11-17-2014

Mixed N-Heterocyclic Carbene–Bis(oxazolinyl)borato Rhodium and Iridium Complexes in Photochemical and Thermal Oxidative Addition Reactions

Songchen Xu
Iowa State University

Kuntal Manna
Iowa State University, kmannachm@gmail.com

Arkady Ellern
Iowa State University, ellern@iastate.edu

Aaron D. Sadow
Iowa State University, sadow@iastate.edu

Mixed N-Heterocyclic Carbene–Bis(oxazolinyl)borato Rhodium and Iridium Complexes in Photochemical and Thermal Oxidative Addition Reactions

Abstract
In order to facilitate oxidative addition chemistry of *fac*-coordinated rhodium(I) and iridium(I) compounds, carbene–bis(oxazolinyl)phenylborate proligands have been synthesized and reacted with organometallic precursors. Two proligands, PhB(OxMe2)2(Im*t*BuH) (H[**1**]; OxMe2 = 4,4-dimethyl-2-oxazoline; Im*t*BuH = 1-*tert*-butylimidazole) and PhB(OxMe2)2(ImMesH) (H[**2**]; ImMesH = 1-mesitylimidazole), are deprotonated with potassium benzyl to generate K[**1**] and K[**2**], and these potassium compounds serve as reagents for the synthesis of a series of rhodium and iridium complexes. Cyclooctadiene and dicarbonyl compounds {PhB(OxMe2)2Im*t*Bu}Rh(η4-C8H12) (**3**), {PhB(OxMe2)2ImMes}Rh(η4-C8H12) (**4**), {PhB(OxMe2)2ImMes}Rh(CO)2 (**5**), {PhB(OxMe2)2ImMes}Ir(η4-C8H12) (**6**), and {PhB(OxMe2)2ImMes}Ir(CO)2 (**7**) are synthesized along with ToMM(η4-C8H12) (M = Rh (**8**); M = Ir (**9**); ToM = tris(4,4-dimethyl-2-oxazolinyl)phenylborate). The spectroscopic and structural properties and reactivity of this series of compounds show electronic and steric effects of substituents on the imidazole (*tert*-butyl vs mesityl), effects of replacing an oxazoline in ToMwith a carbene donor, and the influence of the donor ligand (CO vs C8H12). The reactions of K[**2**] and [M(μ-Cl)(η2-C8H14)2]2 (M = Rh, Ir) provide {κ4-PhB(OxMe2)2ImMes′CH2}Rh(μ-H)(μ-Cl)Rh(η2-C8H14)2 (**10**) and {PhB(OxMe2)2ImMes}IrH(η3-C8H13) (**11**). In the former compound, a spontaneous oxidative addition of a mesityl *ortho*-methyl to give a mixed-valent dirhodium species is observed, while the iridium compound forms a monometallic allyl hydride. Photochemical reactions of dicarbonyl compounds **5** and **7** result in C–H bond oxidative addition providing the compounds {κ4-PhB(OxMe2)2ImMes′CH2}RhH(CO) (**12**) and {PhB(OxMe2)2ImMes}IrH(Ph)CO (**13**). In **12**, oxidative addition results in cyclometalation of the mesityl *ortho*-methyl similar to **10**, whereas the iridium compound reacts with the benzene solvent to give a rare crystallographically characterized *cis*-[Ir](H)(Ph) complex. Alternatively, the rhodium carbonyl **5** or iridium isocyanide {PhB(OxMe2)2ImMes}Ir(CO)CN*t*Bu (**15**) reacts with PhSiH3 in the dark to form the silyl compound {PhB(OxMe2)2ImMes}RhH(SiH2Ph)CO (**14**) or {PhB(OxMe2)2ImMes}IrH(SiH2Ph)CN*t*Bu (**17**). These examples demonstrate the enhanced thermal reactivity of {PhB(OxMe2)2ImMes}-supported iridium and rhodium carbonyl compounds in comparison to tris(oxazolinyl)borate, tris(pyrazolyl)borate, and cyclopentadienyl-supported compounds.

Keywords
addition reactions, carbonyl compounds, iodine, iridium, iridium compounds, ligands, organometallics, photochemical reactions, potassium, rhodium, dicarbonyl compounds

Disciplines
Chemistry

Comments
Reprinted (adapted) with permission from *Organometallics* 33 (2014): 6840, doi:10.1021/om500891h.

ORGANOMETALLICS

Article

pubs.acs.org/Organometallics

Mixed N-Heterocyclic Carbene–Bis(oxazolinyl)borato Rhodium and Iridium Complexes in Photochemical and Thermal Oxidative Addition Reactions

Songchen Xu, Kuntal Manna,‡ Arkady Ellern, and Aaron D. Sadow*

U.S. Department of Energy Ames Laboratory and Department of Chemistry, Iowa State University, 1605 Gilman Hall, Ames, Iowa 50011, United States

Supporting Information

ABSTRACT: In order to facilitate oxidative addition chemistry of *fac*-coordinated rhodium(I) and iridium(I) compounds, carbene–bis(oxazolinyl)phenylborate proligands have been synthesized and reacted with organometallic precursors. Two proligands, $PhB(Ox^{Me2})_2(Im^{tBu}H)$ (H[**1**]; Ox^{Me2} = 4,4-dimethyl-2-oxazoline; $Im^{tBu}H$ = 1-*tert*-butylimidazole) and $PhB(Ox^{Me2})_2(Im^{Mes}H)$ (H[**2**]; $Im^{Mes}H$ = 1-mesitylimidazole), are deprotonated with potassium benzyl to generate K[**1**] and K[**2**], and these potassium compounds serve as reagents for the synthesis of a series of rhodium and iridium complexes. Cyclooctadiene and dicarbonyl compounds $\{PhB(Ox^{Me2})_2Im^{tBu}\}Rh(\eta^4\text{-}C_8H_{12})$ (**3**), $\{PhB(Ox^{Me2})_2Im^{Mes}\}Rh(\eta^4\text{-}C_8H_{12})$ (**4**), $\{PhB(Ox^{Me2})_2Im^{Mes}\}Rh(CO)_2$ (**5**), $\{PhB(Ox^{Me2})_2Im^{Mes}\}Ir(\eta^4\text{-}C_8H_{12})$ (**6**), and $\{PhB(Ox^{Me2})_2Im^{Mes}\}Ir(CO)_2$ (**7**) are synthesized along with $To^MM(\eta^4\text{-}C_8H_{12})$ (M = Rh (**8**); M = Ir (**9**); To^M = tris(4,4-dimethyl-2-oxazolinyl)phenylborate). The spectroscopic and structural properties and reactivity of this series of compounds show electronic and steric effects of substituents on the imidazole (*tert*-butyl vs mesityl), effects of replacing an oxazoline in To^M with a carbene donor, and the influence of the donor ligand (CO vs C_8H_{12}). The reactions of K[**2**] and $[M(\mu\text{-Cl})(\eta^2\text{-}C_8H_{14})_2]_2$ (M = Rh, Ir) provide $\{\kappa^4\text{-}PhB(Ox^{Me2})_2Im^{Mes'}CH_2\}Rh(\mu\text{-H})(\mu\text{-Cl})Rh(\eta^2\text{-}C_8H_{14})_2$ (**10**) and $\{PhB(Ox^{Me2})_2Im^{Mes}\}IrH(\eta^3\text{-}C_8H_{13})$ (**11**). In the former compound, a spontaneous oxidative addition of a mesityl *ortho*-methyl to give a mixed-valent dirhodium species is observed, while the iridium compound forms a monometallic allyl hydride. Photochemical reactions of dicarbonyl compounds **5** and **7** result in C–H bond oxidative addition providing the compounds $\{\kappa^4\text{-}PhB(Ox^{Me2})_2Im^{Mes'}CH_2\}RhH(CO)$ (**12**) and $\{PhB(Ox^{Me2})_2Im^{Mes}\}IrH(Ph)CO$ (**13**). In **12**, oxidative addition results in cyclometalation of the mesityl *ortho*-methyl similar to **10**, whereas the iridium compound reacts with the benzene solvent to give a rare crystallographically characterized *cis*-[Ir](H)(Ph) complex. Alternatively, the rhodium carbonyl **5** or iridium isocyanide $\{PhB(Ox^{Me2})_2Im^{Mes}\}Ir(CO)CN^tBu$ (**15**) reacts with $PhSiH_3$ in the dark to form the silyl compound $\{PhB(Ox^{Me2})_2Im^{Mes}\}RhH(SiH_2Ph)CO$ (**14**) or $\{PhB(Ox^{Me2})_2Im^{Mes}\}IrH(SiH_2Ph)CN^tBu$ (**17**). These examples demonstrate the enhanced thermal reactivity of $\{PhB(Ox^{Me2})_2Im^{Mes}\}$-supported iridium and rhodium carbonyl compounds in comparison to tris(oxazolinyl)borate, tris(pyrazolyl)borate, and cyclopentadienyl-supported compounds.

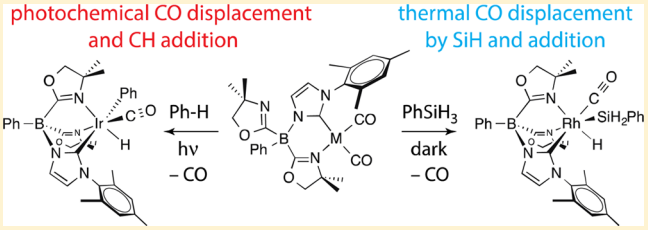

INTRODUCTION

Oxidative addition is an essential part of the rich chemistry of low-valent rhodium and iridium compounds, playing a central role in C–H bond activation chemistry[1] and a large range of catalytic chemistry including hydrogenation,[2] hydrosilylation,[3] hydroformylation,[4] and hydroacylation.[5] Decarbonylation of aldehydes also involves oxidative addition of formyl C–H bonds.[6] Recently, we described a rhodium(I)-catalyzed alcohol and aldehyde decarbonylation reaction that involves oxidative addition of formyl C–H bonds.[7] The $To^MRh(CO)_2$ or $To^MRh(H)_2CO$ (To^M = tris(4,4-dimethyl-2-oxazolinyl)-phenylborate) catalysts require photochemical activation, presumably to generate low-coordinate rhodium centers through CO dissociation. Photochemical CO dissociation is also required for C–H bond oxidative addition mediated by *fac*-coordinated Tp and Cp rhodium dicarbonyl compounds (Tp = tris(pyrazolyl)borate; Cp = cyclopentadienyl) in the classic early examples of hydrocarbon metalation. Despite this similarity, $TpRh(CO)_2$, $CpRh(CO)_2$, and a few of their substituted derivatives are inactive or less active in comparison to $To^MRh(CO)_2$ in the photocatalytic alcohol decarbonylation.

Conversely, To^MRh^I and To^MIr^I compounds are less reactive in a number of oxidative additions than Tp, Cp, and phosphine-coordinated monovalent group 9 compounds that are valuable catalysts for many synthetic transformations. For example, only a few polar C–X bonds are reactive toward $To^MRh(\eta^4\text{-}C_8H_{12})$, and the iridium congeners are unreactive toward oxidative addition of electrophiles such as hydrogen and silanes. In contrast, cyclopentadienyl and tris(pyrazolyl)borate rhodium and iridium compounds have provided the seminal examples of oxidative addition of inert methyl, methylene, and methane

Received: August 29, 2014
Published: November 17, 2014

   dx.doi.org/10.1021/om500891h | *Organometallics* 2014, 33, 6840–6860

C−H bonds.[8] Instead of oxidative addition, reactions of $To^{M}Rh(CO)_2$,[9] $To^{M}Ir(CO)_2$, and $To^{P}Ir(CO)_2$[10] (To^{P} = tris(4*S*-isopropyl-2-oxazolinyl)phenylborate) with strong electrophiles such as MeOTf result in N-methylation of the nitrogen atom on one of the three oxazoline rings. $To^{M}Rh(CO)_2$ reacts with benzene upon photolysis to give $To^{M}RhH(Ph)CO$, but reactions of silanes give mixtures of unidentified products, while $To^{M}Ir(CO)_2$ is inert toward benzene and silanes under a range of photochemical and thermal conditions. For comparison, $Tp^{*}Rh(CO)_2$ (Tp^{*} = tris(3,5-dimethylpyrazolyl)borate) oxidatively adds the Si−H bond in Et_3SiH under photolytic conditions to give $Tp^{*}RhH(SiEt_3)CO$;[11] the photochemical C−H bond oxidative addition chemistry of $Tp^{*}Rh(CO)_2$ noted above is well known. Likewise, $CpRh(\eta^2\text{-}C_2H_4)_2$ also reacts with silanes via oxidative addition under photochemical activation.[12] Thermal C−H bond additions in these systems are observed mainly with olefin leaving groups.[13] A number of factors might be responsible for the reduced reactivity of $To^{M}M$ compounds in oxidative additions of nonpolar bonds including the ancillary ligand's steric properties, its coordination mode, its conformation, and its effect on the electronic properties of the metal center. For example, the varying coordination of tris(pyrazolyl)borate between bidentate and tridentate modes is intimately related to the oxidative addition of C−H bonds.[14−16] While these factors may or may not directly impact catalytic decarbonylation reactivity (or other catalytic processes that invoke oxidative addition), new isoelectronic *fac*-coordinating ligand derivatives may facilitate oxidative additions and/or provide improved catalysis.

In this context, the oxazolinylborate framework remains appealing (despite the limited oxidative addition chemistry of tris(oxazolinyl)borate group 9 compounds) because it allows the synthesis of a range of isoelectronic hybrid ligands through the intermediate $PhB(Ox^{R})_2$. Thus, the electron-donating ability of To^{M} may be modified by substituting an oxazoline by an imidazole to provide mixed carbene−bis(oxazolinyl)borate ligands. N-Heterocyclic carbene donors, derived from imidazole rings, are good electron-donating ligands,[17] and recently we reported the monoanionic ligand bis(4,4-dimethyl-2-oxazolinyl)(1-mesitylimidazolyl)phenylborate ($[PhB(Ox^{Me2})_2Im^{Mes}]^-$) as a supporting ligand for zinc alkylperoxides.[18] The presence of the borate group in oxazolinylborates appears to increase the oxazoline group's electron donation ability,[19] and this may also extend to N-borylated carbenes. In addition, ligands based on N-borylated imidazoles have proven successes in stabilizing high-valent metal centers. Smith and coworkers have demonstrated the electron-donating ability of the tris(imidazol-2-ylidene)phenylborate ligand in the syntheses of four-coordinated iron(IV) nitrido complexes[20] and a cationic iron(V).[21] Furthermore, a rhodium catalyst supported by a mixed carbene−oxazoline ligand was proposed to allow access to a rhodium silylene in a carbonyl hydrosilylation.[22,23] On the basis of these examples, we began to prepare and investigate the reaction chemistry of rhodium and iridium complexes coordinated by mixed oxazoline−carbene ligands.

The current contribution reports the synthesis and structures of carbene−bis(oxazolinyl)borate ligands as their potassium salts and as a series of group 9 compounds for study in oxidative addition chemistry. In particular, the rhodium and iridium compounds $[M(\mu\text{-}Cl)(CO)_2]_2$, $[M(\mu\text{-}Cl)(\eta^4\text{-}C_8H_{12})]_2$, and $[M(\mu\text{-}Cl)(\eta^2\text{-}C_8H_{14})_2]_2$ react with the anionic carbene−bis(oxazolinyl)borate proligands to provide group 9 starting materials. Analysis of the spectroscopic and structural features of the ligands and the series of compounds reveals steric and electronic effects of the N-borylated carbene donor in comparison to related tris(oxazolinyl)borate and tris(pyrazolyl)borate compounds. These steric and electronic features were considered in the context of their importance to oxidative addition chemistry. Furthermore, the resulting compounds show intra- and intermolecular reactivity in oxidative addition of C−H and Si−H bonds under thermal and photochemical conditions that is distinct from the well-known chemistry of cyclopentadienyl and tris(pyrazolyl)borato metal dicarbonyls.

RESULTS AND DISCUSSION

Synthesis and Characterization of Bis(4,4-dimethyl-2-oxazolinyl)(1-*tert*-butylimidazolyl)phenylborate PhB(Ox^{Me2})$_2$(Im^{tBu}H)LiCl(THF) (H[1]·LiCl·THF). The compound $PhB(Ox^{Me2})_2(Im^{tBu}H)LiCl(THF)$ (H[**1**]·LiCl·THF; $Im^{tBu}H$ = 1-*tert*-butylimidazole, Ox^{Me2} = 4,4-dimethyl-2-oxazoline) is prepared by combination of $PhB(Ox^{Me2})_2$[24] and 1-*tert*-butylimidazole in THF at room temperature (eq 1).

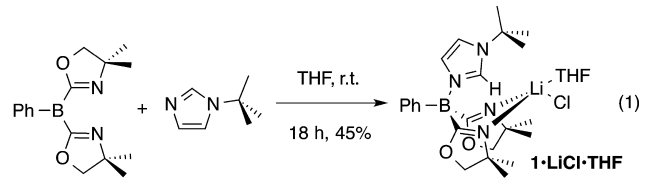

$PhB(Ox^{Me2})_2(LiCl)_n$ (1)

In this compound, the imidazole binds to the boron center through a Lewis acid−base interaction, and the presence of LiCl comes from the preparation of $PhB(Ox^{Me2})_2$.[24]

Compound H[**1**]·LiCl·THF precipitates from the yellow THF solution as an analytically pure white solid in 45% yield after stirring overnight. Compound H[**1**]·LiCl·THF is slightly soluble in benzene, but very soluble in acetonitrile, and the latter solvent is preferable for NMR spectral characterization. The ^{1}H NMR spectrum of H[**1**]·LiCl·THF contained two singlets and one multiplet assigned to the oxazoline methyl and methylene groups, respectively. This pattern suggests a C_s-symmetric structure, as is expected for an imidazole−borane adduct. Signals at 1.58 (9 H) and 8.09 (1 H) ppm were assigned to the *tert*-butyl and 2-H on the imidazolium, respectively. The ^{11}B NMR spectrum revealed one singlet signal at −9.4 ppm; for comparison, the ^{11}B NMR chemical shift of $PhB(Ox^{Me2})_2$ as an acetonitrile adduct (in acetonitrile-d_3) was observed at −8.1 ppm,[24] whereas the borate center in $H[To^{M}]$ was observed at −17.2 ppm.[25] Natural abundance ^{15}N NMR data were obtained through ^{1}H−^{15}N HMBC experiments and differentiated the nitrogen atoms on the imidazolium and oxazoline rings. The 1-N imidazolium signal at −178 ppm was correlated with the ^{1}H NMR signals assigned to the *tert*-butyl group, while the 3-N signal at −184 ppm correlated only with 4-H and 5-H. The heteronuclear ^{1}H−^{15}N correlation experiment also revealed the magnetic equivalence of the oxazoline rings, as both methyl signals were correlated to a single ^{15}N NMR signal at −138 ppm.

An X-ray quality crystal of H[**1**]·LiCl·$NCCD_3$ is obtained by slow evaporation of acetonitrile-d_3 at room temperature. The adduct formation of the imidazole−borane and the presence of LiCl and acetonitrile-d_3 as an additional two-electron donor are verified by an X-ray diffraction study (Figure 1). In the solid-state structure, both oxazolines coordinate to the lithium center through the nitrogen atoms. The pseudotetrahedral

dx.doi.org/10.1021/om500891h | *Organometallics* 2014, 33, 6840−6860

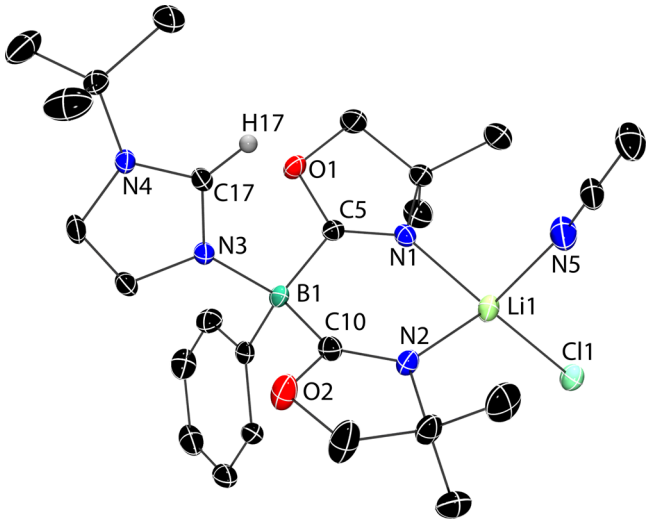

Figure 1. Rendered thermal ellipsoid plot of $PhB(Ox^{Me2})_2(Im^{tBu}H)$-LiCl($NCCD_3$) (H[**1**]·LiCl·$NCCD_3$) with ellipsoids at 35% probability. H and D atoms are not plotted for clarity except for the H17 on the imidazolium C17. Selected interatomic distances (Å): B1−C5, 1.620(4); B1−C10, 1.607(4); B1−N3, 1.594(3); Li1−N1, 2.057(5); Li1−N2, 2.052(5); Li1−N5, 2.118(6). Selected interatomic angles (deg): C5−B1−C10, 111.6(2); C5−B1−N3, 109.1(2); C10−B1−N3, 109.6(2); N1−Li1−N2, 93.5(2).

coordination sphere of the lithium ion is completed by chloride and an acetonitrile ligand, which apparently replaced the THF ligand. The boron center is also pseudotetrahedral. For comparison, $(PhB(Ox^{Me2})_2(Im^{Mes}H)LiCl)_2$ ($(H[\mathbf{2}]\cdot LiCl)_2$, $Im^{Mes}H$ = 1-mesitylimidazole) crystallizes as a dimer with bridging chloride ligands.[18]

Syntheses and Characterizations of Proligands $PhB(Ox^{Me2})_2(Im^{tBu}H)$ (H[1]) and $PhB(Ox^{Me2})_2(Im^{Mes}H)$ (H[2]) and Their Deprotonation. Attempts to deprotonate H[**1**]·LiCl·THF and $(H[\mathbf{2}]\cdot LiCl)_2$ by reaction with ^{n}BuLi, KCH_2Ph, $LiN(SiMe_3)_2$, or $LiN(CHMe_2)_2$ do not provide the desired lithium or potassium borates $[\mathbf{1}]^-$ and $[\mathbf{2}]^-$ in the solvents benzene, toluene, diethyl ether, and tetrahydrofuran over a range of appropriate temperatures. We hypothesized that the LiCl adduct might be interfering with reactions with bases, even though LiCl often enhances the reactivity of alkyl magnesium, zinc, and copper reagents toward metalations.[26] In addition, $(H[\mathbf{2}]\cdot LiCl)_2$ and ZnR_2 (R = Me, Et) react to give {**2**}ZnR, and the LiCl present in the starting material precipitates during those reactions.[18]

Purification of compound H[**1**]·LiCl·THF or $(H[\mathbf{2}]\cdot LiCl)_2$ from their LiCl adducts is accomplished by the addition of excess water to their benzene suspensions. In both cases, an analytically pure white solid is isolated in good yield (eq 2), and

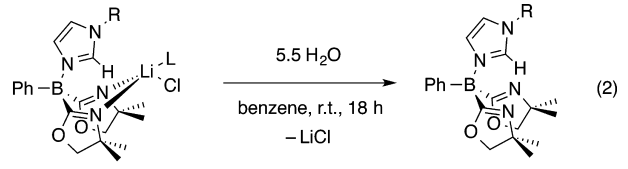

H[**1**]·LiCl·THF; R = *t*Bu, L = THF
(H[**2**]·LiCl)$_2$; R = Mes

H[**1**]; R = *t*Bu (90%)
H[**2**]; R = Mes (70%)

(2)

this isolated product is sufficiently dry for reactions with strong bases such as KCH_2Ph. Flame tests of H[**1**] or H[**2**] gave blue flames in contrast to the red color observed for the tests of H[**1**]·LiCl·THF or $(H[\mathbf{2}]\cdot LiCl)_2$.

The solubility of H[**1**] or H[**2**] in benzene, toluene, tetrahydrofuran, and diethyl ether noticeably increased relative to their LiCl adducts. In contrast to the broad spectrum of H[**1**]·LiCl·THF acquired in benzene-d_6, the spectrum of H[**1**] contained sharp, well-defined resonances with distinct chemical shifts. For example, the 2-H signal in H[**1**] and H[**1**]·LiCl·THF was 9.55 and 8.09 ppm, respectively. The ^{15}N NMR chemical shift value for the oxazoline was slightly downfield in H[**1**] at −125 ppm in comparison to −138 ppm for H[**1**]·LiCl·THF. In addition, the ν_{CN} band in the IR spectrum for H[**1**]·LiCl·THF at 1624 cm^{-1} was at higher energy than for H[**1**] at 1605 cm^{-1}.

Deprotonation of H[**1**] or H[**2**] to generate the potassium complex K[**1**] or K[**2**] is readily accomplished with potassium benzyl in THF (eq 3).

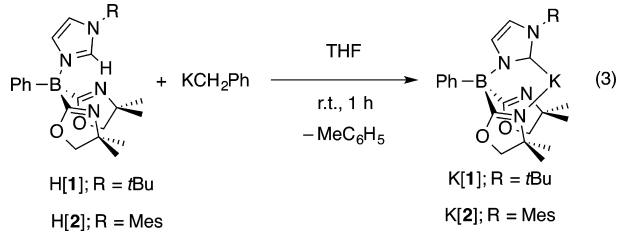

H[**1**]; R = *t*Bu
H[**2**]; R = Mes

K[**1**]; R = *t*Bu
K[**2**]; R = Mes

(3)

A micromolar-scale reaction of H[**1**] and potassium benzyl in tetrahydrofuran-d_8 forms a white precipitate in ca. 20 min. A ^{1}H NMR spectrum of the solution showed the formation of toluene and concomitant disappearance of the 2-H imidazole signal at 9.46 ppm. The resulting product is sparingly soluble in THF, and only a few key oxazoline, imidazole, and phenyl ^{1}H NMR signals could be assigned. The ^{11}B NMR spectrum contained one signal at −11.6 ppm, which was slightly upfield of H[**1**] (−9.4 ppm). Attempts to isolate the white precipitate typically afforded mixtures of K[**1**] and H[**1**] despite careful air- and moisture-free manipulations. Therefore, the most efficient synthetic protocols employ K[**1**] generated *in situ*.

K[**2**], also generated by the reaction of KCH_2Ph and H[**2**], is soluble in THF. The formation of toluene confirmed the expected deprotonation. The 2-H imidazole signal at 8.84 ppm in H[**2**] was absent in the product's ^{1}H NMR spectrum, which is distinct from that of H[**2**]. Although attempts to isolate K[**2**] provided mixtures contaminated with H[**2**], a crystal of K[**2**] was fortuitously obtained from a crystallization in benzene at room temperature. An X-ray diffraction study revealed the 2-C (C22 in Figure 2) bonded to a K center, which affirmed the proposed deprotonation and the proposed connectivity of K[**2**].

The resulting interesting structure (Figure 2) is a polymeric chain of alternating potassium cations and $[\mathbf{2}]^-$, with each potassium atom coordinated to five atoms on two ligands: the *ipso*-carbon of the phenyl group (C23), the NHC carbon (C22), and an oxazoline nitrogen (N2) of one ligand and to one oxazoline nitrogen (N1) and one oxazoline oxygen (O2) of the next [**2**] in the polymer chain. The oxazoline ring that contains N2 and O2 is bridging between two crystal-symmetry-related potassium atoms. Although K[**2**] may be crystallized, its isolation is challenging, and it is most conveniently prepared and used *in situ*.

Synthesis and Characterization of Rhodium(I) and Iridium(I) Compounds Containing $[\mathbf{1}]^-$ and $[\mathbf{2}]^-$. A series of rhodium and iridium compounds have been prepared using

dx.doi.org/10.1021/om500891h | *Organometallics* 2014, 33, 6840−6860

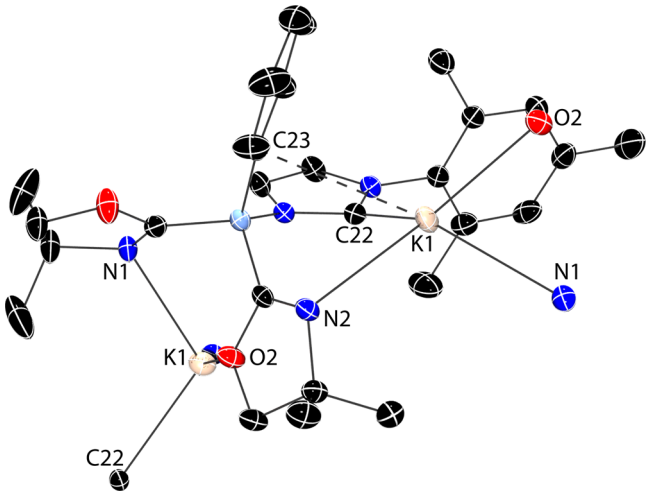

Figure 2. Rendered thermal ellipsoid plot of K[PhB(Ox^{Me2})$_2$Im^{Mes}] (K[**2**]). Ellipsoids are plotted at 35% probability, and H atoms are not illustrated for clarity. Selected interatomic distances (Å): K1−N1, 2.861(2); K1−O2, 2.697(1); K1−C22, 2.991(2); K1−N2, 2.732(2); K1−C23, 3.373(2).

[M(μ-Cl)(η^4-C_8H_{12})]$_2$, [M(μ-Cl)(η^2-C_8H_{14})$_2$]$_2$, and [M(μ-Cl)(CO)$_2$]$_2$ (M = Rh, Ir) as starting materials. A notable difference between [**1**]$^-$ and [**2**]$^-$ is observed, in that [**2**]$^-$ readily provides a rich reactivity on rhodium and iridium, whereas only a single rhodium compound containing [**1**]$^-$ as an ancillary ligand is isolable using these starting materials. In all other cases tested, H[**1**] is the major isolated product from reactions of K[**1**] and rhodium or iridium salts.

Upon addition of the rhodium precursor [Rh(μ-Cl)(η^4-C_8H_{12})]$_2$ to a pink suspension of *in situ* generated K[**1**], the precipitate dissolves immediately to give a red solution (eq 4).

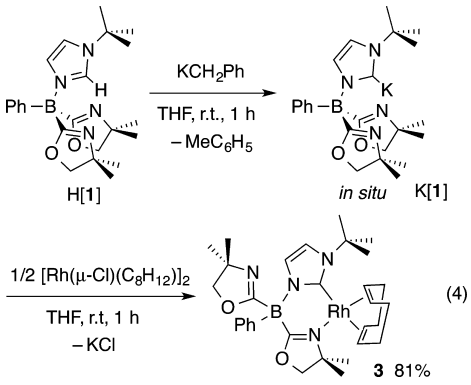

The ^{1}H NMR spectrum of **3**, acquired in benzene-d_6, indicates that the two oxazoline groups are inequivalent. Correlations between the oxazoline methyl groups and nitrogen in a ^{1}H−^{15}N HMBC experiment revealed two distinct chemical shifts for the oxazoline nitrogen. The ^{15}N signal at −183 ppm was assigned to a coordinated oxazoline, while the signal at −123 ppm was assigned to a noncoordinated group based on its similarity to the ^{15}N NMR chemical shift of 2H-4,4-dimethyl-2-oxazoline.[24] Both imidazole nitrogen centers were detected in this experiment at −172 (1-N) and −181 ppm (3-N) and distinguished by a cross-peak from the latter to the *tert*-butyl ^{1}H NMR signal (Table 1). Coordination of the carbene to rhodium was supported by a doublet resonance at 181.1 ppm ($^1J_{RhC}$ = 50 Hz) in the ^{13}C{^{1}H} NMR spectrum.

Table 1. Key Spectroscopic Data from Rhodium and Iridium Compounds

compound	ν_{CO} (cm^{-1}, KBr)	δ ^{13}C of C_8H_{12} or $(CO)_2$	δ $^{15}N_{oxazoline}$
{**1**}Rh(η^4-C_8H_{12}) (**3**)	n.a.	88.61 (7.2 Hz), 88.36 (8.1 Hz), 79.68 (13.7 Hz), 69.13 (12.8 Hz)	−183, −123
{**2**}Rh(η^4-C_8H_{12}) (**4**)	n.a.	90.72 (7.7 Hz), 87.89 (7.8 Hz), 75.22 (12.9 Hz), 70.84 (13.1 Hz)	−182, −125
{**2**}Rh(CO)$_2$ (**5**)	2063, 1993	176.20 (45.0 Hz)	−153
{**2**}Ir(η^4-C_8H_{12}) (**6**)	n.a.	75.66, 72.66, 59.95, 56.37	−188, −124
{**2**}Ir(CO)$_2$ (**7**)	2053, 1979	179.08	−156
To^{M}Rh(CO)$_2$[a]	κ^2: 2070, 2010, 1997; κ^3: 2048, 1968	188.42 (66.6 Hz)	−163
To^{M}Ir(CO)$_2$[b]	2066, 1989	176.63	−167
Tp*Rh(CO)$_2$[c]	2052, 1974	n.a.	n.a.
To^{M}Rh(η^4-C_8H_{12})	n.a.	79.33, 75.65	−169, −161
To^{M}Ir(η^4-C_8H_{12})	n.a.	62.77, 59.25	−193, −155
{PhMeBpz^{Me}}Rh(CO)$_2$[d]	2078, 2012	185.1 (67.6 Hz)	−149
{Acac}Rh(CO)$_2$[e]	2083, 2015	n.a.	n.a.
[(DEAM-MbBI)-Rh(CO)$_2$][BF$_4$][f]	2084, 2026	179.96, 179.93 (45 Hz)	n.a.
{BDI-3}Ir(CO)$_2$[g]	2054, 1986	198.50	n.a.

[a]See ref 9. [b]See ref 10. [c]See ref 27. [d]PhMeBpz^{Me} = bis(3-methylpyrazolyl)methylphenylborate; see ref 32. [e]Acac = acetyl acetonate; see ref 31. [f]DEAM-MbBI = *trans*-9,10-dihydro-9,10-ethanoanthracene-11,12-bis(1-methyl)benzimidazolidine-2-ylidene; see ref 33. [g]BDI-3 = *N*,*N*′-bis(2,6-diisopropylphenyl)-2,4-diketiminate; see ref 34.

Additionally, two ν_{CN} bands in the IR spectrum (acquired in KBr) provided support for coordinated (1570 cm^{-1}) and noncoordinated oxazoline (1613 cm^{-1}).

A single-crystal X-ray diffraction study supports the connectivity and coordination geometry suggested by the solution-phase data (Figure 3). The structure will be discussed below in comparison with {**2**}-coordinated rhodium and iridium compounds.

The syntheses of the red, mesityl-substituted carbene compound {PhB(Ox^{Me2})$_2$Im^{Mes}}Rh(η^4-C_8H_{12}) (**4**) and the yellow dicarbonyl analogue (**5**) follow that of the ^{t}Bu-substituted carbene complex **3** (Scheme 1).

As in **3**, the inequivalent oxazoline groups in **4** do not exchange on the ^{1}H NMR time scale at room temperature. In addition, the methyl groups from the mesityl are inequivalent and the compound appears C_1 symmetric. Thus, seven singlet resonances (3 H each) were observed, assigned to seven inequivalent methyl groups, and these were distinguished with ^{1}H−^{13}C HMBC and ^{1}H−^{15}N HMBC experiments (see Table 1).

Compound **5** is obtained as a yellow solid from the reaction of 2 equiv of K[**2**] and [Rh(μ-Cl)(CO)$_2$]$_2$ at room temperature. The spectroscopy of **5** suggests its structure has higher symmetry than the C_1-symmetric cyclooctadiene-substituted **3**

dx.doi.org/10.1021/om500891h | *Organometallics* 2014, 33, 6840−6860

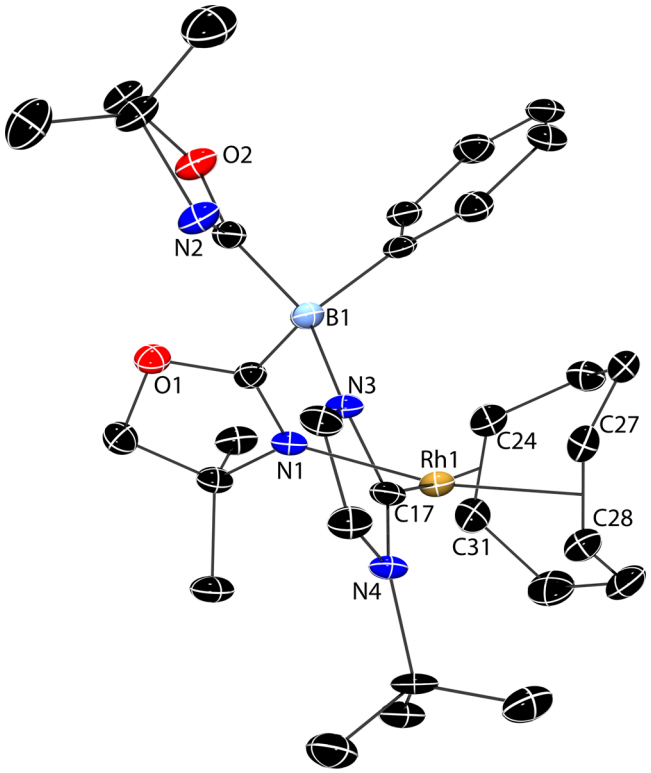

Figure 3. Rendered thermal ellipsoid plot of {PhB(Ox^{Me2})$_2$$Im^{tBu}$}Rh-($\eta^4$-$C_8H_{12}$) (**3**) with ellipsoids at 35% probability. H atoms are not plotted for clarity. Selected interatomic distances (Å) and angle (deg): Rh1−N1, 2.121(4); Rh1−C17, 2.063(5); Rh1−C24, 2.208(4); Rh−C27, 2.116(5); Rh1−C28, 2.147(5); Rh1−C31, 2.173(5); N1−Rh1−C17, 83.0(2).

Scheme 1. Preparation of {PhB(Ox^{Me2})$_2$$Im^{Mes}$}M($\eta^4$-$C_8H_{12}$) (M = Rh (4), Ir (6)) and {PhB(Ox^{Me2})$_2$$Im^{Mes}$}M(CO)$_2$ (M = Rh (5), Ir (7))

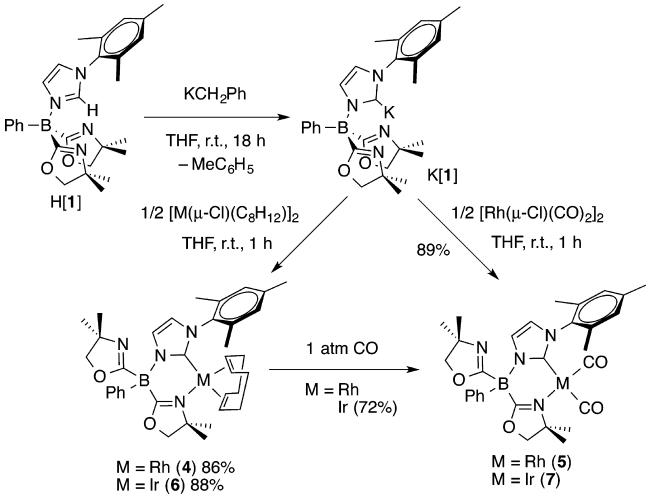

and **4**. Thus, the mesityl group produced only three total ^{1}H NMR signals for methyl and arene hydrogens, and the two oxazolines in **5** appeared equivalent. The oxazoline methyl signals appeared as two singlets in ^{1}H NMR spectra of **5** acquired from room temperature to 195 K in toluene-d_8. Although the signals broadened as the temperature decreased suggesting an exchange process, resolution of the signals into four resonances (expected for a four-coordinated structure) was not observed. A ^{1}H−^{15}N HMBC experiment revealed one nitrogen signal at −153 ppm correlated to the two oxazoline methyl resonances. In contrast, the solid-state infrared spectrum of **5** (precipitated from pentane, KBr) contained two ν_{CN} bands at 1564 and 1626 cm^{-1}. An IR spectrum of **5** dissolved in benzene contained two broad ν_{CN} bands ranging from 1530 to 1560 cm^{-1} and 1620−1650 cm^{-1}. The broad IR signals in the ν_{CN} region suggest the oxazoline exchange process occurs at a rate on the order of the IR time scale. Thus, carbonyl compound **5** is highly fluxional in solution, but only one oxazoline is coordinated in the solid state.

The related iridium compound {PhB(Ox^{Me2})$_2$$Im^{Mes}$}Ir($\eta^4$-$C_8H_{12}$) (**6**) is prepared from [Ir(μ-Cl)(η^4-C_8H_{12})]$_2$ and *in situ* generated K[**2**] analogously to the rhodium congener. Addition of 1 atm of CO to **6** affords {PhB(Ox^{Me2})$_2$$Im^{Mes}$}Ir(CO)$_2$ (**7**). As expected, the spectroscopic properties and structures of the rhodium and iridium compounds are similar. Thus, the oxazoline groups of **6**, like its rhodium analogue **4**, were inequivalent on the ^{1}H NMR time scale, while the oxazoline moieties of the dicarbonyl compounds **5** and **7** appeared to be equivalent because of a rapid exchange process. The reaction of **4** and 1 atm of CO also provides **5**; however, the corresponding reaction of the *tert*-butyl-based carbene compound **3** and CO (1 atm) results in a mixture of unidentified species and cyclooctadiene.

To complete the series for comparison, To^MM(η^4-C_8H_{14}) (M = Rh (**8**), Ir (**9**)) are synthesized by reaction of Tl[To^M] and [M(μ-Cl)(η^4-C_8H_{12})]$_2$ in benzene (eq 5). The use of

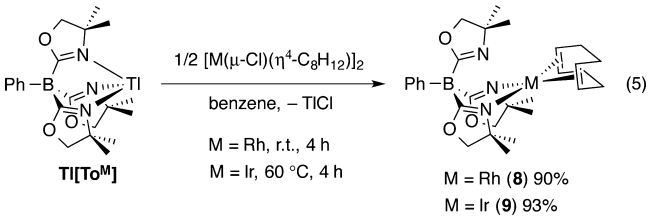

Tl[To^M] is important for formation of To^MM(η^4-C_8H_{14}), as Li[To^M] provided a dimeric lithium chloride adduct.[10] Moreover, the spectroscopy of To^MM(η^4-C_8H_{14}) is complicated in comparison to {PhB(Ox^{Me2})$_2$$Im^R$}M($\eta^4$-$C_8H_{14}$).

The room-temperature ^{1}H NMR spectra of **8** and **9** contained three singlets assigned to the methyl groups and three slightly broad singlets for the methylene groups of the oxazolines. The three methyl signals are consistent with C_s-symmetric structures, but the singlet methylene signals suggest that the To^M ligand's coordination mode is dynamic. In the solid state, infrared spectroscopy provided evidence for the bidentate coordination mode, as indicated by two ν_{CN} bands corresponding to coordinated oxazolines (**8**: 1567 cm^{-1}; **9**: 1558 cm^{-1}) and noncoordinated oxazolines (**8**: 1611 cm^{-1}; **9**: 1607 cm^{-1}). These NMR data suggest a slow dynamic exchange process between the pendent oxazoline and the two coordinated oxazolines that occurs close to the ^{1}H NMR time scale in solution at room temperature. In contrast, the oxazoline groups in previously reported dicarbonyl compounds To^MM(CO)$_2$ (M = Rh, Ir) are rapidly exchanging at room temperature.[7,10] Previously, the denticities of tris(pyrazolyl)-borato group 9 compounds have been correlated to ^{103}Rh NMR chemical shifts,[27] ^{11}B NMR chemical shifts,[28] and ν_{BH} stretching frequencies in the IR spectra,[29] but the latter two methods do not provide insight in the phenyl-oxazolinylborate systems.

dx.doi.org/10.1021/om500891h | *Organometallics* 2014, 33, 6840−6860

Four olefinic ^{13}C NMR signals were detected and assigned to the C_8H_{12} group in compounds **3**, **4**, and **6**; four signals result from the C_1-symmetry of the compounds (see Table 1). In contrast, the $^{13}C\{^1H\}$ spectra for C_s-symmetric $To^MM(\eta^4\text{-}C_8H_{12})$ contained only two olefinic resonances as the result of C_s symmetry. The chemical shifts were further upfield in the iridium complexes than in the rhodium analogues for both To^M and $PhB(Ox^{Me2})_2Im^{Mes}$-supported compounds. The comparison between C_8H_{12} olefinic resonances in To^M and $PhB(Ox^{Me2})_2Im^{Mes}$-supported complexes reveals a common set of upfield chemical shifts as well as an additional downfield set of olefinic chemical shifts for {**1**}- and {**2**}-supported compounds. There were also two sets of two olefinic signals observed in the ^1H NMR spectra, and the downfield set of ^1H NMR resonances correlated to the downfield ^{13}C NMR signals in $^1H-^{13}C$ HMQC experiments. The downfield ^1H and ^{13}C chemical shifts were assigned to the olefin ligand *trans* to the NHC donor, while the upfield signals were assigned to the olefin ligand *trans* to the oxazoline donor based on their similarity to the olefinic chemical shifts in the $To^MM(\eta^4\text{-}C_8H_{12})$ compounds. These assignments were further supported by NOESY experiments on compound **4**. In particular, the downfield ^1H NMR signals assigned to cyclooctadiene at 4.48 and 4.67 ppm showed through-space correlations to the oxazoline methyl signals, and from that the downfield ^1H NMR signals were assigned as *cis* to the oxazoline and *trans* to the carbene. The upfield ^1H NMR signals at 3.11 and 3.52 ppm exhibited through-space correlations to the two *ortho*-methyl groups on the NHC-mesityl ring in the NOESY experiment, and these signals and the corresponding upfield ^{13}C NMR signals were assigned as *trans* to oxazoline. Satisfyingly, two out of the four cyclooctadiene olefinic signals at 4.48 and 3.52 ppm correlated to the *meta*-C_6H_5 in the NOESY experiment, and these data placed those two hydrogen atoms *syn* with the pseudoaxial phenyl group on boron. The other two olefinic hydrogens were *anti* with the phenyl group, and no cross-peak was detected.

In the rhodium $PhB(Ox^{Me2})_2Im^R$ cyclooctadiene compounds, the $^1J_{RhC}$ values are larger for the upfield signals (12−14 Hz) than for downfield, *trans*-to-NHC olefinic signals (7−8 Hz). This effect was previously observed.[30] Unfortunately, the $^{13}C\{^1H\}$ NMR signals in $To^MRh(\eta^4\text{-}C_8H_{12})$ for the diene are broad, and the coupling constants could not be measured.

The CO stretching frequencies in the four-coordinate complexes **5** and **7** appeared at lower energy than those in corresponding $\kappa^2\text{-}To^MM(CO)_2$ compounds (measured on four-coordinate square planar compounds in a KBr matrix), which supports the expectation that $PhB(Ox^{Me2})_2Im^{Mes}$ is more electron-donating than To^M. The five-coordinate rhodium complex $Tp^*Rh(CO)_2$ has CO bonds that are lower energy than **5**, but that compound is 18-electron.[27] Better comparisons are with four-coordinate compounds such as $\{Acac\}Rh(CO)_2$ or $\{PhMeBp^{Me}\}Rh(CO)_2$, which show higher energy CO stretching frequencies.[31,32] The ν_{CO} bands for cationic bis(carbene) rhodium dicarbonyl compounds appear at even higher energy.[33] The carbonyl stretching frequencies of **7** and strongly electron-donating diketiminate iridium dicarbonyls are similar, suggesting similar electron-donating capabilities of zwitterionic $PhB(Ox^{Me2})Im^{Mes}$ (as a bidentate ligand) to the monoanionic diketiminate ligands.[34]

The upfield nitrogen signals observed in the $^1H-^{15}N$ HMBC experiments of compounds **3**, **4**, and **6** were assigned to the coordinated oxazoline nitrogen. The downfield ^{15}N cross-peak was assigned to the noncoordinated oxazoline because that signal was closer to the chemical shift of the oxazoline nitrogen in H[**1**] and H[**2**] (−125 ppm). Although the two nitrogen chemical shift values in the cyclooctadiene compounds **4** and **6** were different from the ones observed in the carbonyl compounds **5** and **7** (−153 and −156 ppm, respectively), the average values of the former are very close (−154 ppm, **4**; −156 ppm, **6**) to those of **5** and **7**. This similarity is attributed to the chemical averaging of signals in **5** and **7** that results from the fluxionality of the carbonyl compounds. The $^{13}C\{^1H\}$ NMR signals for the carbene 2-C for the series of compounds range from 178 to 187 ppm without a clear affect of the metal center or other ligand (CO, cyclooctadiene).

X-ray quality crystals of all five $PhB(Ox^{Me2})_2Im^R$-supported compounds **3**, **4**, **5**, **6**, and **7** are obtained from pentane at −30 °C. The conformations of cyclooctadiene-coordinated compounds **3**, **4**, and **6** are similar to one another, as are the structural features of the dicarbonyls **5** and **7**. Thermal ellipsoid-rendered representations for rhodium compounds **3**, **4**, and **5** are shown in Figures 3, 4, and 5, while illustrations of iridium complexes **6** and **7** are available in the Supporting Information. The molecular structure of $To^MRh(\eta^4\text{-}C_8H_{12})$ (**8**) is shown in Figure 6. In all six compounds, the metal center is coordinated in the square planar geometry that is expected for monovalent group 9 compounds. To achieve this geometry, the $PhB(Ox^{Me2})_2Im^{Mes}$ ligand coordinates in a bidentate fashion through the NHC and one of the two oxazoline donors. The bidentate-coordinated $PhB(Ox^{Me2})_2Im^{Mes}$ ligand forms a boat-like conformation with the boron and metal centers occupying the "bow" and "stern" positions. A similar boat conformation is obtained in the crystal structure of *tert*-butyl-substituted

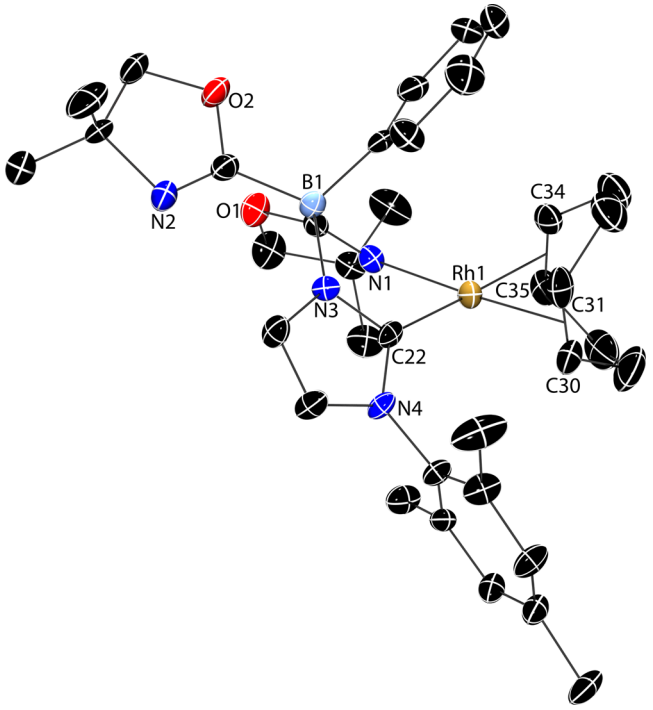

Figure 4. Rendered thermal ellipsoid plot of $\{PhB(Ox^{Me2})_2Im^{Mes}\}Rh(\eta^4\text{-}C_8H_{12})$ (**4**). The ellipsoids are plotted at 35% probability, and H atoms are not illustrated for clarity. Selected interatomic distances (Å) and angle (deg): Rh1−N1, 2.132(6); Rh1−C22, 2.051(7); Rh1−C30, 2.139(8); Rh1−C31, 2.105(8); Rh1−C34, 2.198(7); Rh1−C35, 2.189(7); C22−Rh1−N1, 84.6(2).

dx.doi.org/10.1021/om500891h | *Organometallics* 2014, 33, 6840−6860

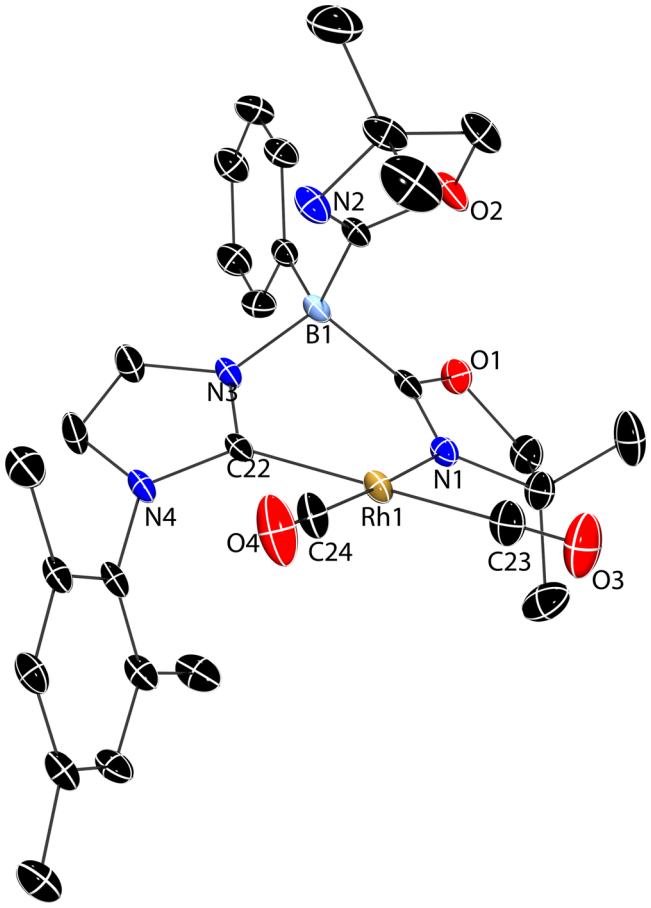

Figure 5. Rendered thermal ellipsoid plot of $\{PhB(Ox^{Me2})_2Im^{Mes}\}$-$Rh(CO)_2$ (**5**) at 35% probability. H atoms are not included in the depiction for clarity. Selected interatomic distances (Å): Rh1−N1, 2.087(2); Rh1−C22, 2.062(3), Rh1−C23, 1.896(4); Rh1−C24, 1.836(3). Selected interatomic angles (deg): C22−Rh1−N1, 87.4(1); N1−Rh1−C23, 96.0(1); C23−Rh1−C24, 85.3(1); C24−Rh1−C22, 91.3(1).

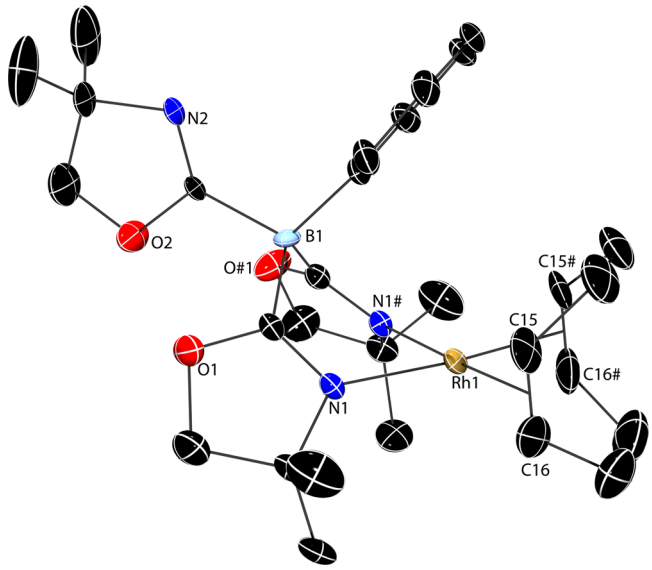

Figure 6. Rendered thermal ellipsoid plot of $To^{M}Rh(\eta^4\text{-}C_8H_{12})$ (**8**). Ellipsoids are plotted at 35% probability, and H atoms are not illustrated for clarity. Selected interatomic distances (Å) and angle (deg): Rh1−N1, 2.116(6); Rh1−C15, 2.099(9); Rh1−C16, 2.12(1), N1−Rh1−N1#, 84.4(3).

complex **3** (shown above in Figure 3) and To^{M}-supported compound **8**.

The six-membered boat conformation places the pendent oxazoline and phenyl groups bonded to boron in either axial or equatorial positions. The boat conformation results in steric interactions between the axial group on boron and the other ligand(s) on the metal center. Interestingly, the pendent oxazoline is axial and points toward the metal center in the two carbonyl compounds **5** and **7**, while in the cyclooctadiene compounds **3**, **4**, and **6**, the phenyl ring occupies the axial position and the oxazoline group points away from the metal center. The combination of bulky cyclooctadiene on the metal center and nonplanar 4,4-dimethyl-2-oxazoline in the axial position likely would result in unfavorable steric interactions. For this reason, the conformation that places the planar phenyl group in the axial position is more favorable for the cyclooctadiene-coordinated compounds. Because the CO ligands have significantly diminished steric demand in comparison to cyclooctadiene, the carbonyl compounds can adopt a conformation in which the pendent oxazoline group is axial and points at the metal center. Presumably, a weak interaction between the metal center and the axial oxazoline might favor that conformation; however, the Rh1−N2 and Rh1−O2 distances in **5** are 3.713 and 4.213 Å and probably too long for a meaningful interaction (the sum of van der Waals radii of Rh−N and Rh−O are 3.6 and 3.5 Å).[35] A related conformation was reported from the results of single-crystal X-ray diffraction studies of $Tp^{3R,5R}Rh(CO)_2$ (R = Me or CF_3) and $Tp^{4\text{-}tBu\text{-}3,5\text{-}Me2}Rh(CO)_2$, in which the noncoordinated pyrazolyl is located in the axial position of the boat, above the coordination plane of the rhodium center; however, in the pyrazolylborate case, the pyrazolyl plane and square plane are orthogonal.[16,36] $Tp^*Ir(\eta^4\text{-}C_8H_{12})$ adopts a conformation in the solid state in which the noncoordinated pyrazole is axial, but this is attributed to steric repulsions of the 5-methyl groups.[37] This literature compound is fluxional. Moreover, the coordination of the ancillary ligand in $Tp^*Rh(CO)_2$ is proposed to be $\kappa^{2,5}$, and this configuration is suggested to be essential for the C−H bond oxidative addition chemistry of that complex.

In fact, an interesting pattern emerges upon analysis of the ancillary ligands' solid-state conformations in comparison to the fluxionality of the complexes. As noted above, carbonyl compounds **5** and **7** are fluxional from 190 to 298 K, whereas the cyclooctadiene compounds are not fluxional at room temperature. Thus, the conformations in the solid state and the rates of oxazoline exchange are similarly partitioned by the ancillary cyclooctadiene or carbon monoxide ligands. Likewise, the $To^{M}Rh(\eta^4\text{-}C_8H_{12})$ (**8**) is nonfluxional at room temperature (400 MHz), while $To^{M}Rh(CO)_2$ is highly fluxional under the same conditions.

The $M-C_{NHC}$ distances in compounds **3**−**7** are equivalent within 3σ, and apparently the imidazole N-substituent and the ancillary ligand do not influence this interaction (Table 2). Also, the $M-N_{oxazoline}$ distances are similar in compounds **3**−**8**. A large and systematic *trans* influence of the NHC donor is observed, such that the metal−carbon bonds *trans* to the carbene moiety are longer than the bonds *trans* to the oxazoline donor. This observation is consistent with observations for carbene-imine-supported compounds, in which the *trans* influence of carbene is greater than that of the imine donor.[38]

Cyclooctene Group 9 Precursors Give Nonanalogous Rh(III) and Ir(III) Products. Interestingly, the products

dx.doi.org/10.1021/om500891h | *Organometallics* 2014, 33, 6840−6860

Table 2. Characteristic Interatomic Distances in Compounds 3−8

compound	M−C_{NHC} [a]	M−N [a]	M−$C_{trans\ to\ NHC}$ [a]	M−$C_{trans\ to\ N}$ [a]
{**1**}Rh(C_8H_{12}) (**3**)	2.063(5)	2.121(4)	2.208(4), 2.173(5)	2.116(5), 2.147(5)
{**2**}Rh(C_8H_{12}) (**4**)	2.051(7)	2.132(6)	2.198(7), 2.189(7)	2.139(8), 2.105(8)
{**2**}Rh(CO)$_2$ (**5**)	2.062(3)	2.087(2)	1.896(4)	1.836(2)
{**2**}Ir(C_8H_{12}) (**6**)	2.069(3)	2.116(2)	2.192(3), 2.161(3)	2.124(3), 2.126(3)
{**2**}Ir(CO)$_2$ (**7**)	2.075(3)	2.085(2)	1.891(3)	1.836(3)
To^{M}Rh(C_8H_{12}) (**8**)	n.a.	2.116(6)	n.a.	2.099(9), 2.12(1)

[a]In angstroms (Å).

obtained from reactions of *in situ* generated K[**2**] with [Rh(μ-Cl)(η^2-C_8H_{14})$_2$]$_2$ or [Ir(μ-Cl)(η^2-C_8H_{14})$_2$]$_2$ are not isostructural, although both transformations involve formation of trivalent metal centers through oxidative addition reactions. The reaction of K[**2**] with 0.5 equiv of the rhodium starting material gives a red-brown solid that is difficult to purify. Recrystallization of the reaction product provides an interesting asymmetric dimer, {κ^4-PhB(Ox^{Me2})$_2$$Im^{Mes'}CH_2$}Rh($\mu$-H)($\mu$-Cl)Rh($\eta^2$-$C_8H_{14}$)$_2$ (**10**), in which only one PhB(Ox^{Me2})$_2$$Im^{Mes}$ ligand is present per two rhodium centers even though 2 equiv of K[**2**] were allowed to react with [Rh(μ-Cl)(η^2-C_8H_{14})$_2$]$_2$ in the initial exploratory experiments. An upfield signal in the ^{1}H NMR spectrum at −21.70 ppm revealed that a rhodium hydride formed, and the doublet of doublets splitting pattern indicated that the hydride interacts inequivalently with two rhodium centers ($^1J_{RhH}$ = 30 and 18 Hz). Four singlet resonances at 1.90, 1.28, 1.23, and 1.10 ppm were assigned to four inequivalent oxazoline methyl groups based on 2D NMR correlation spectroscopy and suggested a C_1-symmetric product. In addition, cyclooctene resonances were evident in the ^{1}H and ^{13}C{^{1}H} NMR spectra. Although the product is asymmetric, only two mesityl-derived signals at 2.23 and 2.08 ppm (3 H each) were observed. The missing mesityl methyl group was transformed into a Rh-CH_2-aryl moiety via a cyclometalation event and appeared as a multiplet at 2.80 ppm (2 H). Further evidence for cyclometalation was provided by a ^{1}H−^{13}C HMQC experiment, which showed a correlation between this ^{1}H NMR signal and a doublet in the ^{13}C{^{1}H} NMR spectrum at 12.78 ppm ($^1J_{RhC}$ = 21 Hz). The carbene is coordinated to a rhodium center based on its appearance as a doublet in the ^{13}C{^{1}H} NMR spectrum at 175.98 ppm ($^1J_{RhC}$ = 50 Hz).

In addition, both of the oxazoline groups are coordinated to rhodium. This assignment was based upon their ^{15}N NMR chemical shifts of −162 and −178 ppm, which were upfield of noncoordinated oxazoline (∼−125 ppm). Moreover, the groups disposed *trans* to these oxazolines are clearly not identical based on the different ^{15}N NMR chemical shifts of the oxazolines. The *trans* ligands, however, could not be assigned because cross-peaks to the other ligands bonded to rhodium, such as the upfield hydride signal, were not detected in the ^{1}H−^{15}N HMBC experiment. Thus, the PhB(Ox^{Me2})$_2$$Im^{Mes'}$$CH_2$ ligand is coordinated in a tetradentate fashion to rhodium having undergone a cyclometalation, a hydride is formed, the compound contains at least two rhodium centers, and cyclooctene ligands are present. Ultimately, the identity of **10** was clarified by a single-crystal X-ray diffraction study (Figure 7), and this allowed a rational ratio of reactants for a more efficient preparation based on the product's constitution (Scheme 2). The same product is obtained after longer reaction times (18 h) or heating at 60 °C.

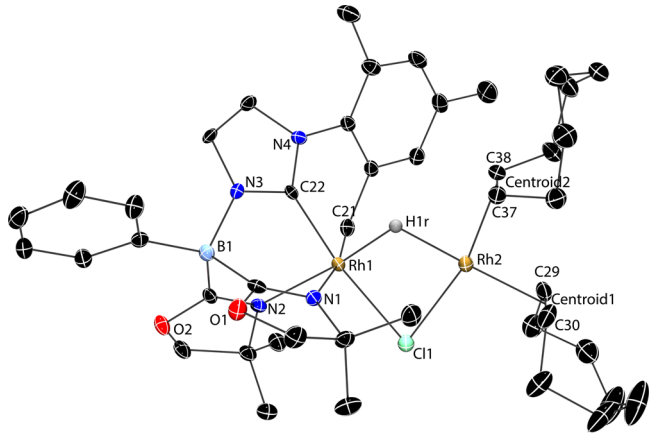

Figure 7. Rendered thermal ellipsoid plot of {κ^4-PhB(Ox^{Me2})$_2$$Im^{Mes'}$-$CH_2$}Rh($\mu$-H)($\mu$-Cl)Rh($\eta^2$-$C_8H_{14}$)$_2$ (**10**) with ellipsoids depicted at 35% probability. A disordered pentane and hydrogen atoms are not included in the representation, with the exception of the rhodium hydride, which was located in the Fourier difference map and refined isotropically. Selected interatomic distances (Å): Rh1−N1, 2.221(3); Rh1−N2, 2.110(3); Rh1−C21, 2.069(4); Rh1−C22, 1.941(4); Rh1−Cl1, 2.434(1); Rh1−H1r, 1.61(4); Rh1−Rh2, 2.8586(5); Rh2−Cl1, 2.363(1); Rh2−H1r, 1.81(5); Rh2−C29, 2.155(5); Rh2−C30, 2.154(5); Rh2−C37, 2.150(3); Rh2−C38, 2.158(3). Selected interatomic angles (deg): N1−Rh1−N2, 83.5(1); C22−Rh1−N1, 89.5(1); C22−Rh1−N2, 87.2(1); C22−Rh1−C21, 82.2(1); C22−Rh1−Rh2, 121.5(1); C21−Rh1−Rh2, 87.5(1); Rh2−Rh1−Cl1, 52.29(3); N1−Rh1−Cl1, 97.32(8); N2−Rh1−Cl1, 98.69(8); Rh1−Cl1−Rh2, 73.13(3); Rh1−Rh2−Cl1, 54.59(3).

Compound **10** has a unique structure that features two inequivalent rhodium centers with bridging hydride and chloride ligands. One rhodium center is bonded to six ligands, the C−H bond-cleaved mesityl methylene group, two oxazolines, the carbene, and bridging hydride and chloride groups; the other rhodium atom is bonded to two η^2-cyclooctenes in addition to the bridging ligands. The overall valence requirement of the Rh_2 dimer is four, creating possible valence assignments of the rhodium atoms as either Rh(I)/Rh(III) or Rh(II)/Rh(II). The Rh−Rh distance is 2.8586(5) Å, which is significantly longer than the distance in $Rh_2(OAc)_4$ of 2.386 Å.[39] In addition, **10** contains one six-coordinate rhodium center in a distorted octahedral configuration, while the second rhodium is four-coordinate square planar. The Rh1−Rh2 axis splits the bridging H and Cl ligands. Moreover, the Rh1−Cl1 (2.434(1) Å) and Rh2−Cl1 (2.363(1) Å) distances are inequivalent, as are the Rh1−H1r (1.61(4) Å) and Rh2−H1r (1.81(5) Å) distances. On the basis of these data, it is more appropriate to assign six-coordinate Rh1 as trivalent and Rh2 as monovalent, following an approach applied previously.[40] A search of the Cambridge Structural Database revealed eight dirhodium compounds bridged by chloride and hydride; however these were all symmetrical

dx.doi.org/10.1021/om500891h | *Organometallics* 2014, 33, 6840−6860

Scheme 2. Contrasting Reactions of $[M(\mu\text{-Cl})(\eta^2\text{-}C_8H_{14})_2]_2$ (M = Rh, Ir) with *in Situ* Generated K[2]

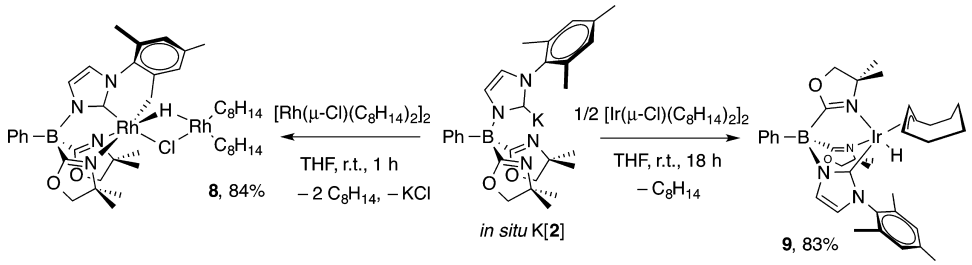

Rh(III)/Rh(III) dimers. Unlike most Rh(II)−Rh(II) compounds in which the square planar coordination is orthogonal to the Rh−Rh vector, the Rh(I) coordination plane contains the Rh−Rh vector. In addition, cyclometalations of IMes and I^{t}Bu (IMes = 1,3-bis(2,3,5-trimethylphenyl)imidazole-2-ylidene; I^{t}Bu = *N*,*N*-di(*tert*-butyl)imidazol-2-ylidene) are reported for their reactions with the same rhodium precursor used for **10**, namely, $[Rh(\mu\text{-Cl})(\eta^2\text{-}C_8H_{14})_2]_2$.[41] Cyclometalation of tris(pyrazolyl)borate rhodium and iridium are discussed below.

In contrast, the iridium system forms a yellow compound, $\{PhB(Ox^{Me2})_2Im^{Mes}\}IrH(\eta^3\text{-}C_8H_{13})$ (**11**) from K[**2**] and $[Ir(\mu\text{-Cl})(\eta^2\text{-}C_8H_{14})_2]_2$ after stirring overnight. Compound **11** is C_1-symmetric rather than C_s-symmetric, as evidenced by seven methyl resonances in the ^{1}H NMR spectrum. A resonance at −27.49 ppm was assigned to an iridium hydride, while a triplet at 4.90 ppm ($^3J_{HH}$ = 7.2 Hz, 1 H), a quartet at 4.09 ($^3J_{HH}$ = 8.4 Hz, 1 H), and a multiplet at 3.43 ppm (1 H, overlapped with CH_2 of the oxazoline ring) were assigned to the allyl protons on the C−H bond activated cyclooctene ring. The symmetry of the molecule suggests that the hydride is not *trans* to the carbene, as this configuration would produce a C_s-symmetric species. Instead, one of the oxazoline ligands is disposed *trans* to the iridium hydride, as evidenced by a correlation between the nitrogen signal at −184 ppm and the hydride resonance in a ^{1}H−^{15}N HMBC experiment. Unfortunately, signals associated with imidazole nitrogen were not detected in the ^{1}H−^{15}N HMBC spectrum.

There are a few other reported iridium allyl hydrides formed through metalation of an olefin upon coordination of a monoanionic tridentate *fac*-coordinating ligand, and these include $\{PhB(CH_2PR_2)_3\}$ (R = Ph, *i*-C_3H_7),[42,43] Tp,[44] and To^M.[45] Cp*RhH(C_3H_5) is formed by photolysis of Cp*Rh(η^2-C_3H_6)$_2$,[46] and the iridium analogue is synthesized by reduction of Cp*Ir(η^3-C_3H_5)Cl.[47] The hydride resonance of **11** at −27.49 ppm appeared further upfield than the other iridium allyl hydride compounds following the trend $\{PhB(CH_2PPh_2)_3\}IrH(\eta^3\text{-}C_8H_{13})$ (at −12.55 ppm)[42] > $\{PhB(CH_2P^iPr_2)_3\}IrH(\eta^3\text{-}C_8H_{13})$ (at −15.3 ppm)[43] > $\{PhB(CH_2P^iPr_2)_3\}IrH(\eta^3\text{-}C_3H_5)$ (at −15.60 ppm) > Cp*IrH(η^3-C_3H_5) (at −16.7) > TpIrH(η^3-C_8H_{13}) (at −18.10 ppm).[44] Attempts to synthesize To^{M}IrH(η^3-C_8H_{13}) were unsuccessful with K[To^M] or Li[To^M], but TlTo^M gives the product (δ_{IrH} = −28.54).[45] To^{M}RhH(η^3-C_8H_{13}) has a comparable hydride doublet at −24.27 ppm (in benzene-d_6, $^1J_{RhH}$ = 11.6 Hz).[45] In addition, a unique feature of **11** is that the ligands *trans* to the allyl group are inequivalent.

X-ray quality crystals of **11** are obtained from a concentrated benzene solution at room temperature. A single-crystal X-ray diffraction study of **11** confirms the C_1-symmetry of the complex and the configuration that disposes one of the oxazolines and the hydride ligand *trans* (Figure 8). The Ir−N

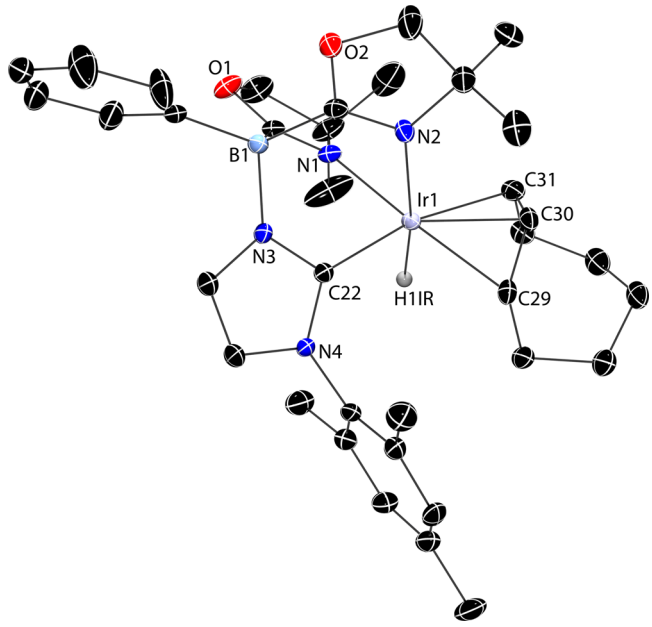

Figure 8. Rendered thermal ellipsoid plot of $\{PhB(Ox^{Me2})_2Im^{Mes}\}IrH(\eta^3\text{-}C_8H_{13})$ (**11**) with ellipsoids at 35% probability. H atoms are not plotted for clarity with the exception of the iridium hydride, which was located objectively on a difference Fourier map. Selected interatomic distances (Å): Ir1−N1, 2.286(2); Ir1−N2, 2.125(2); Ir1−C22, 2.029(3); Ir1−H1IR, 1.55(3); Ir1−C29, 2.183(3); Ir1−C30, 2.110(3); Ir1−C31, 2.278(4). Selected interatomic angles (deg): C22−Ir1−N1, 85.8(1); C22−Ir1−N2, 85.5(1); C22−Ir1−C29, 103.2(1); C22−Ir1−C30, 137.8(1); C22−Ir1−C31, 167.7(1); N1−Ir1−N2, 82.46(9).

distance *trans* to hydride (Ir1−N1, 2.286(2) Å) is elongated compared to the Ir−N bond *trans* to the allyl group (Ir1−N2, 2.125(2) Å). This is presumably due to the strong *trans* influence of the hydride ligand, as also observed in $\{PhB(CH_2PPh_2)_3\}IrH(\eta^3\text{-}C_8H_{13})$. Moreover, the allylic coordination of C_8H_{13} to the iridium center is also affected by the inequivalent donors. Within the [Ir]-(η^3-C_8H_{13}) interaction of **11**, the iridium−carbon distances vary (Ir1−C29, 2.183(3) Å; Ir1−C30, 2.110(3) Å; Ir1−C31, 2.278(4) Å). The allylic carbon (C31) *cis* to the oxazoline and pseudo-*trans* to the carbene has the longest iridium−carbon distance, whereas the carbon pseudo-*trans* to oxazoline is ca. 0.1 Å shorter. The mesityl group on the NHC is rotated to accommodate the C_8H_{13} group (C22−N4−C13−C14, 88.38°), while the oxazoline methyl groups are directed toward the C_8H_{13} ligand. Thus, the inequivalent allyl bonding may be a combination of complementary steric and electronic influences. The related Ir−C distances in $\{PhB(CH_2PPh_2)_3\}IrH(\eta^3\text{-}C_8H_{13})$ are longer than in **11** at 2.302(9), 2.176(8), and 2.261(9) Å.

dx.doi.org/10.1021/om500891h | *Organometallics* 2014, 33, 6840−6860

Scheme 3. Divergent Photochemical Reactivity of Rhodium and Iridium Congeners of $\{PhB(Ox^{Me2})_2Im^{Mes}\}M(CO)_2$

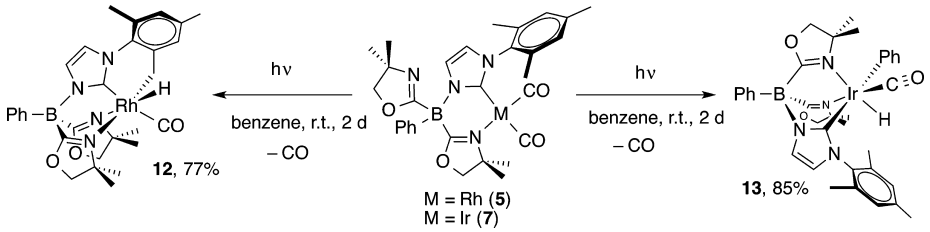

Photochemical Intra- and Intermolecular Oxidative Addition Reactions of $\{PhB(Ox^{Me2})_2Im^{Mes}\}M(CO)_2$ (M = Rh (5), Ir (7)). The metal dicarbonyl compounds **5** and **7** react under photolytic conditions in a Rayonet reactor (254 nm) to give inequivalent products. Photolysis of **5** in benzene-d_6 for 2 d provides cyclometalated rhodium hydride $\{\kappa^4\text{-}PhB(Ox^{Me2})_2(Im^{Mes'}CH_2)\}RhH(CO)$ as a yellow solid in 77% yield (**12**, Scheme 3). Compound **12** is persistent in solution even after extended photolysis, and the hydride resonance at −14.21 ppm ($^1J_{RhH}$ = 23.4 Hz) was observed in the ^{1}H NMR spectrum even at long reaction times in benzene-d_6. Unlike the symmetric-appearing fluxional starting material, the product's overall C_1-symmetry was indicated by the observation of six methyl signals for inequivalent oxazolines and the cyclometalated mesityl group. The diastereotopic cyclometalated CH_2 resonances appeared as a virtual triplet at 2.78 ppm.

In a ^{1}H−^{15}N HMBC experiment, two methyl signals at 0.90 and 1.02 ppm and the rhodium hydride provided cross-peaks to the same oxazoline nitrogen signal at −162 ppm. On the basis of this through-rhodium correlation, the rhodium hydride is assigned as *trans* to one of the oxazoline donors. The other two upfield methyl signals at 0.72 and 0.83 ppm (3 H each) correlated to a nitrogen signal at −171 ppm. The IR spectrum (KBr) contained bands at 2015 and 2064 cm^{-1} assigned to the carbonyl and hydride vibrations, respectively. An additional two absorptions at 1587 and 1568 cm^{-1} were assigned to the oxazoline ν_{CN}. Light yellow crystals of **12** are obtained from a pentane solution cooled at −30 °C. A single-crystal X-ray diffraction study confirms the proposed structure and reveals that the NHC and carbonyl ligands are disposed in a *trans* configuration, as are the mesityl-derived benzyl ligand and an oxazoline (Figure 9). The hydride (H1r), which was located and refined isotropically, is *trans* to one of the oxazolines; the Rh1−H1r distance is ca. 0.2 Å shorter than in the bridging hydride of dirhodium compound **10**.

The resulting compound contains three types of carbon-based ligands coordinated to rhodium in a meridonal fashion: an NHC, a carbonyl, and a benzyl group. The Rh−C distance associated with the benzyl ligand (Rh1−C21, 2.103(3) Å) is longer than the benzyl in **10** (Figure 7, Rh1−C21, 2.069(4) Å) and the previously reported Rh(IMes)(H)(IMes′)Cl (2.079(2) Å).[41c] The intramolecular C−H bond activation on the substituent of the imidazole ring has been reported for thermal activation for both rhodium and iridium complexes.[41,48] In addition, thermal and photolytic conditions can lead to intramolecular C−H bond cleavage of tris(pyrazolyl)borate ligands in rhodium and iridium compounds.[49] For instance, optically active $Tp^{Menth}Rh(CO)_2$ (Tp^{Menth} = tris(7*R*-isopropyl-4*R*-methyl-4,5,6,7-tetrahydroindazolyl)borate) undergoes cyclometalation upon photolysis.[49a]

In contrast to the intramolecular C−H bond oxidative addition observed with rhodium, the iridium dicarbonyl (**7**) reacts under photolytic conditions over 2 d with the benzene solvent to give an intermolecular metalated product, $\{PhB(Ox^{Me2})_2Im^{Mes}\}IrH(Ph)CO$ (**13**), in 85% yield. Further UV photolysis of isolated **13** leads to a complicated mixture of unidentified species. In addition, compound **7** decomposes in methylene chloride under photolytic conditions, and apparently the cyclometalated iridium analogue of **12** is not accessible under these conditions. Although the photolytic chemistry is not clean in methylene chloride, the benzene-activated product **13** is persistent in methylene chloride-d_2. In the ^{1}H NMR spectrum of **13** in methylene chloride-d_2, a singlet

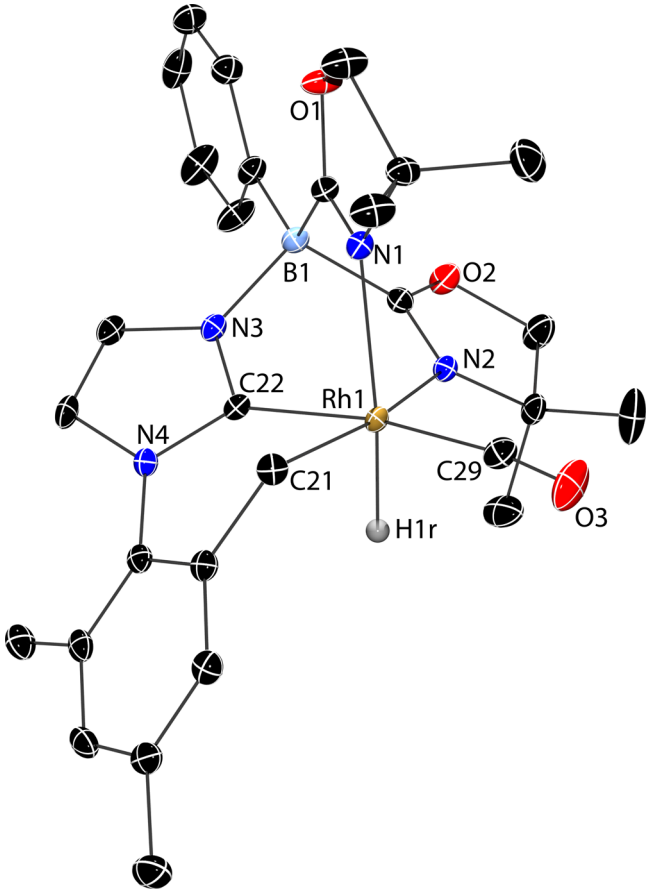

Figure 9. Rendered thermal ellipsoid plot of $\{\kappa^4\text{-}PhB(Ox^{Me2})_2Im^{Mes'}CH_2\}RhH(CO)$ (**12**) with ellipsoids at 35% probability. With the exception of the hydrogen bonded to rhodium, which was located in the Fourier difference map and refined isotropically, H atoms are not plotted for clarity. Selected interatomic distances (Å): Rh1−N1, 2.191(2); Rh1−N2, 2.147(2); Rh1−C21, 2.106(3); Rh1−C22, 2.016(3); Rh1−C29, 1.882(3); Rh1−H1r, 1.44(3). Selected interatomic angles (deg): C22−Rh1−N1, 85.05(8); C22−Rh1−N2, 86.76(9); N1−Rh1−N2, 83.04(8); C21−Rh1−C22, 81.0(1); C21−Rh1−C29, 89.5(1).

dx.doi.org/10.1021/om500891h | *Organometallics* 2014, 33, 6840−6860

at −16.51 ppm was assigned to the iridium hydride. All seven methyl groups were inequivalent in the C_1-symmetric complex. The $^1H-^{15}N$ HMBC experiment showed a correlation between the hydride and the nitrogen signal at −182 ppm, suggesting that this oxazoline ring is *trans* to hydride. However, a $^1H-^{13}C$ HMBC experiment revealed two strong cross-peaks between the hydride and carbon signals at 139.32 and 171.70 ppm and a faint correlation to a ^{13}C NMR signal at 170.07 ppm. The signal at 139.32 ppm was assigned to *ipso*-IrC_6H_5, while the signal at 170.07 ppm, which also correlated to the 4-H and 5-H signals of the $N_2C_3H_2Mes$, was assigned to the carbene carbon on the imidazole ring, and the signal at 171.70 ppm was assigned to the carbon atom in the carbonyl group. These multiple correlations to the iridium hydride resonance complicate the assignments of the iridium center's configuration, although the carbonyl, phenyl group, and hydride are most likely *fac* disposed.

The iridium center's configuration in **13** is unambiguously determined by a single-crystal X-ray diffraction study (Figure 10),

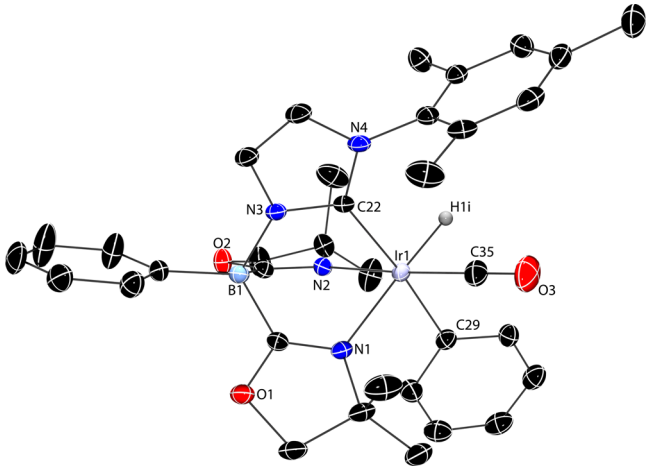

Figure 10. Rendered thermal ellipsoid plot of {PhB(Ox^{Me2})$_2$Im^{Mes}}-IrH(Ph)CO (**13**) with ellipsoids at 35% probability. H atoms are not plotted for clarity. The Ir1−H1i was located in the Fourier difference map and fixed without refinement. Selected interatomic distances (Å): Ir1−C22, 2.84(4); Ir1−N1, 2.182(3); Ir1−N2, 2.136(3); Ir1−C29, 2.101(4); Ir1−C35, 1.813(5); Ir1−H1i, 1.67. Selected interatomic angles (deg): C22−Ir1−N1, 85.1(1); C22−Ir1−N2, 84.0(1); N1−Ir1−N2, 85.8(1); C22−Ir1−C35, 97.4(2); C29−Ir1−C35, 88.6(2); C29−Ir1−C35, 88.6(2); C22−Ir1−C29, 173.9(1).

which shows that the phenyl and NHC ligands are *trans*, one oxazoline and the hydride are *trans*, and the second oxazoline and carbonyl are *trans* in an overall distorted octahedral geometry. This configuration is remarkable because all the other monometallic rhodium(III) and iridium(III) compounds reported here contain the neutral donor ligand *trans* to the NHC. In cyclometalated **12**, the NHC and metalated mesityl are geometrically required to be *cis* because the groups are connected through the multidentate ligand. However, in the silyl compounds described below, that geometric constraint is lifted but the carbene and the two electron-donor π-acid ligands remain *trans*.

Compound **13** is one of the few examples of crystallographically characterized rhodium or iridium complexes with the hydride, the hydrocarbyl, and a third ancillary group *fac*-coordinated to the metal. To the best of our knowledge, the only other example is the carbene-stabilized compound Tp*IrH(C_6H_5)(C_5H_3MeNH) (C_5H_3MeNH = pyridylidene),[50] in which the hydride, the phenyl, and the pyridylidene are *fac*-coordinated to iridium and formed from heterolytic addition of H_2 to an iridium(III) 2-pyridyl phenyl compound and not from C−H bond oxidative addition. The air-stable iridium vinyl hydride {HBPf$_3$}IrH(C_2H_3)CO (HBPf$_3$ = tris(3-trifluoromethyl-5-methylpyrazol-1-yl)borate) is also stabilized relative to its monovalent η^2-C_2H_4 isomer.[13a] For comparison in the To^{M}Rh(CO)$_2$-catalyzed photochemical decarbonylation chemistry in benzene-d_6, extensive H/D exchange suggests that reversible C−H oxidative addition/reductive elimination occurs from To^{M}RhH(Ph)CO. Likewise To^{M}RhH(η^3-C_8H_{13}) reacts by reductive elimination in the presence of alcohols.[45] The cyclopentadienyl rhodium(III) alkyl hydride compounds are also unstable with respect to hydrocarbon reductive elimination and form dimeric $Cp_2Rh_2(CO)_3$.[51] Typically, rhodium and iridium hydrocarbyl hydride compounds such as Tp*RhH(Ph)CO that are formed from C−H bond oxidative addition are converted into halide complexes for isolation.[8,52] Examples of *trans*-[Ir](H)Ph are more common, presumably because C−H reductive elimination is less facile with *trans*-disposed ligands.[53]

Thus, in two instances, the rhodium precursor reacts via cyclometalation of the *ortho*-methyl of the mesityl-imidazole, whereas the iridium congener reacts with the C−H bond of a substrate (either benzene or cyclooctene). We have not yet observed the reductive elimination reaction of either of the cyclometalated rhodium compounds into a tridentate monoanionic *C,N,N*-coordinating ligand, and a few reactions provide compound **12**. The tendency for **10** and **12** to form from a few different conditions and a few starting materials may reflect a thermodynamic preference of the cyclometalated structure for rhodium with PhB(Ox^{Me2})$_2$Im^{Mes}. Attempts to generate the cyclometalated iridium analogue have been unsuccessful.

Oxidative Addition of Phenylsilane. Synthesis and Characterization of {PhB(Ox^{Me2})$_2$Im^{Mes}}RhH(SiH$_2$Ph)CO (14). Complex **5** and $PhSiH_3$ react at room temperature to give a clean and isolable rhodium silyl complex, {PhB(Ox^{Me2})$_2$Im^{Mes}}-RhH(SiH_2Ph)CO (**14**). The yellow-brown solution leads to the isolation of **14** as a brown solid after evaporation of solvent and volatiles (eq 6). In contrast, To^{M}Rh(CO)$_2$ and $PhSiH_3$ are the

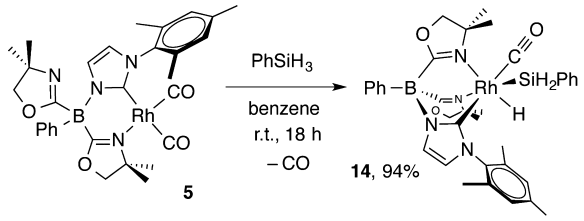

(6)

only species detected by ^1H NMR spectroscopy even at elevated temperature (60 °C) for extended time (24 h). In addition, the rhodium cyclooctadiene compounds **3** and **4** remain unchanged after heating at 120 °C in the presence of $PhSiH_3$, Ph_2SiH_2, $PhMeSiH_2$, and Mes_2SiH_2. Also, the reaction of iridium carbonyl congener **7** and $PhSiH_3$ affords a mixture of unidentified products. Secondary silanes such as Mes_2SiH_2, Ph_2SiH_2, and $PhMeSiH_2$ do not react with **5** even at elevated temperature. In fact, the lack of phenylsilane redistribution and/or polymerization is unusual given the tendency for rhodium to catalyze these processes.[54,55]

The reaction of eq 6 occurs under ambient light and in the dark, and it is complete after 1 h at 60 °C in the dark. This reactivity also contrasts with the reactions of Cp^{R}Rh(CO)$_2$ (Cp^R = C_5H_5, C_5H_4Me, C_5Me_5) and Et_3SiH, which require

dx.doi.org/10.1021/om500891h | Organometallics 2014, 33, 6840−6860

photolytically activated CO dissociation.[56] Most likely, CO dissociation requires hydrosilane preassociation because **5** persists in benzene and thermal C−H bond activation (e.g., of benzene solvent) by **5** is not detected. Although thermal C−H bond oxidative addition chemistry of Tp*RhL_2 monovalent systems is known, such reactivity typically requires a labile ligand such as ethylene.[57]

Evidence for phenylsilane oxidative addition was provided by a rhodium hydride resonance at −13.22 ppm in the ^{1}H NMR spectrum, which appeared as a doublet of doublets resulting from rhodium and silicon-hydride coupling ($^1J_{RhH}$ = 21 Hz; $^3J_{HH}$ = 1.2 Hz). As in the C_1-symmetric compounds described above, a combination of 1D NMR and 2D correlation spectroscopy suggested that oxazoline and hydride are disposed *trans*. Two doublets at 4.43 and 4.91 ppm (1 H each; $^2J_{HH}$ = 6.0 Hz; $^1J_{SiH}$ = 170 and 188 Hz) were assigned to the diastereotopic silicon hydrides. The ^{13}C{^{1}H} NMR spectrum of **14** contained a doublet at 194.53 ppm that was assigned to the carbene 2-C ($^1J_{RhC}$ = 51 Hz). Likewise, the carbonyl carbon signal appeared as a doublet at 178.39 ppm ($^1J_{RhC}$ = 41 Hz). The IR spectrum (KBr) showed a broad peak at 1593 cm^{-1} associated with the CN stretching mode, peaks at 2064 and 2016 cm^{-1} assigned to the ν_{RhH} and ν_{CO}, and one band at 1998 cm^{-1} for the ν_{SiH}. The ν_{CO} and ν_{RhH} were assigned by comparison with the cyclometalated Rh(III) hydrido carbonyl **12**, which contains a RhH and carbonyl and similar IR peaks at 2064 and 2015 cm^{-1} but lacks both the SiH_2Ph group and the IR band at 1998 cm^{-1} and by comparison with the IR spectrum of Tp*RhH($SiEt_3$)CO, which contained absorptions at 2086 (ν_{RhH}) and 2020 cm^{-1} (ν_{CO}).[11]

X-ray quality crystals of **14** are obtained from a concentrated pentane solution at −30 °C, and an ORTEP diagram is shown in Figure 11. The coordination environment of the rhodium center in **14** is related to that of cyclometalated **12**, with *trans* carbene/carbonyl ligands and *trans* oxazoline/hydride ligands; however, the cyclometalated mesityl of **12** is replaced with a silyl ligand in **14**. The strong *trans* influence of the silyl group on the rhodium-oxazoline interaction in **14** is evidenced by the longer Rh1−N2 distance of 2.206(5) Å versus the Rh1−N1 distance of 2.184(5) Å in **12**. The other rhodium−ligand distances (Rh1−CO, Rh1−$N1_{oxazoline}$, Rh1−$C22_{NHC}$) are similar for **12** and **14**.

Photolysis of **14** at 254 nm results in elimination of $PhSiH_3$ and formation of the cyclometalated **12** (eq 7). On a

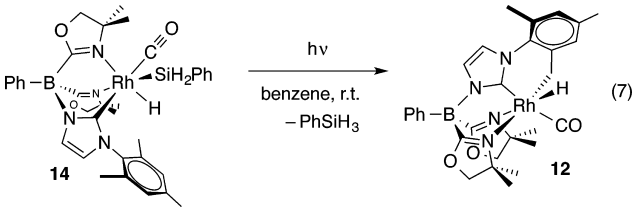

(7)

micromolar scale, the process takes 2 d to finish, which is as slow as the formation of **12** from **5**. This process appears to involve a sequence of reductive elimination of a Si−H bond followed by oxidative addition of the C−H bond on the basis of photolysis of **14**-d_3, which gives unlabeled **12**.

Synthesis and Characterization of {PhB(Ox^{Me2})$_2$Im^{Mes}}-Ir(CO)CN^{t}Bu (15). As noted above and in contrast to {PhB(Ox^{Me2})$_2$Im^{Mes}}Rh(CO)$_2$ (**5**), the reaction of iridium congener **7** and $PhSiH_3$ provides a mixture of products. Because **5** likely reacts with $PhSiH_3$ through an associative substitution

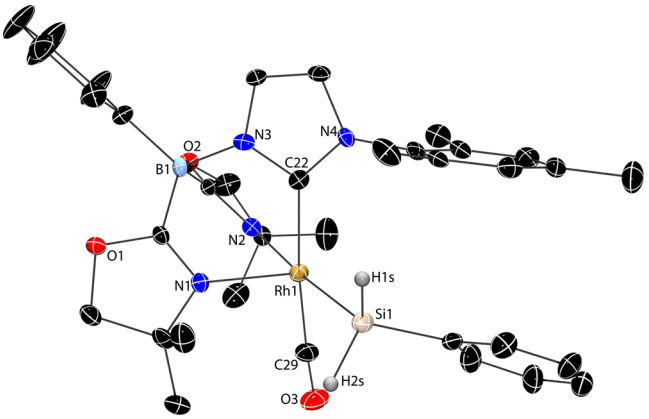

Figure 11. Rendered thermal ellipsoid plot of {PhB(Ox^{Me2})$_2$Im^{Mes}}-RhH(SiH_2Ph)CO (**14**) with ellipsoids drawn at 35% probability. A cocrystallized toluene solvent molecule and H atoms, with the exception of the SiH, are not plotted for clarity. The H1s and H2s were located objectively in a difference Fourier map and refined isotropically; however, the H1r was placed in a calculated position with a Rh1−H1r of 1.61 Å. Its temperature factor was set based on the rhodium atom and is not included in the illustration. Selected interatomic distances (Å): Rh1−N1, 2.184(5); Rh1−N2, 2.206(5); Rh1−C22, 2.068(5); Rh1−C29, 1.857(7); Rh1−Si1, 2.328(2). Selected interatomic angles (deg): C22−Rh1−N1, 85.7(2); C22−Rh1−N2, 84.2(2); N1−Rh1−N2, 85.2(2); N1−Rh1−C29, 99.4(3); N2−Rh1−C29, 97.3(2); N1−Rh1−Si1, 99.9(2); C22−Rh1−Si1, 95.1(2).

that precedes oxidative addition, the substitution of CO with other ligands was tested for the iridium compound. Complex **7** reacts with *tert*-butyl isocyanide in benzene to give {PhB(Ox^{Me2})$_2$Im^{Mes}}Ir(CO)CN^{t}Bu (**15**, eq 8). Under the photolytic

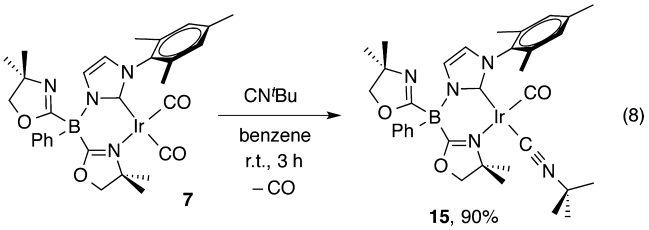

(8)

conditions in which the iridium dicarbonyl reacts with benzene, compound **15** decomposes to H[**2**].

The oxazoline groups appeared equivalent in ^{1}H NMR spectra of **15** acquired at 195 K to room temperature. The integration of the *tert*-butyl peak (9 H, relative to oxazoline methyl peaks being 6 H each) shows that only one carbonyl moiety is replaced by the isocyanide group. A ^{15}N NMR signal at −196 ppm was assigned to the isocyanide nitrogen on the basis of its correlation to the *tert*-butyl signal in a ^{1}H−^{15}N HMBC experiment. In the ^{15}N dimension, one signal (−154 ppm) correlated to the oxazoline protons and two signals (−176 and −188 ppm) correlated to imidazole protons. The IR spectrum (KBr) contained characteristic bands assigned to isocyanide (2144 cm^{-1}), CO (1973 cm^{-1}), and oxazoline ν_{CN} (1616 and 1579 cm^{-1}). Although the NMR and IR spectra suggest that compound **15** is four-coordinate square planar containing an axial noncoordinated oxazoline, the stereochemical disposition of the isocyanide group (*cis* or *trans* to NHC) was unknown.

X-ray quality crystals of **15** are obtained from a pentane solution cooled to −30 °C (Figure 12), and the single-crystal X-ray diffraction study reveals that the isocyanide ligand is

dx.doi.org/10.1021/om500891h | *Organometallics* 2014, 33, 6840−6860

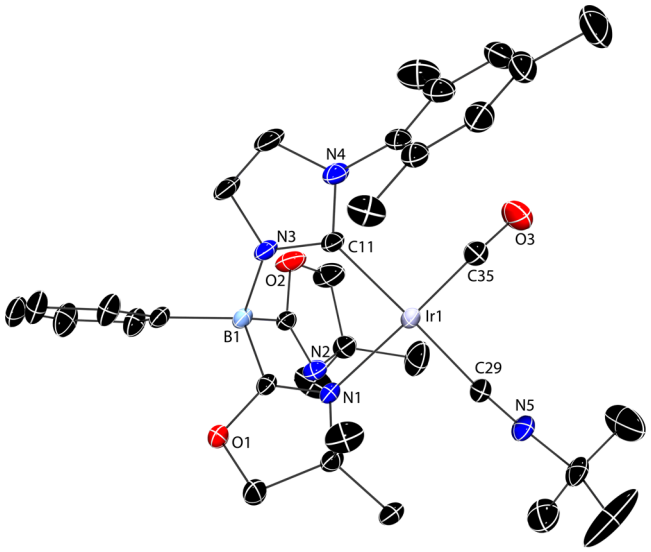

Figure 12. Rendered thermal ellipsoid plot of {PhB(Ox^{Me2})$_2$$Im^{Mes}$}-Ir(CO)C$N^t$Bu (**15**) with ellipsoids at 35% probability. A disordered benzene solvent molecule and H atoms are not plotted for clarity. Selected interatomic distances (Å): Ir1−C11, 2.052(2); Ir1−N1, 2.099(2); Ir1−C29, 1.955(2); Ir1−C35, 1.817(2). Selected interatomic angles (deg): C11−Ir1−N1, 85.22(7); N1−Ir1−C29, 94.12(7); C29−Ir1−C35, 87.05(9); C11−Ir1−C35, 93.41(9).

disposed *trans* to the NHC donor. The PhB(Ox^{Me2})Im^{Mes} ligand's conformation is similar to that of the dicarbonyl compounds, and this conformation was suggested by the fluxionality of the oxazoline donors as discussed above. The Ir−CN^tBu distance (*trans* to carbene, Ir1−C29, 1.955(2) Å) is longer than the Ir−CO distance (*trans* to oxazoline, Ir1−C35, 1.817(2) Å). In addition the Ir−CO distance in **15** is shorter than in **7** (*trans* to oxazoline, Ir1−C30, 1.836(3) Å).

Although oxazoline groups rapidly exchange in **15**, the substitution reaction of the carbonyl *trans* to the NHC donor is remarkably stereoselective, and only one stereoisomer is obtained. The selectivity suggests an associative substitution, as is typical in reactions of square planar d^8 compounds, but may also be related to unfavorable steric interactions between the mesityl substituent on the imidazole ring and the *tert*-butyl isocyanide in the unobserved stereoisomer. Still, this substitution reaction demonstrates the stronger *trans* effect of the carbene donor with respect to oxazoline, while the crystallographically determined structures of starting materials and products show the *trans* influence of the NHC donor.

The reaction of excess *tert*-butyl isocyanide and **7** results in the replacement of both carbonyl groups to give {PhB-(Ox^{Me2})$_2$$Im^{Mes}$}Ir(C$N^t$Bu)$_2$ (**16**). Because **7** is prepared from **4**, it is more convenient to add 2 equiv of CN^tBu to **4** to more directly obtain **16** (Scheme 4).

As in the dicarbonyl compounds, compound **16** is fluxional, and apparently rapid processes exchange oxazoline groups and isocyanide groups. Two oxazoline methyl singlets at 1.38 and 1.35 ppm (6 H each) were observed in the ^{1}H NMR spectrum that correlated to the oxazoline nitrogen signal at −154 ppm in a ^{1}H−^{15}N HMBC experiment. The *tert*-butyl isocyanide ligands exhibited one broad peak at 0.96 ppm (18 H), compared to a sharp singlet at 0.73 ppm in the ^{1}H NMR spectrum of **15**. The chemical shift of the *tert*-butyl group in **16** and free *tert*-butyl isocyanide were identical, and that signal increased in intensity upon addition of excess *tert*-butyl isocyanide, indicating that free and coordinated isocyanide undergo rapid exchange. The ^{1}H NMR spectrum of isolated **16** also contained a broad signal, and the two inequivalent isocyanides are not distinguished. However, both exchange processes are slower than the vibrational time scale because symmetric and asymmetric $\nu_{C\equiv N}$ bands were observed in the solid state (2124 and 2029 cm^{-1}) and in solution (2120 and 2028 cm^{-1}). In addition, coordinated and noncoordinated oxazoline bands are observed in the solid state (1616 and 1581 cm^{-1}) and in solution at 1617 and 1587 cm^{-1}. The solution-phase IR spectrum of **16** with 2 equiv of *tert*-butyl isocyanide revealed the $\nu_{C\equiv N}$ signals from **16** and an additional band from noncoordinated isocyanide at 2134 cm^{-1}. In addition, the two oxazoline ν_{CN} absorptions of the mixture of CN^tBu and **16** appeared at 1610 and 1564 cm^{-1}. These bands are lower in energy than the oxazoline ν_{CN} peaks in **16** alone, and perhaps this results from a transient associative interaction of CN^tBu and **16** in the mixture.

Thermal Oxidative Addition of $PhSiH_3$ to Form {PhB(Ox^{Me2})$_2$$Im^{Mes}$}IrH($SiH_2$Ph)C$N^t$Bu (17). In contrast to the mixture obtained in reactions of iridium dicarbonyl **7** and silanes, compound **15** reacts with phenylsilane at elevated temperature to give an isolable iridium silyl complex, {PhB(Ox^{Me2})$_2$$Im^{Mes}$}IrH($SiH_2$Ph)C$N^t$Bu (**17**; eq 9). Remarkably,

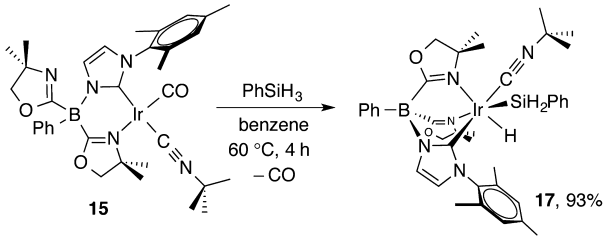

(9)

the carbonyl is replaced by the silyl and hydride ligands, rather than the isocyanide ligand, and the final crystallographically determined structure reveals that the isocyanide is *trans* to the carbene moiety.

As in the rhodium(III) carbonyl analogue, the hydride resonance at −18.76 ppm correlated with a nitrogen signal at −189 ppm in a ^{1}H−^{15}N HMBC experiment to establish their *trans* disposition. In the ^{1}H NMR spectrum, the diastereotopic

Scheme 4. Synthesis of {PhB(Ox^{Me2})$_2$$Im^{Mes}$}Ir(C$N^t$Bu)$_2$ (16)

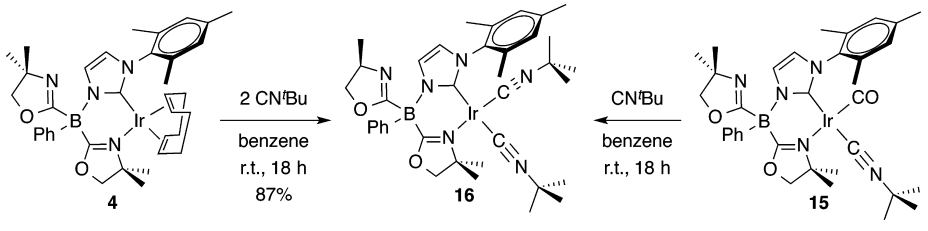

dx.doi.org/10.1021/om500891h | *Organometallics* 2014, 33, 6840−6860

SiH's appeared as doublet resonances at 4.10 and 4.61 ppm ($^1J_{SiH}$ = 169 and 155 Hz; $^2J_{HH}$ = 3.6 Hz). This observation is consistent with the formation of a stereogenic iridium center in a C_1-symmetric product. Moreover, the *tert*-butyl resonance at 0.92 ppm revealed that the isocynanide is not replaced in the reaction.

X-ray quality crystals of **17** are obtained from a concentrated benzene solution at room temperature, and the results are depicted in Figure 13. The *trans* hydride-oxazoline configurational

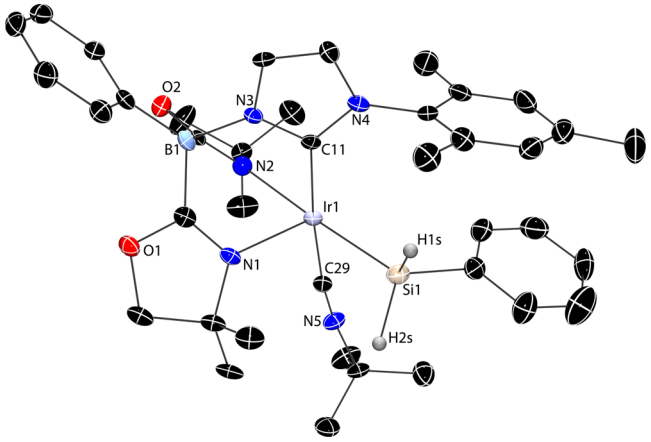

Figure 13. Rendered thermal ellipsoid plot of {PhB(Ox^{Me2})$_2$Im^{Mes}}-IrH(SiH$_2$Ph)CN^{t}Bu (**17**) with ellipsoids at 35% probability. H1s and H2s on Si1 are located objectively in the Fourier difference map, refined isotropically, and included in the plot. All other H atoms are placed in calculated positions, and the location of the H atom on Ir1 is not determined. Selected interatomic distances (Å): Ir1−N1, 2.191(5); Ir1−N2, 2.198(5); Ir1−C11, 2.060(8); Ir1−C29, 1.943(8); Ir1−Si1, 2.336(2). Selected interatomic angles (deg): C11−Ir1−N1, 86.5(2); C11−Ir1−N2, 84.4(2); N1−Ir1−N2, 83.0(2); N1−Ir1−C29, 97.9(3); N2−Ir1−C29, 98.4(3); N1−Ir1−Si1, 101.8(1); C11−Ir1−Si1, 97.5(2).

assignment suggested by ^{1}H−^{15}N correlation is confirmed by the diffraction experiment. Furthermore, the isocyanide and NHC donor are mutually *trans*.

CONCLUSION

This work has demonstrated that the substitution of an oxazoline donor in the tris(oxazolinyl)phenylborate ligand PhB(Ox^{Me2})$_3$ for an N-heterocyclic carbene donor in PhB(Ox^{Me2})$_2$Im^{Mes} has a significant effect on the reactivity of iridium and rhodium compounds. This effect has been evaluated through the comparison of the reactivity of a series of compounds supported by the related tris(oxazolinyl)borate ligand, as well as tris(pyrazolyl)-borate and cyclopentadienyl-coordinated group 9 metal complexes. The enhanced reactivity imparted by the PhB(Ox^{Me2})$_2$Im^{Mes} ligand is demonstrated by the thermal displacement of CO during the oxidative addition of Si−H bonds to rhodium(I) and iridium(I) centers. For comparison, oxidative additions of C−H and Si−H bonds to To^{M}Rh(CO)$_2$, TpRh(CO)$_2$, and CpM(CO)$_2$ require photochemically mediated CO dissociation. However, C−H bond activation by {PhB(Ox^{Me2})$_2$Im^{Mes}}M(CO)$_2$ requires photochemical activation, as well as higher energy and more intense light than the corresponding photochemical reactions of Tp*Rh(CO)$_2$. Currently, we are exploring the potential application of these compounds in catalytic thermal decarbonylation reactions given the enhanced reactivity toward CO dissociation. Thermal C−H oxidative additions that involve displacement of CO might facilitate transformations involving carbonylation of hydrocarbons or decarbonylations of oxygenates.

Presumably, the mechanisms of thermal oxidative addition of Si−H bonds and photochemical C−H bonds are different, and this is suggested by the inequivalent configurations of the products. In particular, photoinduced benzene metalation provides an [Ir](H)Ph species with Ph and NHC disposed *trans*, whereas thermal oxidative addition of Si−H gives [M](H)SiH$_2$Ph with both hydride and silyl ligands *trans* to weaker oxazoline donors. The reactivity of PhB(Ox^{Me2})$_2$Im^{Mes}-supported compounds may be attributed to the electron-donating ability of the carbene donor, which manifests itself in low-energy ν_{CO} stretching frequencies, systematic changes in ^{1}H and ^{13}C NMR chemical shifts and $^1J_{RhH}$ coupling constants, the *trans* influence evident in monovalent species, and the observed stereoselective substitution chemistry. The first point, regarding the electron-donating ability of the carbene-containing ligand, is that the CO stretching frequencies of the dicarbonyl compounds **5** and **7** appeared at similar energy to β-diketiminate dicarbonyl compounds and at lower energy than those of κ^2-To^{M}Rh(CO)$_2$ and κ^2-To^{M}Ir(CO)$_2$. Within the mixed oxazoline−carbene borate ligand, the carbene donor exhibits a stronger *trans* influence than the oxazoline. Interestingly, substitution reactions of **7** also show that the carbene donor has a greater *trans* effect on the substitution of CO donors than the oxazoline donor, as evidenced by reactions of **7** and isocyanide as well as the photochemical reaction of **7** and benzene. Detailed mechanistic investigations of thermal oxidative addition reactions of PhSiH$_3$ and **5** or **15**, as well as application of these compounds in catalytic Si−H addition chemistry, are currently under way.

In addition, the synthetic aspects of this work demonstrate the breadth and initial limitations of heavier group 9 centers supported by PhB(Ox^{Me2})$_2$Im^R monoanionic ligands. The mesityl-imidazole substitution provides a range of compounds that are promising for future transformations, mechanistic investigations, and catalysis, whereas the chemistry of the *tert*-butyl-imidazole derivative is currently limited. This limitation of PhB(Ox^{Me2})$_2$Im^{tBu} in rhodium and iridium chemistry is unexpected, given the successful application of bulkier PhB(Im^{tBu})$_3$ as a supporting ligand for smaller first-row metal centers such as iron.[20a] Alternative synthetic approaches for PhB(Ox^{Me2})$_2$Im^{tBu}H metalation reactions and other substitutions of oxazoline are currently under investigation based on the initial reaction chemistry reported here.

EXPERIMENTAL SECTION

General Procedures. All reactions were performed under a dry argon atmosphere using standard Schlenk techniques or under a nitrogen atmosphere in a glovebox, unless otherwise indicated. Benzene, toluene, methylene chloride, pentane, and tetrahydrofuran were dried and deoxygenated using an IT PureSolv system. Benzene-d_6, toluene-d_8, and tetrahydrofuran-d_8 were heated to reflux over Na/K alloy and vacuum transferred. Acetonitrile-d_3 and methylene chloride-d_2 were heated to reflux over CaH$_2$ and vacuum transferred. [PhB(Ox^{Me2})$_2$]$_n$,[24] 1-*tert*-butylimidazole,[58] 1-mesitylimidazole,[59] [PhB(Ox^{Me2})$_2$(Im^{Mes}H)-LiCl]$_2$ ((H[**2**]·LiCl)$_2$),[18] Tl[To^M],[9] [Rh(μ-Cl)(η^4-C$_8$H$_{12}$)]$_2$,[60] [Rh(μ-Cl)(η^2-C$_8$H$_{14}$)$_2$]$_2$,[61] [Rh(μ-Cl)(CO)$_2$]$_2$,[62] [Ir(μ-Cl)(η^4-C$_8$H$_{12}$)]$_2$, and [Ir(μ-Cl)(η^2-C$_8$H$_{14}$)$_2$]$_2$[63] were synthesized according to literature procedures. *tert*-Butyl isocyanide and phosphorus pentoxide were purchased from Sigma-Aldrich and stored inside a glovebox. Anhydrous sodium sulfate was purchased from Fisher Scientific and predried at 180 °C before use. Potassium benzyl was synthesized by

dx.doi.org/10.1021/om500891h | *Organometallics* 2014, 33, 6840−6860

reacting potassium *tert*-butoxide with ^{n}BuLi in toluene. Phenylsilane was synthesized by reduction of trichlorophenylsilane with $LiAlH_4$.

^{1}H, ^{13}C{^{1}H}, ^{11}B, ^{15}N, and ^{29}Si NMR spectra were collected on Avance II 600 or 700 MHz NMR spectrometers. NMR signals (^{1}H, ^{13}C, and ^{15}N) were assigned based on COSY, HMQC, and HMBC experiments. ^{15}N chemical shifts were determined by ^{1}H−^{15}N HMBC experiments. ^{15}N chemical shifts were originally referenced to an external liquid NH_3 standard and recalculated to the CH_3NO_2 chemical shift scale by adding −381.9 ppm. ^{29}Si chemical shifts were determined by ^{1}H−^{29}Si HMQC experiments and calibrated to an external standard of $PhSiH_3$ in a capillary (at −59 ppm). Infrared spectra were recorded on a Bruker Vertex spectrometer. Elemental analyses were performed using a PerkinElmer 2400 Series II CHN/S in the Iowa State Chemical Instrumentation Facility. Photolyses were performed in sealed storage vessels placed in a Rayonet photochemical reactor (model RPR-100) at an operating temperature of 35 °C at 254 nm and intensity of 1.65×10^{16} photon·s^{-1} cm^{-3}.

PhB(Ox^{Me2})$_2$(Im^{tBu}H)LiCl(THF) (H[1]·LiCl·THF). A 100 mL Schlenk flask was charged with $[PhB(Ox^{Me2})_2]_n$ (2.50 g, 8.80 mmol) and tetrahydrofuran (20 mL). 1-*tert*-Butylimidazole (1.09 g, 8.78 mmol) was added, and the solution was stirred at room temperature for 18 h. The clear yellow solution became cloudy after ca. 3 h. The resulting yellow suspension was filtered, and the solid was washed with pentane (2 × 20 mL) and dried *in vacuo* to afford the product as a yellowish solid (1.61 g, 3.96 mmol, 45.1%). ^{1}H NMR (acetonitrile-d_3, 600 MHz): δ 8.09 (s, 1 H, 2H-$N_2C_3H_3CMe_3$), 7.49 (s, 1 H, 4,5H-$N_2C_3H_3CMe_3$), 7.25−7.13 (m, 6 H, C_6H_5 (5 H) and 4,5H-$N_2C_3H_3CMe_3$ (1 H)), 3.71 (m, 4 H, CNCMe$_2$C*H*$_2$O), 3.63 (m, 4 H, THF), 1.79 (m, 4 H, THF), 1.58 (s, 9 H, CMe$_3$), 1.36 (s, 6 H, CNC*Me*$_2$CH$_2$O), 1.26 (s, 6 H, CNC*Me*$_2$CH$_2$O). ^{13}C{^{1}H} NMR (acetonitrile-d_3, 150 MHz): δ 180 (br, *C*NCMe$_2$CH$_2$O), 148 (br, *ipso*-C_6H_5), 136.18 (2C-$N_2C_3H_3CMe_3$), 133.31 (*o*-C_6H_5), 128.28 (*m*-C_6H_5), 127.10 (*p*-C_6H_5), 126.67 (4,5C-$N_2C_3H_3CMe_3$), 119.39 (4,5C-$N_2C_3H_3CMe_3$), 78.05 (CNCMe$_2$*C*H$_2$O), 68.26 (THF), 68.18 (CNCMe$_2$CH$_2$O), 59.22 (*C*Me$_3$), 29.96 (*C*Me$_3$), 28.70 (CNC*Me*$_2$CH$_2$O), 28.58 (CNC*Me*$_2$CH$_2$O), 26.19 (THF). ^{11}B NMR (acetonitrile-d_3, 192 MHz): δ −9.4. ^{15}N{^{1}H} NMR (acetonitrile-d_3, 61 MHz): δ −138 (CNCMe$_2$CH$_2$O), −178 (1N-$N_2C_3H_3CMe_3$), −184 (3N-$N_2C_3H_3CMe_3$). IR (KBr, cm^{-1}): 3089 w, 2964 m, 2928 m, 2883 m, 1624 s (CN), 1251 m, 1191 m, 1126 s, 991 m, 751 m. Anal. Calcd for $C_{27}H_{41}BClLiN_4O_3$: C, 62.14; H, 7.73; N, 10.74. Found: C, 62.11; H, 7.79; N, 10.72. Mp: 218−221 °C.

PhB(Ox^{Me2})$_2$(Im^{tBu}H) (H[1]). A 100 mL round-bottom flask was charged with PhB(Ox^{Me2})$_2$(Im^{tBu}H)LiCl(THF) (H[**1**]·LiCl·THF, 0.842 g, 1.61 mmol) and bench grade benzene (50 mL) in air. Water (160 μL, 8.88 mmol) was added, and the white suspension was stirred at room temperature in air for 18 h. The mixture became noticeably more transparent after ca. 3 h. The white suspension was stirred with Na_2SO_4 and then filtered, and the benzene solvent was evaporated to give a white solid. The white solid was redissolved in dry benzene (15 mL) in the glovebox and dried over P_2O_5 for 18 h. The mixture was filtered, and the solvent was evaporated. Trituration with pentane and drying *in vacuo* afforded the product as a white solid (0.591 g, 1.45 mmol, 89.9%). Spectral data are given in benzene-d_6, as well as in tetrahydrofuran-d_8 for comparison with the deprotonated product K[**1**]. ^{1}H NMR (benzene-d_6, 600 MHz): δ 9.55 (s, 1 H, 2H-$N_2C_3H_3CMe_3$), 8.02 (d, $^3J_{HH}$ = 7.2 Hz, 2 H, *o*-C_6H_5), 7.58 (s, 1 H, 4,5H-$N_2C_3H_3CMe_3$), 7.40 (t, $^3J_{HH}$ = 7.2 Hz, 2 H, *m*-C_6H_5), 7.22 (t, $^3J_{HH}$ = 6.6 Hz, 1 H, *p*-C_6H_5), 6.11 (s, 1 H, 4,5H-$N_2C_3H_3CMe_3$), 3.73 (d, $^2J_{HH}$ = 7.8 Hz, 2 H, CNCMe$_2$C*H*$_2$O), 3.68 (d, $^2J_{HH}$ = 7.8 Hz, 2 H, CNCMe$_2$C*H*$_2$O), 1.29 (s, 6 H, CNC*Me*$_2$CH$_2$O), 1.28 (s, 6 H, CNC*Me*$_2$CH$_2$O), 0.68 (s, 9 H, CMe$_3$). ^{1}H NMR (tetrahydrofuran-d_8, 600 MHz): δ 9.46 (s, 1 H, 2H-$N_2C_3H_3CMe_3$), 7.38 (d, $^3J_{HH}$ = 7.2 Hz, 2 H, *o*-C_6H_5), 7.34 (s, 1 H, 4,5H-$N_2C_3H_3CMe_3$), 7.29 (s, 1 H, 4,5H-$N_2C_3H_3CMe_3$), 7.02 (t, $^3J_{HH}$ = 7.2 Hz, 2 H, *m*-C_6H_5), 6.96 (t, $^3J_{HH}$ = 7.2 Hz, 1 H, *p*-C_6H_5), 3.58 (br, 4 H, CNCMe$_2$C*H*$_2$O, overlapping with tetrahydrofuran-d_8), 1.60 (s, 9 H, CMe$_3$), 1.16 (s, 6 H, CNC*Me*$_2$CH$_2$O), 1.15 (s, 6 H, CNC*Me*$_2$CH$_2$O). ^{13}C{^{1}H} NMR (benzene-d_6, 150 MHz): δ 179 (br, *C*NCMe$_2$CH$_2$O), 150 (br, *ipso*-C_6H_5), 136.91 (2C-$N_2C_3H_3CMe_3$), 134.33 (*o*-C_6H_5), 127.90 (*m*-C_6H_5), 127.76 (4,5C-$N_2C_3H_3CMe_3$), 126.48 (*p*-C_6H_5), 116.10 (4,5C-$N_2C_3H_3CMe_3$), 77.66 (CNCMe$_2$*C*H$_2$O), 68.00 (CNCMe$_2$CH$_2$O), 56.67 (*C*Me$_3$), 29.59 (CNC*Me*$_2$CH$_2$O), 29.45 (*C*Me$_3$), 29.44 (CNC*Me*$_2$CH$_2$O). ^{13}C{^{1}H} NMR (tetrahydrofuran-d_8, 150 MHz): δ 178.47 (br, *C*NCMe$_2$CH$_2$O), 149.43 (br, *ipso*-C_6H_5), 137.44 (2C-$N_2C_3H_3CMe_3$), 134.02 (*o*-C_6H_5), 127.33 (4,5C-$N_2C_3H_3CMe_3$), 127.06 (*m*-C_6H_5), 125.59 (*p*-C_6H_5), 116.94 (4,5C-$N_2C_3H_3CMe_3$), 77.46 (CNCMe$_2$*C*H$_2$O), 67.94 (CNCMe$_2$CH$_2$O), 57.91 (*C*Me$_3$), 29.94 (*C*Me$_3$), 29.13 (CNC*Me*$_2$CH$_2$O), 29.07 (CNC*Me*$_2$CH$_2$O). ^{11}B NMR (benzene-d_6, 192 MHz): δ −8.8. ^{11}B NMR (tetrahydrofuran-d_8, 192 MHz): δ −9.4. ^{15}N{^{1}H} NMR (benzene-d_6, 61 MHz): δ −125 (CNCMe$_2$CH$_2$O), −177 (3N-$N_2C_3H_3CMe_3$), −186 (1N-$N_2C_3H_3CMe_3$). ^{15}N{^{1}H} NMR (tetrahydrofuran-d_8, 61 MHz): δ −125 (CNCMe$_2$CH$_2$O), −183 ($N_2C_3H_3CMe_3$). IR (KBr, cm^{-1}): 3138 w, 3049 w, 2964 s, 2881 w, 1605 s (CN), 1423 w, 1359 w, 1259 m, 1189 m, 1114 s, 1017 m, 969 m, 801 w, 731 w, 697 w, 658 w. Anal. Calcd for $C_{23}H_{33}BN_4O_2$: C, 67.65; H, 8.15; N, 13.72. Found: C, 67.96; H, 8.11; N, 13.68. Mp: 120−123 °C.

K[PhB(Ox^{Me2})$_2$Im^{tBu}] (K[1]). This material was most conveniently generated *in situ*. Compound H[**1**] (0.0223 g, 0.0546 mmol) and potassium benzyl (0.072 g, 0.0553 mmol) were allowed to react in tetrahydrofuran-d_8 (0.50 mL). Instantaneously, a clear brown solution formed, which turned red and cloudy in 5 min. ^{1}H NMR (tetrahydrofuran-d_8, 600 MHz): δ 7.9 (br, 1 H, 5H-$N_2C_3H_2CMe_3$), 7.43−6.86 (m, C_6H_5, 4H-$N_2C_3H_2CMe_3$, and toluene), 3.48 (br, 4 H, CNCMe$_2$C*H*$_2$O), 2.31 (s, 9 H, CMe$_3$), 1.51 (s, 6 H, CNC*Me*$_2$CH$_2$O), 1.13 (br, 6 H, CNC*Me*$_2$CH$_2$O). ^{13}C{^{1}H} NMR (tetrahydrofuran-d_8, 150 MHz): δ 135.18 (2C-$N_2C_3H_2CMe_3$), 129.01 (4,5C-$N_2C_3H_2CMe_3$), 126.39 (4,5C-$N_2C_3H_2CMe_3$), 76.97 (CNCMe$_2$CH$_2$O), 30.73 (*C*Me$_3$), 28.89 (CNC*Me*$_2$CH$_2$O), 28.79 (CNC*Me*$_2$CH$_2$O). ^{11}B NMR (tetrahydrofuran-d_8, 192 MHz): δ −11.6.

PhB(Ox^{Me2})$_2$(Im^{Mes}H) (H[2]). The procedure for preparation of H[**2**] follows the one for H[**1**] described above, using [PhB(Ox^{Me2})$_2$(Im^{Mes}H)LiCl]$_2$ ([H[**2**]·LiCl]$_2$, 1.052 g, 2.051 mmol), 50 mL of bench grade benzene, and water (203 μL, 11.3 mmol). The white solid product was obtained in good yield (0.675 g, 1.44 mmol, 70.0%). ^{1}H NMR (benzene-d_6, 600 MHz): δ 9.06 (s, 1 H, 2H-$N_2C_3H_3$Mes), 8.04 (d, $^3J_{HH}$ = 7.2 Hz, 2 H, *o*-C_6H_5), 7.74 (s, 1 H, 4,5H-$N_2C_3H_3$Mes), 7.42 (t, $^3J_{HH}$ = 7.2 Hz, 2 H, *m*-C_6H_5), 7.25 (t, $^3J_{HH}$ = 7.2 Hz, 1 H, *p*-C_6H_5), 6.48 (s, 2 H, *m*-$C_6H_2Me_3$), 5.83 (s, 1 H, 4,5H-$N_2C_3H_3$Mes), 3.73 (d, $^2J_{HH}$ = 7.8 Hz, 2 H, CNCMe$_2$C*H*$_2$O), 3.69 (d, $^2J_{HH}$ = 7.8 Hz, 2 H, CNCMe$_2$C*H*$_2$O), 1.99 (s, 3 H, *p*-$C_6H_2Me_3$), 1.67 (s, 6 H, *o*-$C_6H_2Me_3$), 1.23 (s, 12 H, CNC*Me*$_2$CH$_2$O). ^{1}H NMR (tetrahydrofuran-d_8, 600 MHz): δ 8.84 (s, 1 H, 2H-$N_2C_3H_3$Mes), 7.49 (m, 3 H, *o*-C_6H_5 (2 H) and 4,5H-$N_2C_3H_3$Mes (1 H)), 7.09 (m, 3 H, *m*-C_6H_5 (2 H) and 4,5H-$N_2C_3H_3$Mes (1 H)), 7.04 (m, 3 H, *p*-C_6H_5 (1 H) and *m*-$C_6H_2Me_3$ (2 H)), 3.64 (br, 4 H, CNCMe$_2$C*H*$_2$O), 2.33 (s, 3 H, *p*-$C_6H_2Me_3$), 2.07 (s, 6 H, *o*-$C_6H_2Me_3$), 1.15 (s, 6 H, CNC*Me*$_2$CH$_2$O), 1.14 (s, 6 H, CNC*Me*$_2$CH$_2$O). ^{13}C{^{1}H} NMR (benzene-d_6, 150 MHz): δ 179 (br, *C*NCMe$_2$CH$_2$O), 149 (br, *ipso*-C_6H_5), 140.71 (2C-$N_2C_3H_3$Mes), 139.97 (*p*-$C_6H_2Me_3$), 135.37 (*ipso*-$C_6H_2Me_3$), 134.50 (*o*-C_6H_5), 132.74 (*o*-$C_6H_2Me_3$), 129.69 (*m*-$C_6H_2Me_3$), 128.00 (*m*-C_6H_5), 127.79 (4,5C-$N_2C_3H_3$Mes), 126.65 (*p*-C_6H_5), 119.48 (4,5C-$N_2C_3H_3$Mes), 77.94 (CNCMe$_2$*C*H$_2$O), 67.84 (CNCMe$_2$CH$_2$O), 29.56 (CNC*Me*$_2$CH$_2$O), 29.33 (CNC*Me*$_2$CH$_2$O), 21.21 (*p*-$C_6H_2Me_3$), 17.47 (*o*-$C_6H_2Me_3$). ^{13}C{^{1}H} NMR (tetrahydrofuran-d_8, 150 MHz): δ 179 (br, *C*NCMe$_2$CH$_2$O), 149 (br, *ipso*-C_6H_5), 141.45 (2C-$N_2C_3H_3$Mes), 140.68 (*p*-$C_6H_2Me_3$), 136.05 (*ipso*-$C_6H_2Me_3$), 134.53 (*o*-C_6H_5), 133.62 (*o*-$C_6H_2Me_3$), 130.00 (*m*-$C_6H_2Me_3$), 127.43 (4,5C-$N_2C_3H_3$Mes), 127.38 (*m*-C_6H_5), 126.05 (*p*-C_6H_5), 120.49 (4,5C-$N_2C_3H_3$Mes), 77.96 (CNCMe$_2$*C*H$_2$O), 67.94 (CNCMe$_2$CH$_2$O), 29.20 (CNC*Me*$_2$CH$_2$O), 29.08 (CNC*Me*$_2$CH$_2$O), 21.09 (*p*-$C_6H_2Me_3$), 17.58 (*o*-$C_6H_2Me_3$). ^{11}B NMR (benzene-d_6, 192 MHz): δ −8.3. ^{11}B NMR (tetrahydrofuran-d_8, 192 MHz): δ −11.0. ^{15}N{^{1}H} NMR (benzene-d_6, 61 MHz): δ −125 (CNCMe$_2$CH$_2$O), −174 (3N-$N_2C_3H_3$Mes), −206 (1N-$N_2C_3H_3$Mes). ^{15}N{^{1}H} NMR (tetrahydrofuran-d_8, 61 MHz): δ −127 (CNCMe$_2$CH$_2$O), −176 (3N-$N_2C_3H_3$Mes), −207 (1N-$N_2C_3H_3$Mes). IR (KBr, cm^{-1}): 3166 m, 3133 m, 3068 w, 2963 s, 1606 s (CN), 1532 s, 1133 s, 1066 s, 907 s, 801 m,

dx.doi.org/10.1021/om500891h | *Organometallics* 2014, 33, 6840−6860

737 s, 707 s. Anal. Calcd for $C_{28}H_{35}BN_4O_2$: C, 71.49; H, 7.50; N, 11.91. Found: C, 71.73; H, 7.48; N, 12.08. Mp: 149−152 °C.

K[PhB(Ox^{Me2})$_2$Im^{Mes}] (K[2]). As with K[**1**], K[**2**] is most conveniently generated *in situ*, and the data given here are from an *in situ* reaction. An X-ray quality crystal was obtained from benzene solution at room temperature; however, spectroscopic analysis of the supernatant revealed both H[**2**] and K[**2**]. H[**2**] (0.0257 g, 0.0546 mmol) and potassium benzyl (0.0072 g, 0.055 mmol) were allowed to react in tetrahydrofuran-d_8 (0.50 mL) to give a transparent brown solution. ^{1}H NMR (tetrahydrofuran-d_8, 600 MHz): δ 8.43 (s, 1 H, $N_2C_3H_2$Mes), 7.52 (d, $^3J_{HH}$ = 7.2 Hz, 2 H, *o*-C_6H_5), 7.00 (t, $^3J_{HH}$ = 7.2 Hz, 2 H, *m*-C_6H_5), 6.91 (t, $^3J_{HH}$ = 7.2 Hz, 1 H, *p*-C_6H_5), 6.86 (s, 2 H, *m*-$C_6H_2Me_3$), 6.61 (s, 1 H, $N_2C_3H_2$Mes), 3.47 (d, $^2J_{HH}$ = 7.8 Hz, 2 H, CNCMe$_2$CH_2O), 3.44 (d, $^2J_{HH}$ = 7.2 Hz, 2 H, CNCMe$_2$CH_2O), 2.26 (s, 3 H, *p*-$C_6H_2Me_3$), 1.99 (s, 6 H, *o*-$C_6H_2Me_3$), 1.09 (s, 6 H, CNCMe_2CH$_2$O), 1.07 (s, 6 H, CNCMe_2CH$_2$O). ^{13}C{^{1}H} NMR (tetrahydrofuran-d_8, 150 MHz): δ 183 (br, *C*NCMe$_2$CH$_2$O), 156 (br, *ipso*-C_6H_5), 141.62 (*p*-$C_6H_2Me_3$), 136.63 (*ipso*-$C_6H_2Me_3$), 136.42 (*o*-$C_6H_2Me_3$), 135.21 (*o*-C_6H_5), 129.07 (*m*-$C_6H_2Me_3$), 126.81 (4,5C-$N_2C_3H_2$Mes), 126.53 (*m*-C_6H_5), 124.58 (*p*-C_6H_5), 116.09 (4,5C-$N_2C_3H_2$Mes), 77.07 (CNCMe$_2$CH$_2$O), 67.95 (CNCMe$_2$CH$_2$O), 29.01 (CNCMe_2CH$_2$O), 28.94 (CNCMe_2CH$_2$O), 21.10 (*p*-$C_6H_2Me_3$), 18.32 (*o*-$C_6H_2Me_3$). ^{11}B NMR (tetrahydrofuran-d_8, 192 MHz): δ −11.6. ^{15}N{^{1}H} NMR (tetrahydrofuran-d_8, 61 MHz): δ −134 (CNCMe$_2$CH$_2$O), −170 ($N_2C_3H_2$Mes), −189 ($N_2C_3H_2$Mes).

{PhB(Ox^{Me2})$_2$Im^{tBu}}Rh(η^4-C$_8$H$_{12}$) (3). The compound PhB(Ox^{Me2})$_2$(Im^{tBu}H) (H[**1**], 0.127 g, 0.312 mmol) was dissolved in tetrahydrofuran (10 mL), and potassium benzyl (0.0495 g, 0.380 mmol) was added. This combination provided a transparent, but dark red solution, which became a pink opaque suspension upon stirring for 1 h at room temperature. Addition of [Rh(μ-Cl)(η^4-C_8H_{12})]$_2$ (0.0768 g, 0.156 mmol) gave a dark brown mixture, which was stirred for 1 h at room temperature. The solvent was removed *in vacuo*, and the residual solid was extracted with benzene (2 × 5 mL). The benzene extracts were combined, filtered, and evaporated to dryness. Trituration with pentane and *in vacuo* drying afforded the product as a yellow solid (0.156 g, 0.252 mmol, 80.8%). ^{1}H NMR (benzene-d_6, 600 MHz): δ 8.93 (br, 1 H, $N_2C_3H_2$CMe$_3$), 7.83 (d, $^3J_{HH}$ = 7.2 Hz, 2 H, *o*-C_6H_5), 7.43 (t, $^3J_{HH}$ = 7.2 Hz, 2 H, *m*-C_6H_5), 7.27 (t, $^3J_{HH}$ = 7.2 Hz, 1 H, *p*-C_6H_5), 6.65 (s, 1 H, $N_2C_3H_2$CMe$_3$), 4.93 (m, 1 H, C_8H_{12}), 4.35 (m, 1 H, C_8H_{12}), 3.66 (d, $^2J_{HH}$ = 7.2 Hz, 1 H, CN(Rh)CMe$_2$CH_2O), 3.58 (d, $^2J_{HH}$ = 8.4 Hz, 1 H, CN(Rh)CMe$_2$CH_2O), 3.54 (br, 3 H, CNCMe$_2$CH_2O (1 H) and C_8H_{12} (2 H)), 3.30 (d, $^2J_{HH}$ = 8.4 Hz, 1 H, CN(Rh)CMe$_2$CH_2O), 2.31 (m, 1 H, C_8H_{12}), 1.98 (m, 1 H, C_8H_{12}), 1.84 (m, 1 H, C_8H_{12}), 1.61 (s, 9 H, CMe$_3$), 1.45 (m, 1 H, C_8H_{12}), 1.40 (m, 1 H, C_8H_{12}), 1.33 (s, 3 H, CNCMe_2CH$_2$O), 1.23 (s, 3 H, CNCMe_2CH$_2$O), 1.12 (m, 2 H, C_8H_{12}), 0.90 (s, 3 H, CN(Rh)CMe_2CH$_2$O), 0.84 (s, 3 H, CN(Rh)CMe_2CH$_2$O), 0.78 (m, 1 H, C_8H_{12}). ^{13}C{^{1}H} NMR (benzene-d_6, 150 MHz): δ 189 (br, *C*N(Rh)CMe$_2$CH$_2$O), 181.06 (d, $^1J_{RhC}$ = 49.8 Hz, 2C-$N_2C_3H_2$CMe$_3$), 154 (br, CNCMe$_2$CH$_2$O), 179 (br, *ipso*-C_6H_5), 133.74 (*o*-C_6H_5), 128.92 (4,5C-$N_2C_3H_2$CMe$_3$), 127.89 (*m*-C_6H_5), 125.72 (*p*-C_6H_5), 117.62 (4,5C-$N_2C_3H_2$CMe$_3$), 88.61 (d, $^1J_{RhC}$ = 7.2 Hz, C_8H_{12}), 88.36 (d, $^1J_{RhC}$ = 8.1 Hz, C_8H_{12}), 80.29 (CN(Rh)-CMe$_2$CH$_2$O), 79.68 (d, $^1J_{RhC}$ = 13.7 Hz, C_8H_{12}), 77.13 (CNCMe$_2$CH$_2$O), 69.13 (d, $^1J_{RhC}$ = 12.8 Hz, C_8H_{12}), 68.29 (CNCMe$_2$CH$_2$O), 68.05 (CN(Rh)CMe$_2$CH$_2$O), 56.85 (*C*Me$_3$), 32.84 (*C*Me$_3$), 32.27 (C_8H_{12}), 31.69 (C_8H_{12}), 29.59 (C_8H_{12}), 29.38 (CNCMe_2CH$_2$O), 29.24 (CNCMe_2CH$_2$O), 28.39 (CN(Rh)-CMe_2CH$_2$O), 28.28 (CN(Rh)CMe_2CH$_2$O), 27.46 (C_8H_{12}). ^{11}B NMR (benzene-d_6, 192 MHz): δ −8.0. ^{15}N{^{1}H} NMR (benzene-d_6, 61 MHz): δ −123 (CNCMe$_2$CH$_2$O), −172 (1N-$N_2C_3H_2$CMe$_3$), −181 (3N-$N_2C_3H_2$CMe$_3$), −183 (CN(Rh)Me$_2$CH$_2$O). IR (KBr, cm^{-1}): 3128 w, 2962 s, 2928 s, 2870 s, 2823 m, 1613 s (CN), 1570 s (CN), 1463 m, 1370 m, 1262 m, 1197 s, 1152 s, 1123 m, 1019 m, 998 m, 977 s, 965 s, 734 s, 703 s, 688 w. Anal. Calcd for $C_{31}H_{44}BN_4O_2Rh$: C, 60.21; H, 7.17; N, 9.06. Found: C, 60.00; H, 7.65; N, 9.35. Mp: 201−202 °C.

{PhB(Ox^{Me2})$_2$Im^{Mes}}Rh(η^4-C$_8$H$_{12}$) (4). PhB(Ox^{Me2})$_2$(Im^{Mes}H) (H[**2**], 0.102 g, 0.217 mmol) and potassium benzyl (0.0341 g, 0.262 mmol) were allowed to react in tetrahydrofuran (10 mL) to give a transparent, yet dark red solution, which was stirred at room temperature for 1 h. Addition of [Rh(μ-Cl)(η^4-C_8H_{12})]$_2$ (0.0535 g, 0.109 mmol) provided a dark brown solution, which was stirred at room temperature for 1 h. A solid residue was obtained by evaporation of the volatile materials. Extraction with benzene (2 × 5 mL), evaporation of the benzene, trituration with pentane, and drying gave **4** as a yellow solid (0.127 g, 0.187 mmol, 86.2%). ^{1}H NMR (benzene-d_6, 600 MHz): δ 9.59 (s, 1 H, $N_2C_3H_2$Mes), 7.74 (d, $^3J_{HH}$ = 7.2 Hz, 2 H, *o*-C_6H_5), 7.42 (t, $^3J_{HH}$ = 7.2 Hz, 2 H, *m*-C_6H_5), 7.24 (t, $^3J_{HH}$ = 7.2 Hz, 1 H, *p*-C_6H_5), 6.84 (s, 1 H, *m*-$C_6H_2Me_3$), 6.62 (s, 1 H, *m*-$C_6H_2Me_3$), 6.32 (s, 1 H, $N_2C_3H_2$Mes), 4.67 (m, 1 H, C_8H_{12}), 4.48 (m, 1 H, C_8H_{12}), 3.75 (d, $^2J_{HH}$ = 7.8 Hz, 1 H, CNCMe$_2$CH_2O), 3.66 (d, $^2J_{HH}$ = 7.8 Hz, 1 H, CN(Rh)CMe$_2$CH_2O), 3.57 (d, $^2J_{HH}$ = 7.8 Hz, 1 H, CNCMe$_2$CH_2O), 3.52 (m, 1 H, C_8H_{12}), 3.31 (d, $^2J_{HH}$ = 8.4 Hz, 1 H, CN(Rh)CMe$_2$CH_2O), 3.11 (m, 1 H, C_8H_{12}), 2.39 (s, 3 H, *o*-$C_6H_2Me_3$), 2.12 (s, 3 H, *p*-$C_6H_2Me_3$), 1.93 (m, 1 H, C_8H_{12}), 1.87 (s, 3 H, *o*-$C_6H_2Me_3$), 1.57 (m, 1 H, C_8H_{12}), 1.52 (m, 1 H, C_8H_{12}), 1.40 (s, 3 H, CNCMe_2CH$_2$O), 1.38 (m, 1 H, C_8H_{12}), 1.23 (s, 3 H, CNCMe_2CH$_2$O), 1.19 (m, 4 H, C_8H_{12}), 1.02 (s, 3 H, CN(Rh)-CMe_2CH$_2$O), 0.87 (s, 3 H, CN(Rh)CMe_2CH$_2$O). ^{13}C{^{1}H} NMR (benzene-d_6, 150 MHz): δ 191 (br, *C*N(Rh)CMe$_2$CH$_2$O), 179.90 (d, $^1J_{RhC}$ = 51.5 Hz, 2C−$N_2C_3H_2$Mes), 178 (br, *C*NCMe$_2$CH$_2$O), 155 (br, *ipso*-C_6H_5), 138.53 (*p*-$C_6H_2Me_3$), 137.93 (*o*-$C_6H_2Me_3$), 136.14 (*ipso*-$C_6H_2Me_3$), 135.33 (*o*-$C_6H_2Me_3$), 133.72 (*o*-C_6H_5), 129.46 (*m*-$C_6H_2Me_3$), 129.37 (*m*-$C_6H_2Me_3$), 127.69 (4,5C-$N_2C_3H_2$Mes), 127.61 (*m*-C_6H_5), 125.67 (*p*-C_6H_5), 120.63 (4,5C-$N_2C_3H_2$Mes), 90.72 (d, $^1J_{RhC}$ = 7.7 Hz, C_8H_{12}), 87.89 (d, $^1J_{RhC}$ = 7.8 Hz, C_8H_{12}), 81.24 (CNCMe$_2$CH$_2$O), 77.00 (CN(Rh)CMe$_2$CH$_2$O), 75.22 (d, $^1J_{RhC}$ = 12.9 Hz, C_8H_{12}), 70.84 (d, $^1J_{RhC}$ = 13.1 Hz, C_8H_{12}), 68.40 (CNCMe$_2$CH$_2$O), 68.26 (CN(Rh)CMe$_2$CH$_2$O), 31.96 (C_8H_{12}), 31.32 (C_8H_{12}), 30.15 (C_8H_{12}), 29.50 (CNCMe_2CH$_2$O), 29.27 (CNCMe_2CH$_2$O), 28.63 (CN(Rh)CMe_2CH$_2$O), 28.00 (C_8H_{12}), 27.74 (CN(Rh)CMe_2CH$_2$O), 21.31 (*p*-$C_6H_2Me_3$), 20.52 (*o*-$C_6H_2Me_3$), 18.54 (*o*-$C_6H_2Me_3$). ^{11}B NMR (benzene-d_6, 192 MHz): δ −8.8. ^{15}N{^{1}H} NMR (benzene-d_6, 61 MHz): δ −125 (CNCMe$_2$CH$_2$O), −176 ($N_2C_3H_2$Mes), −182 (CN(Rh)CMe$_2$CH$_2$O), −191 ($N_2C_3H_2$Mes). IR (KBr, cm^{-1}): 3041 w, 2960 s, 2925 s, 2873 s, 2829 w, 1613 m (CN), 1576 m (CN), 1459 m, 1394 m, 1310 m, 1191 s, 1123 w, 1011 m, 990 s, 810 m, 731 s, 700 m. Anal. Calcd for $C_{36}H_{46}BN_4O_2Rh$: C, 63.54; H, 6.81; N, 8.23. Found: C, 63.43; H, 7.12; N, 8.27. Mp: 246−248 °C.

{PhB(Ox^{Me2})$_2$Im^{Mes}}Rh(CO)$_2$ (5). PhB(Ox^{Me2})$_2$(Im^{Mes}H) (H[**2**], 0.308 g, 0.655 mmol) and potassium benzyl (0.0939 g, 0.721 mmol) were allowed to react in tetrahydrofuran (10 mL) to form K[**2**] as above. [Rh(μ-Cl)(CO)$_2$]$_2$ (0.127 g, 0.328 mmol) was added to provide a dark green solution. The solution was stirred at room temperature for 1 h, the solvent was removed *in vacuo*, and the residue was extracted with benzene (2 × 5 mL). The benzene extracts were combined, filtered, and evaporated to give a solid. The solid was triturated with pentane and dried *in vacuo* to afford the product as a yellowish-green solid (0.366 g, 0.583 mmol, 89.0%). ^{1}H NMR (benzene-d_6, 600 MHz): δ 7.82 (m, 3 H, *o*-C_6H_5 (2 H) and $N_2C_3H_2$Mes (1 H)), 7.43 (t, $^3J_{HH}$ = 7.2 Hz, 2 H, *m*-C_6H_5), 7.27 (t, $^3J_{HH}$ = 7.2 Hz, 1 H, *p*-C_6H_5), 6.74 (s, 2 H, *m*-$C_6H_2Me_3$), 6.20 (s, 1 H, $N_2C_3H_2$Mes), 3.60 (m, 4 H, CNCMe$_2$CH_2O), 2.08 (s, 3 H, *p*-$C_6H_2Me_3$), 2.02 (s, 6 H, *o*-$C_6H_2Me_3$), 1.16 (s, 6 H, CNCMe_2CH$_2$O), 1.12 (s, 6 H, CNCMe_2CH$_2$O). ^{13}C{^{1}H} NMR (benzene-d_6, 150 MHz): δ 188 (br, *C*NCMe$_2$CH$_2$O), 186 (br, 2C-$N_2C_3H_2$Mes), 176.20 (d, $^1J_{RhC}$ = 45.0 Hz, CO), 149 (br, *ipso*-C_6H_5), 139.17 (*ipso*-$C_6H_2Me_3$), 137.36 (*p*-$C_6H_2Me_3$), 136.45 (*o*-$C_6H_2Me_3$), 134.70 (*o*-C_6H_5), 129.69 (*m*-$C_6H_2Me_3$), 127.84 (*m*-C_6H_5), 127.01 (4,5C-$N_2C_3H_2$Mes), 126.75 (*p*-C_6H_5), 120.50 (4,5C-$N_2C_3H_2$Mes), 78.94 (CNCMe$_2$CH$_2$O), 67.94 (CNCMe$_2$CH$_2$O), 29.03 (CNCMe_2CH$_2$O), 28.80 (CNCMe_2CH$_2$O), 21.37 (*p*-$C_6H_2Me_3$), 18.91 (*o*-$C_6H_2Me_3$). ^{11}B NMR (benzene-d_6, 192 MHz): δ −8.8. ^{15}N{^{1}H} NMR (benzene-d_6, 61 MHz): δ −153 (CNCMe$_2$CH$_2$O), −173 (3N-$N_2C_3H_2$Mes), −189 (1N-$N_2C_3H_2$Mes). IR (KBr, cm^{-1}): 3124 w, 3071 w, 3050 w, 2964 m, 2925 m, 2872 w, 2063 s (CO), 1993 s (CO), 1959 w, 1626 m (CN), 1564 m (CN), 1490 m, 1459 m, 1434 m, 1407 w, 1367 w, 1347 w, 1319 w, 1283 m, 1250 w, 1189 m, 1163 m, 1131 w, 1021 m, 988 w, 963 m, 853 w, 732 m, 701 m. Anal. Calcd for $C_{30}H_{34}BN_4O_4Rh$: C,

dx.doi.org/10.1021/om500891h | *Organometallics* 2014, 33, 6840−6860

57.35; H, 5.45; N, 8.92. Found: C, 57.36; H, 5.55; N, 9.38. Mp: 132−135 °C.

{PhB(Ox^{Me2})$_2$Im^{Mes}}Ir(η^4-C$_8$H$_{12}$) (6). PhB(Ox^{Me2})$_2$(Im^{Mes}H) (H[**2**], 0.307 g, 0.653 mmol) and potassium benzyl (0.102 g, 0.783 mmol) were stirred in tetrahydrofuran (10 mL) at room temperature for 1 h. [Ir(μ-Cl)(η^4-C$_8$H$_{12}$)]$_2$ (0.219 g, 0.326 mmol) was added to give a transparent red solution, which was stirred at room temperature for 1 h. The product was isolated following the procedure described for compound **4**, giving a red solid (0.442 g, 0.574 mmol, 87.9%). ^{1}H NMR (benzene-d_6, 600 MHz): δ 9.44 (s, 1 H, N$_2$C$_3$*H*$_2$Mes), 7.61 (d, $^3J_{HH}$ = 7.2 Hz, 2 H, *o*-C$_6$H$_5$), 7.37 (t, $^3J_{HH}$ = 7.2 Hz, 2 H, *m*-C$_6$H$_5$), 7.20 (t, $^3J_{HH}$ = 7.2 Hz, 1 H, *p*-C$_6$H$_5$), 6.80 (s, 1 H, *m*-C$_6$*H*$_2$Me$_3$), 6.63 (s, 1 H, *m*-C$_6$*H*$_2$Me$_3$), 6.35 (s, 1 H, N$_2$C$_3$*H*$_2$Mes), 4.35 (m, 1 H, C$_8$H$_{12}$), 4.08 (m, 1 H, C$_8$H$_{12}$), 3.73 (d, $^2J_{HH}$ = 7.8 Hz, 1 H, CNCMe$_2$C*H*$_2$O), 3.66 (d, $^2J_{HH}$ = 8.4 Hz, 1 H, CN(Ir)CMe$_2$C*H*$_2$O), 3.56 (d, $^2J_{HH}$ = 7.8 Hz, 1 H, CNCMe$_2$C*H*$_2$O), 3.33 (d, $^2J_{HH}$ = 8.4 Hz, 1 H, CN(Ir)CMe$_2$C*H*$_2$O), 3.20 (m, 1 H, C$_8$H$_{12}$), 2.90 (m, 1 H, C$_8$H$_{12}$), 2.27 (s, 3 H, *o*-C$_6$H$_2$*Me*$_3$), 2.11 (s, 3 H, *p*-C$_6$H$_2$*Me*$_3$), 1.92 (s, 3 H, *o*-C$_6$H$_2$*Me*$_3$), 1.81 (m, 1 H, C$_8$H$_{12}$), 1.54 (m, 1 H, C$_8$H$_{12}$), 1.38 (s, 3 H, CNC*Me*$_2$CH$_2$O), 1.32 (m, 1 H, C$_8$H$_{12}$), 1.21 (s, 6 H, CNC*Me*$_2$CH$_2$O (3 H) and C$_8$H$_{12}$ (3 H)), 1.03 (s, 4 H, CN(Ir)C*Me*$_2$CH$_2$O (3 H) and C$_8$H$_{12}$ (1 H)), 0.92 (s, 4 H, CN(Ir)C*Me*$_2$CH$_2$O (3 H) and C$_8$H$_{12}$ (1 H)). ^{13}C{^{1}H} NMR (benzene-d_6, 150 MHz): δ 193 (br, *C*N(Ir)CMe$_2$CH$_2$O), 178.33 (2C-N$_2$C$_3$H$_2$Mes), 177 (br, *C*NCMe$_2$CH$_2$O), 154 (br, *ipso*-C$_6$H$_5$), 138.31 (*ipso*-C$_6$H$_2$Me$_3$), 138.10 (*p*-C$_6$H$_2$Me$_3$), 136.09 (*o*-C$_6$H$_2$Me$_3$), 135.40 (*o*-C$_6$H$_2$Me$_3$), 133.18 (*o*-C$_6$H$_5$), 129.41 (*m*-C$_6$H$_2$Me$_3$), 129.35 (*m*-C$_6$H$_2$Me$_3$), 127.62 (*m*-C$_6$H$_5$), 127.05 (4,5C-N$_2$C$_3$H$_2$Mes), 125.61 (*p*-C$_6$H$_5$), 121.05 (4,5C-N$_2$C$_3$H$_2$Mes), 82.32 (CN(Ir)C*Me*$_2$CH$_2$O), 77.05 (CNC*Me*$_2$CH$_2$O), 75.66 (C$_8$H$_{12}$), 72.66 (C$_8$H$_{12}$), 69.29 (CN(Ir)*C*Me$_2$CH$_2$O), 68.36 (CNCMe$_2$CH$_2$O), 59.95 (C$_8$H$_{12}$), 56.37 (C$_8$H$_{12}$), 33.16 (C$_8$H$_{12}$), 31.52 (C$_8$H$_{12}$), 30.48 (C$_8$H$_{12}$), 29.48 (CNC*Me*$_2$CH$_2$O), 29.24 (CNC*Me*$_2$CH$_2$O), 29.19 (C$_8$H$_{12}$), 28.73 (CN(Ir)C*Me*$_2$CH$_2$O), 27.46 (CN(Ir)C*Me*$_2$CH$_2$O), 21.32 (*p*-C$_6$H$_2$*Me*$_3$), 20.44 (*o*-C$_6$H$_2$*Me*$_3$), 18.56 (*o*-C$_6$H$_2$*Me*$_3$). ^{11}B NMR (benzene-d_6, 192 MHz): δ −9.0. ^{15}N{^{1}H} (benzene-d_6, 61 MHz): δ −124 (CNCMe$_2$CH$_2$O), −178 (N$_2$C$_3$H$_2$Mes), −188 (CN(Ir)CMe$_2$CH$_2$O), −192 (N$_2$C$_3$H$_2$Mes). IR (KBr, cm^{-1}): 2960 s, 2923 s, 2872 m, 1611 m (CN), 1564 m (CN), 1461 m, 1384 m, 1363 m, 1194 m, 1134 m, 994 m, 965 m, 732 m, 701 m, 677 m. Anal. Calcd for C$_{36}$H$_{46}$BIrN$_4$O$_2$: C, 56.17; H, 6.02; N, 7.28. Found: C, 56.03; H, 6.36; N, 7.33. Mp: 242−245 °C.

{PhB(Ox^{Me2})$_2$Im^{Mes}}Ir(CO)$_2$ (7). {PhB(Ox^{Me2})$_2$Im^{Mes}}Ir(η^4-C$_8$H$_{12}$) (**6**, 0.407 g, 0.529 mmol) was dissolved in benzene (10 mL), the clear red solution was degassed three times, and the vessel was charged with 1 atm of CO. The solution turned yellow after 5 min. The flask was sealed, and the solution was stirred at room temperature for 3 h. The volatile materials were evaporated under reduced pressure, and the residue was triturated with pentane and dried *in vacuo* to afford the product as a yellow solid (0.273 g, 0.380 mmol, 71.8%). Although the combustion analysis gave a >0.5% difference between calculated and experimental values, derivatives of **7** gave the expected analysis (compounds **13** and **15**), and likely the difference results from imperfect combustion. ^{1}H NMR (benzene-d_6, 600 MHz): δ 7.81 (d, $^3J_{HH}$ = 7.8 Hz, 2 H, *o*-C$_6$H$_5$), 7.52 (s, 1 H, N$_2$C$_3$*H*$_2$Mes), 7.43 (t, $^3J_{HH}$ = 7.2 Hz, 2 H, *m*-C$_6$H$_5$), 7.27 (t, $^3J_{HH}$ = 7.2 Hz, 1 H, *p*-C$_6$H$_5$), 6.74 (s, 2 H, *m*-C$_6$*H*$_2$Me$_3$), 6.16 (s, 1 H, N$_2$C$_3$*H*$_2$Mes), 3.61 (d, $^2J_{HH}$ = 8.4 Hz, 2 H, CNCMe$_2$C*H*$_2$O), 3.58 (d, $^2J_{HH}$ = 8.4 Hz, 2 H, CNCMe$_2$C*H*$_2$O), 2.08 (s, 3 H, *p*-C$_6$H$_2$*Me*$_3$), 2.02 (s, 6 H, *o*-C$_6$H$_2$*Me*$_3$), 1.18 (s, 6 H, CNC*Me*$_2$CH$_2$O), 1.13 (s, 6 H, CNC*Me*$_2$CH$_2$O). ^{13}C{^{1}H} NMR (benzene-d_6, 150 MHz): δ 187 (br, *C*NCMe$_2$CH$_2$O), 179 (br, CO), 176.07 (2C-N$_2$C$_3$H$_2$Mes), 149 (br, *ipso*-C$_6$H$_5$), 139.43 (*p*-C$_6$H$_2$Me$_3$), 136.97 (*ipso*-C$_6$H$_2$Me$_3$), 136.53 (*o*-C$_6$H$_2$Me$_3$), 134.77 (*o*-C$_6$H$_5$), 129.75 (*m*-C$_6$H$_2$Me$_3$), 127.96 (*m*-C$_6$H$_5$), 126.96 (*p*-C$_6$H$_5$), 126.69 (4,5C-N$_2$C$_3$H$_2$Mes), 120.99 (4,5C-N$_2$C$_3$H$_2$Mes), 79.19 (CNCMe$_2$*C*H$_2$O), 68.75 (CN*C*Me$_2$CH$_2$O), 28.94 (CNC*Me*$_2$CH$_2$O), 28.58 (CNC*Me*$_2$CH$_2$O), 21.38 (*p*-C$_6$H$_2$*Me*$_3$), 18.95 (*o*-C$_6$H$_2$*Me*$_3$). ^{11}B NMR (benzene-d_6, 192 MHz): δ −8.7. ^{15}N{^{1}H} NMR (benzene-d_6, 61 MHz): δ −156 (CNCMe$_2$CH$_2$O), −173 (3N-N$_2$C$_3$H$_2$Mes), −187 (1N-N$_2$C$_3$H$_2$Mes). IR (KBr, cm^{-1}): 2964 w, 2872 w, 2053 s (CO), 1979 s (CO), 1612 w, 1551 w (CN), 1461 w, 1361 w, 1292 w, 1188 w, 967 m, 732 m, 703 m. Anal. Calcd for C$_{30}$H$_{34}$BIrN$_4$O$_4$: C, 50.21; H, 4.78; N, 7.81. Found: C, 50.84; H, 4.97; N, 8.47. Mp: 143−146 °C.

To^{M}Rh(η^4-C$_8$H$_{12}$) (8). Tl[To^M] (0.440 g, 0.749 mmol) and [Rh(μ-Cl)(η^4-C$_8$H$_{12}$)]$_2$ (0.189 g, 0.384 mmol) were allowed to react in benzene (20 mL) for 4 h at room temperature. The reaction mixture was filtered, the filtrate was evaporated, and the residue was extracted with benzene. The solvent was removed under reduced pressure to afford the product as a yellow solid (0.205 g, 0.345 mmol, 90.3%). ^{1}H NMR (benzene-d_6, 700 MHz): δ 7.77 (d, $^3J_{HH}$ = 6.4 Hz, 2 H, *o*-C$_6$H$_5$), 7.44 (t, $^3J_{HH}$ = 7.6 Hz, 2 H, *m*-C$_6$H$_5$), 7.29 (t, $^3J_{HH}$ = 7.6 Hz, 1 H, *p*-C$_6$H$_5$), 4.24 (br, 2 H, C$_8$H$_{12}$), 3.96 (br, 2 H, C$_8$H$_{12}$), 3.75 (s, 2 H, CNCMe$_2$C*H*$_2$O), 3.57 (s, 2 H, CNCMe$_2$C*H*$_2$O), 3.46 (s, 2 H, CNCMe$_2$C*H*$_2$O), 1.99 (br, 2 H, C$_8$H$_{12}$), 1.33 (br, 10 H C$_8$H$_{12}$ (4 H) and CNC*Me*$_2$CH$_2$O (6 H)), 1.08 (s, 8 H, C$_8$H$_{12}$ (2 H) and CNC*Me*$_2$CH$_2$O (6 H)), 0.72 (s, 6 H, CNC*Me*$_2$CH$_2$O). ^{13}C{^{1}H} NMR (benzene-d_6, 175 MHz): δ 193 (br, CNCMe$_2$CH$_2$O), 135.41 (*o*-C$_6$H$_5$), 127.83 (*m*-C$_6$H$_5$), 125.57 (*p*-C$_6$H$_5$), 81.79 (CNCMe$_2$CH$_2$O), 79.34 (C$_8$H$_{12}$), 77.40 (CNCMe$_2$CH$_2$O), 75.65 (C$_8$H$_{12}$), 68.47 (CNCMe$_2$CH$_2$O), 67.62 (CNCMe$_2$CH$_2$O), 30.83 (C$_8$H$_{12}$), 29.51 (CNC*Me*$_2$CH$_2$O and C$_8$H$_{12}$), 28.14 (CNC*Me*$_2$CH$_2$O), 27.56 (CNC*Me*$_2$CH$_2$O). ^{11}B NMR (benzene-d_6, 192 MHz): δ −16.3. IR (KBr, cm^{-1}): 3063 w, 3042 w, 2999 m, 2963 s, 2927 s, 2879 s, 2834 m, 1611 m (CN), 1567 s (CN), 1485 w, 1461 m, 1432 w, 1387 w, 1365 m, 1335 w, 1303 w, 1276 s, 1252 m, 1194 s, 1155 m, 1130 w, 995 s, 968 s, 894 w, 874 w, 838 w, 816 w, 775 w, 729 m, 704 m. Anal. Calcd for C$_{29}$H$_{41}$BN$_3$O$_3$Rh: C, 58.70; H, 6.96; N, 7.08. Found: C, 58.57; H, 6.77; N, 7.01. Mp: 180−185 °C (dec).

To^{M}Ir(η^4-C$_8$H$_{12}$) (9). Compound **9** was prepared following the procedure for the rhodium analogue, with Tl[To^M] (0.700 g, 1.19 mmol) and [Ir(μ-Cl)(η^4-C$_8$H$_{12}$)]$_2$ (0.411 g, 0.611 mmol) providing **9** (0.758 g, 1.11 mmol, 93.3%). ^{1}H NMR (benzene-d_6, 700 MHz): δ 7.62 (d, $^3J_{HH}$ = 6.4 Hz, 2 H, *o*-C$_6$H$_5$), 7.39 (t, $^3J_{HH}$ = 7.2 Hz, 2 H, *m*-C$_6$H$_5$), 7.24 (t, $^3J_{HH}$ = 7.2 Hz, 1 H, *p*-C$_6$H$_5$), 4.05 (br, 2 H, C$_8$H$_{12}$), 3.74 (br, 4 H, CNCMe$_2$C*H*$_2$O (2 H) and C$_8$H$_{12}$ (2 H)), 3.59 (s, 2 H, CNCMe$_2$C*H*$_2$O), 3.49 (s, 2 H, CNCMe$_2$C*H*$_2$O), 1.92 (br, 2 H, C$_8$H$_{12}$), 1.34 (s, 6 H, CNC*Me*$_2$CH$_2$O), 1.21 (br, 4 H, C$_8$H$_{12}$), 1.06 (s, 6 H, CNC*Me*$_2$CH$_2$O), 0.89 (br, 2 H, C$_8$H$_{12}$), 0.81 (s, 6 H, CNC*Me*$_2$CH$_2$O). ^{13}C{^{1}H} NMR (benzene-d_6, 175 MHz): δ 194.0 (br, *C*NCMe$_2$CH$_2$O), 152.99 (*ipso*-C$_6$H$_5$), 134.83 (*o*-C$_6$H$_5$), 127.75 (*m*-C$_6$H$_5$), 125.45 (*p*-C$_6$H$_5$), 82.98 (2 CNCMe$_2$*C*H$_2$O overlapped), 77.41 (CNCMe$_2$CH$_2$O), 68.62 (2 CNCMe$_2$CH$_2$O overlapped), 63.13 (C$_8$H$_{12}$), 59.61 (C$_8$H$_{12}$), 31.54 (2 C$_8$H$_{12}$ overlapped), 30.26 (C$_8$H$_{12}$), 29.51 (CNC*Me*$_2$CH$_2$O), 28.16 (CNC*Me*$_2$CH$_2$O), 27.15 (CNC*Me*$_2$CH$_2$O). ^{11}B NMR (benzene-d_6, 192 MHz): δ −16.4. IR (KBr, cm^{-1}): 3063 w, 3036 w, 3000 m, 2965 s, 2928 s, 2881 s, 2835 m, 1607 m (CN), 1558 s (CN), 1462 m, 1433 w, 1388 w, 1370 m, 1329 w, 1284 s, 1254 w, 1198 s, 1158 s, 1131 m, 1002 s, 967 s, 892 w, 875 w, 839 w, 817 w, 785 w, 739 m, 704 m. Anal. Calcd for C$_{29}$H$_{41}$BIrN$_3$O$_3$: C, 51.02; H, 6.05; N, 6.16. Found: C, 51.00; H, 5.53; N, 6.03. Mp: 175−180 °C.

{κ^4-PhB(Ox^{Me2})$_2$Im$^{Mes'}$CH$_2$}Rh(μ-H)(μ-Cl)Rh(η^2-C$_8$H$_{14}$)$_2$ (10). PhB(Ox^{Me2})$_2$(Im^{Mes}H) (H[**2**], 0.107 g, 0.228 mmol) was deprotonated with potassium benzyl (0.0365 g, 0.280 mmol) in tetrahydrofuran (10 mL) as above, [Rh(μ-Cl)(η^2-C$_8$H$_{14}$)]$_2$ (0.164 g, 0.228 mmol) was added, and the dark brown solution was stirred at room temperature for 1 h. The volatile materials were evaporated *in vacuo*, and the residue was extracted with benzene (2 × 5 mL). The benzene extracts were combined, filtered, and evaporated. The residue was triturated with pentane and dried *in vacuo* to afford the product as a yellow solid (0.179 g, 0.192 mmol, 84.2%). ^{1}H NMR (benzene-d_6, 600 MHz): δ 8.55 (d, $^3J_{HH}$ = 7.2 Hz, 2 H, *o*-C$_6$H$_5$), 7.60 (t, $^3J_{HH}$ = 7.2 Hz, 2 H, *m*-C$_6$H$_5$), 7.47 (s, 1 H, 3H-C$_6$*H*$_2$(CH$_2$Rh)Me$_2$), 7.44 (t, $^3J_{HH}$ = 7.2 Hz, 1 H, *p*-C$_6$H$_5$), 6.79 (s, 1 H, N$_2$C$_3$*H*$_2$Mes′), 6.59 (s, 1 H, 5H-C$_6$*H*$_2$(CH$_2$Rh)Me$_2$), 6.56 (s, 1 H, N$_2$C$_3$*H*$_2$Mes′), 4.30 (br, 1 H, C$_8$H$_{14}$), 3.67 (m, 4 H, CNCMe$_2$C*H*$_2$O (1 H) and C$_8$H$_{14}$ (3 H)), 3.30 (d, $^2J_{HH}$ = 7.8 Hz, 1 H, CNCMe$_2$C*H*$_2$O), 3.02 (m, 1 H, C$_8$H$_{14}$), 2.95 (br, 2 H, CHCMe$_2$C*H*$_2$O (1 H) and C$_8$H$_{14}$ (1 H)), 2.80 (m, 4 H, CNCMe$_2$C*H*$_2$O (1 H), C$_8$H$_{14}$ (1 H), and CH$_2$Rh (2 H)), 2.42

dx.doi.org/10.1021/om500891h | *Organometallics* 2014, 33, 6840−6860

(m, 1 H, C_8H_{14}), 2.23 (s, 3 H, *p*-$C_6H_2(CH_2Rh)Me_2$), 2.08 (s, 3 H, *o*-$C_6H_2(CH_2Rh)Me_2$), 1.90 (s, 3 H, CNC$Me_2$$CH_2O$), 1.75 (m, 1 H, C_8H_{14}), 1.57 (m, 5 H, C_8H_{14}), 1.39 (m, 9 H, C_8H_{14}), 1.28 (s, 3 H, CNC$Me_2$$CH_2O$), 1.23 (s, 3 H, CNC$Me_2$$CH_2O$), 1.17 (m, 3 H, C_8H_{14}), 1.10 (s, 3 H, CNC$Me_2$$CH_2O$), 1.04 (m, 2 H, C_8H_{14}), −21.70 (dd, 1 H, $^1J_{RhH}$ = 30 and 18 Hz). $^{13}C\{^1H\}$ NMR (benzene-d_6, 150 MHz): δ 187 (br, *C*NCMe$_2$CH$_2$O), 184 (br, *C*NCMe$_2$CH$_2$O), 175.98 (d, $^1J_{RhC}$ = 50.1 Hz, 2C-$N_2C_3H_2Mes'$), 150.61 (*ipso*-$C_6H_2(CH_2Rh)Me_2$), 143 (br, *ipso*-C_6H_5), 136.77 (*o*-C_6H_5), 136.60 (2C and 6C-$C_6H_2(CH_2Rh)Me_2$), 135.53 (4C-$C_6H_2(CH_2Rh)Me_2$), 128.92 (5C-$C_6H_2(CH_2Rh)Me_2$), 127.91 (*m*-C_6H_5), 127.31 (3C-$C_6H_2(CH_2Rh)Me_2$), 127.07 (*p*-C_6H_5), 124.55 (4,5C-$N_2C_3H_2Mes'$), 119.58 (4,5C-$N_2C_3H_2Mes'$), 81.06 (CNCMe$_2$*C*H$_2$O), 80.78 (d, $^1J_{RhC}$ = 10.8 Hz, C_8H_{14}), 80.39 (CNCMe$_2$*C*H$_2$O), 75.99 (d, $^1J_{RhC}$ = 11.6 Hz, C_8H_{14}), 71.57 (d, $^1J_{RhC}$ = 11.4 Hz, C_8H_{14}), 69.36 (d, $^1J_{RhC}$ = 12.2 Hz, C_8H_{14}), 69.18 (CNCMe$_2$*C*H$_2$O), 68.58 (CNCMe$_2$*C*H$_2$O), 33.0 (br, C_8H_{14}), 31.8 (br, C_8H_{14}), 31.7 (br, C_8H_{14}), 30.1 (br, C_8H_{14}), 29.9 (br, C_8H_{14}), 29.88 (C_8H_{14}), 29.55 (CNC*Me*$_2$CH$_2$O), 29.31 (CNC*Me*$_2$CH$_2$O), 29.1 (br, C_8H_{14}), 28.31 (CNC*Me*$_2$CH$_2$O), 28.0 (br, C_8H_{14}), 27.3 (br, C_8H_{14}), 27.23 (C_8H_{14}), 27.16 (C_8H_{14}), 26.71 (C_8H_{14}), 25.44 (CNC*Me*$_2$CH$_2$O), 21.47 (*p*-$C_6H_2(CH_2Rh)Me_2$), 20.34 (*o*-$C_6H_2(CH_2Rh)Me_2$), 12.78 ($^1J_{RhH}$ = 21.2 Hz, RhCH$_2$). ^{11}B NMR (benzene-d_6, 192 MHz): δ −9.6. $^{15}N\{^1H\}$ NMR (benzene-d_6, 61 MHz): δ −162 (CNCMe$_2$CH$_2$O), −178 (CNCMe$_2$CH$_2$O). IR (KBr, cm^{-1}): 2956 m, 2921 s, 2849 m, 1582 s (CN), 1559 w (CN), 1480 m, 1464 m, 1413 m, 1354 s, 1278 m, 1187 s, 1166 m, 967 s, 888 w, 850 w, 837 w, 821 w, 743 w, 728 w, 703 s, 670 w, 645 w. Anal. Calcd for $C_{44}H_{62}BClN_4O_2Rh_2$: C, 56.76; H, 6.71; N, 6.02. Found: C, 57.11; H, 6.78; N, 6.44. Mp: 189−192 °C.

{PhB(Ox^{Me2})$_2$Im^{Mes}}IrH(η^3-C$_8$H$_{13}$) (11). PhB(Ox^{Me2})$_2$(Im^{Mes}H) (H[**2**], 0.0914 g, 0.194 mmol) was deprotonated with potassium benzyl (0.0317 g, 0.243 mmol) in tetrahydrofuran (10 mL). [Ir(μ-Cl)(η^2-C_8H_{14})$_2$]$_2$ (0.0871 g, 0.0972 mmol) was added, and the dark brown solution was stirred at room temperature for 18 h. The solvent was removed *in vacuo*, and the residue was extracted with benzene (2 × 5 mL). The benzene extracts were combined, filtered, and evaporated to give a solid, which was triturated with pentane and dried *in vacuo* to afford the product as a yellow solid (0.124 g, 0.161 mmol, 83.0%). ^1H NMR (benzene-d_6, 600 MHz): δ 8.49 (d, $^3J_{HH}$ = 7.2 Hz, 2 H, *o*-C_6H_5), 7.57 (t, $^3J_{HH}$ = 7.2 Hz, 2 H, *m*-C_6H_5), 7.41 (t, $^3J_{HH}$ = 7.2 Hz, 1 H, *p*-C_6H_5), 6.85 (s, 1 H, $N_2C_3H_2$Mes), 6.78 (s, 1 H, *m*-$C_6H_2Me_3$), 6.70 (s, 1 H, *m*-$C_6H_2Me_3$), 6.09 (s, 1 H, $N_2C_3H_2$Mes), 4.90 (t, $^3J_{HH}$ = 7.2 Hz, 1 H, *C*H(CH)$_2$(CH$_2$)$_5$), 4.09 (q, $^3J_{HH}$ = 8.4 Hz, 1 H, CH(*C*H)$_2$(CH$_2$)$_5$), 3.85 (d, $^2J_{HH}$ = 8.4 Hz, 1 H, CNCMe$_2$*C*H$_2$O *trans* to C_8H_{13}), 3.69 (d, $^2J_{HH}$ = 8.4 Hz, 1 H, CNCMe$_2$*C*H$_2$O *trans* to C_8H_{13}), 3.43 (m, 2 H, CNCMe$_2$*C*H$_2$O *trans* to H (1 H) and CH(*C*H)$_2$(CH$_2$)$_5$ (1 H)), 3.34 (d, $^2J_{HH}$ = 8.4 Hz, 1 H, CNCMe$_2$*C*H$_2$O *trans* to H), 2.58 (m, 1 H, C_8H_{13}), 2.43 (m, 1 H, C_8H_{13}), 2.19−2.17 (m, 4 H, $C_6H_2Me_3$ (3 H) and C_8H_{13} (1 H)), 2.10 (s, 3 H, $C_6H_2Me_3$), 2.00 (s, 3 H, $C_6H_2Me_3$), 1.55 (m, 3 H, C_8H_{13}), 1.24 (s, 3 H, CNC*Me*$_2$CH$_2$O *trans* to C_8H_{13}), 1.20 (m, 3 H, C_8H_{13}), 1.09 (s, 3 H, CNC*Me*$_2$CH$_2$O *trans* to C_8H_{13}), 0.84 (s, 3 H, CNC*Me*$_2$CH$_2$O *trans* to H), 0.76 (s, 3 H, CNC*Me*$_2$CH$_2$O *trans* to H), 0.70 (m, 1 H, C_8H_{13}), −27.49 (s, 1 H, IrH). $^{13}C\{^1H\}$ NMR (benzene-d_6, 150 MHz): δ 186.4 (br, *C*NCMe$_2$CH$_2$O), 183.9 (br, *C*NCMe$_2$CH$_2$O), 164.12 (2C-$N_2C_3H_2$Mes), 144.1 (*ipso*-C_6H_5), 139.73 (*o*-$C_6H_2Me_3$), 139.70 (*o*-$C_6H_2Me_3$), 138.19 (*ipso*-$C_6H_2Me_3$), 137.17 (*o*-C_6H_5), 136.87 (*p*-$C_6H_2Me_3$), 129.70 (*m*-$C_6H_2Me_3$), 129.19 (4,5C-$N_2C_3H_2$Mes), 127.62 (*m*-C_6H_5), 127.10 (*p*-C_6H_5), 124.19 (*m*-$C_6H_2Me_3$), 120.23 (4,5C-$N_2C_3H_2$Mes), 89.26 (C_8H_{13}), 82.99 (CNCMe$_2$*C*H$_2$O *trans* to H), 80.70 (CNCMe$_2$*C*H$_2$O *trans* to C_8H_{13}), 69.42 (CNCMe$_2$*C*H$_2$O *trans* to C_8H_{13}), 69.36 (CNCMe$_2$*C*H$_2$O *trans* to H), 54.82 (C_8H_{13}), 48.43 (C_8H_{13}), 38.57 (C_8H_{13}), 37.52 (C_8H_{13}), 31.56 (C_8H_{13}), 31.50 (C_8H_{13}), 31.38 (C_8H_{13}), 28.45 (CNC*Me*$_2$CH$_2$O *trans* to H), 28.23 (CNC*Me*$_2$CH$_2$O *trans* to H), 28.18 (CNC*Me*$_2$CH$_2$O *trans* to C_8H_{13}), 28.12 (CNC*Me*$_2$CH$_2$O *trans* to C_8H_{13}), 27.03 (C_8H_{13}), 21.36 (*o*-$C_6H_2Me_3$), 18.51 (*p*-$C_6H_2Me_3$), 18.50 (*o*-$C_6H_2Me_3$). ^{11}B NMR (benzene-d_6, 192 MHz): δ −10.5. $^{15}N\{^1H\}$ NMR (benzene-d_6, 61 MHz): δ −184 (CNCMe$_2$CH$_2$O, *trans* to H), −196 (CNCMe$_2$CH$_2$O *trans* to C_8H_{13}). IR (KBr, cm^{-1}): 3126 w, 2960 s, 2922 s, 2245 s (IrH), 1585 s (CN), 1567 m (CN), 1490 m, 1456 m, 1404 s, 1338 s, 1324 m, 1261 m, 1186 s, 1161 m, 1020 m, 993 m, 972 m, 927 w, 853 w, 823 w, 745 m, 704 s, 672 m, 643 m. Anal. Calcd for $C_{36}H_{48}BIrN_4O_2$: C, 56.02; H, 6.27; N, 7.26. Found: C, 56.25; H, 5.89; N, 7.23. Mp: 183−185 °C.

{κ^4-PhB(Ox^{Me2})$_2$Im$^{Mes'}$CH$_2$}RhH(CO) (12). A 10 mL benzene solution of {PhB(Ox^{Me2})Im^{Mes}}Rh(CO)$_2$ (**5**, 0.144 g, 0.230 mmol) was exposed to UV light in a Rayonet reactor for 2 d. The reaction mixture was evaporated to dryness, and the solid residue was triturated with pentane and dried *in vacuo* to provide the brown product (0.106 g, 0.177 mmol, 77.0%). ^1H NMR (benzene-d_6, 600 MHz): δ 8.54 (d, $^3J_{HH}$ = 7.8 Hz, 2 H, *o*-C_6H_5), 7.62 (t, $^3J_{HH}$ = 7.8 Hz, 2 H, *m*-C_6H_5), 7.45 (t, $^3J_{HH}$ = 7.2 Hz, 1 H, *p*-C_6H_5), 7.18 (s, 1 H, 5H-$C_6H_2(CH_2Rh)Me_2$), 6.84 (s, 1 H, $N_2C_3H_2Mes'$), 6.63 (s, 1 H, $N_2C_3H_2Mes'$), 6.61 (s, 1 H, 3H-$C_6H_2(CH_2Rh)Me_2$), 3.67 (d, $^2J_{HH}$ = 8.4 Hz, 1 H, CNCMe$_2$*C*H$_2$O), 3.44 (m, 2 H, CNCMe$_2$*C*H$_2$O), 3.38 (d, $^2J_{HH}$ = 8.4 Hz, 1 H, CNCMe$_2$*C*H$_2$O), 2.78 (m, 2 H, CH$_2$Rh), 2.15 (s, 3 H, *o*-$C_6H_2(CH_2Rh)Me_2$), 1.92 (s, 3 H, *p*-$C_6H_2(CH_2Rh)Me_2$), 1.02 (s, 3 H, CNC*Me*$_2$CH$_2$O *trans* to H), 0.90 (s, 3 H, CNC*Me*$_2$CH$_2$O *trans* to H), 0.83 (s, 3 H, CNC*Me*$_2$CH$_2$O *trans* to CH$_2$), 0.72 (s, 3 H, CNC*Me*$_2$CH$_2$O *trans* to CH$_2$), −14.21 (d, $^1J_{RhH}$ = 23.4 Hz, 1 H, RhH). $^{13}C\{^1H\}$ NMR (benzene-d_6, 150 MHz): δ 197.06 (d, $^1J_{RhC}$ = 52.5 Hz, CO), 186 (br, *C*NCMe$_2$CH$_2$O), 185.74 (d, $^1J_{RhC}$ = 40.2 Hz, 2C-$N_2C_3H_2Mes'$), 185 (br, *C*NCMe$_2$CH$_2$O), 148.64 (2C-$C_6H_2(CH_2Rh)Me_2$), 143 (br, *ipso*-C_6H_5), 137.15 (4,6C-$C_6H_2(CH_2Rh)Me_2$), 137.14 (4,6C-$C_6H_2(CH_2Rh)Me_2$), 136.68 (*o*-C_6H_5), 136.28 (*ipso*-$C_6H_2(CH_2Rh)Me_2$), 129.01 (3C-$C_6H_2(CH_2Rh)Me_2$), 127.98 (*m*-C_6H_5), 127.45 (*p*-C_6H_5), 126.06 (5C-$C_6H_2(CH_2Rh)Me_2$), 123.97 (4,5C-$N_2C_3H_2Mes'$), 119.40 (4,5C-$N_2C_3H_2Mes'$), 80.35 (CNCMe$_2$*C*H$_2$O *trans* to H), 79.77 (CNCMe$_2$CH$_2$O *trans* to CH$_2$), 67.87 (CNCMe$_2$CH$_2$O *trans* to H), 66.70 (CNCMe$_2$CH$_2$O *trans* to CH$_2$), 28.71 (CNC*Me*$_2$CH$_2$O *trans* to H), 28.00 (CNC*Me*$_2$CH$_2$O *trans* to CH$_2$), 27.93 (CNC*Me*$_2$CH$_2$O *trans* to CH$_2$), 27.32 (CNC*Me*$_2$CH$_2$O *trans* to H), 21.29 (*o*-$C_6H_2(CH_2Rh)Me_2$), 20.39 (*p*-$C_6H_2(CH_2Rh)Me_2$), 6.58 (d, $^1J_{RhC}$ = 20.6 Hz, CH$_2$Rh). ^{11}B NMR (benzene-d_6, 192 MHz): δ −9.7. $^{15}N\{^1H\}$ NMR (benzene-d_6, 61 MHz): δ −162 (CNCMe$_2$CH$_2$O *trans* to H), −171 (CNCMe$_2$CH$_2$O *trans* to CH$_2$), −183 ($N_2C_3H_2Mes'$), −188 ($N_2C_3H_2Mes'$). IR (KBr, cm^{-1}): 2976 m, 2929 m, 2892 w, 2064 m (RhH), 2015 s (CO), 1967 w, 1587 m (CN), 1568 m (CN), 1479 m, 1430 m, 1362 m, 1274 m, 1164 m, 968 m, 957 m, 819 w, 705 m. Anal. Calcd for $C_{29}H_{34}BN_4O_3Rh$: C, 58.02; H, 5.71; N, 9.33. Found: C, 58.46; H, 5.51; N, 9.42. Mp: 196−199 °C.

{PhB(Ox^{Me2})$_2$Im^{Mes}}IrH(Ph)CO (13). A 10 mL benzene solution of {PhB(Ox^{Me2})$_2$Im^{Mes}}Ir(CO)$_2$ (7, 0.0930 g, 0.130 mmol) was irradiated with UV light in a Rayonet reactor for 2 d. The volatile materials were evaporated, and the residue was triturated with pentane and dried *in vacuo* to afford the product as a brown solid (0.0843 g, 0.110 mmol, 84.6%). ^1H NMR (methylene chloride-d_2, 600 MHz): δ 8.04 (d, $^3J_{HH}$ = 7.2 Hz, 2 H, *o*-BC_6H_5), 7.39 (m, 4 H, *m*-BC_6H_5 (2 H) and IrC_6H_5 (2 H)), 7.32 (t, $^3J_{HH}$ = 7.2 Hz, 1 H, *p*-BC_6H_5), 7.07 (s, 1 H, *m*-$C_6H_2Me_3$), 7.00 (s, 1 H, *m*-$C_6H_2Me_3$), 6.81 (br, 3 H, $N_2C_3H_2$Mes (1 H) and IrC_6H_5 (2 H)), 6.69 (m, 2 H, $N_2C_3H_2$Mes (1 H) and IrC_6H_5 (1 H)), 4.24 (d, $^2J_{HH}$ = 7.8 Hz, 1 H, CNCMe$_2$*C*H$_2$O), 4.17 (d, $^2J_{HH}$ = 8.4 Hz, 1 H, CNCMe$_2$*C*H$_2$O), 3.92 (d, $^2J_{HH}$ = 8.4 Hz, 1 H, CNCMe$_2$*C*H$_2$O), 3.80 (d, $^2J_{HH}$ = 8.4 Hz, 1 H, CNCMe$_2$*C*H$_2$O), 2.39 (s, 3 H, *p*-$C_6H_2Me_3$), 2.05 (s, 3 H, *o*-$C_6H_2Me_3$), 1.94 (s, 3 H, *o*-$C_6H_2Me_3$), 0.94 (s, 3 H, CNC*Me*$_2$CH$_2$O *trans* to H), 0.89 (s, 6 H, CNC*Me*$_2$CH$_2$O), 0.54 (s, 3 H, CNC*Me*$_2$CH$_2$O *trans* to CO), −16.51 (s, 1 H, IrH). $^{13}C\{^1H\}$ NMR (methylene chloride-d_2, 150 MHz): δ 187.92 (br, *C*NCMe$_2$CH$_2$O), 184.71 (br, *C*NCMe$_2$CH$_2$O), 171.70 (CO), 170.07 (2C-$N_2C_3H_2$Mes), 143.86 (br, IrC_6H_5), 143.44 (IrC_6H_5), 143.26 (*ipso*-BC_6H_5), 139.32 (*ipso*-IrC_6H_5), 139.30 (*p*-$C_6H_2Me_3$), 139.16 (*ipso*-$C_6H_2Me_3$), 136.99 (*o*-$C_6H_2Me_3$), 136.58 (*o*-$C_6H_2Me_3$), 136.18 (*o*-BC_6H_5), 129.34 (*m*-$C_6H_2Me_3$), 129.25 (*m*-$C_6H_2Me_3$), 127.46 (*m*-BC_6H_5), 127.16 (*p*-BC_6H_5), 124.31 (4,5C-$N_2C_3H_2$Mes), 122.67 (IrC_6H_5), 120.92 (4,5C-$N_2C_3H_2$Mes), 80.22 (CNCMe$_2$*C*H$_2$O *trans* to H), 79.78 (CNCMe$_2$*C*H$_2$O *trans* to CO), 70.24 (CNCMe$_2$*C*H$_2$O), 70.09 (CNCMe$_2$*C*H$_2$O), 29.47 (CNC*Me*$_2$CH$_2$O *trans* to H), 29.40

dx.doi.org/10.1021/om500891h | *Organometallics* 2014, 33, 6840−6860

(CNCMe_2CH$_2$O *trans* to CO), 26.29 (CNCMe_2CH$_2$O *trans* to H), 25.45 (CNCMe_2CH$_2$O *trans* to CO), 21.45 (*p*-C$_6$H$_2$$Me_3$), 18.85 (*o*-C$_6H_2$$Me_3$), 18.13 (*o*-C$_6H_2$$Me_3$). ^{11}B NMR (methylene chloride-d_2, 192 MHz): δ −10.0. ^{15}N{^{1}H} NMR (benzene-d_6, 61 MHz): δ −182 (CNCMe$_2$CH$_2$O *trans* to H), −193 (CNCMe$_2$CH$_2$O *trans* to CO). IR (KBr, cm^{-1}): 3139 w, 3046 w, 2969 m, 2925 m, 2885 w, 2177 m (IrH), 1999 s (CO), 1578 m (CN), 1558 m (CN), 1404 m, 1291 m, 1205 m, 1183 m, 1162 m, 967 m, 744 m, 704 m. Anal. Calcd for $C_{35}H_{40}BIrN_4O_3$: C, 54.75; H, 5.25; N, 7.30. Found: C, 54.84; H, 5.17; N, 7.23. Mp: 281−282 °C.

{PhB(Ox^{Me2})$_2$Im^{Mes}}RhH(SiH$_2$Ph)CO (14). PhSiH$_3$ (70.0 μL, 0.567 mmol) was allowed to react with {PhB(Ox^{Me2})$_2$Im^{Mes}}Rh(CO)$_2$ (**5**, 0.351 g, 0.559 mmol) in benzene (10 mL) at room temperature for 18 h. The volatiles were removed *in vacuo*, and the brown residue was triturated with pentane and dried to give a brown solid (0.372 g, 0.525 mmol, 94.1%). ^{1}H NMR (benzene-d_6, 600 MHz): δ 8.41 (d, $^3J_{HH}$ = 7.2 Hz, 2 H, *o*-BC$_6$H$_5$), 7.59 (m, 2 H, *o*-SiC$_6$H$_5$), 7.55 (t, $^3J_{HH}$ = 7.2 Hz, 2 H, *m*-BC$_6$H$_5$), 7.40 (t, $^3J_{HH}$ = 7.2 Hz, 1 H, *p*-BC$_6$H$_5$), 7.11 (m, 3 H, *m*- and *p*-SiC$_6$H$_5$), 6.54 (d, $^3J_{HH}$ = 1.8 Hz, 1 H, N$_2$C$_3$H$_2$Mes), 6.50 (s, 1 H, *m*-C$_6$H$_2$Me$_3$), 6.40 (s, 1 H, *m*-C$_6$H$_2$Me$_3$), 5.93 (d, $^3J_{HH}$ = 1.8 Hz, 1 H, N$_2$C$_3$H$_2$Mes), 4.91 (d, $^2J_{HH}$ = 6.0 Hz, $^1J_{SiH}$ = 170 Hz, 1 H, SiH), 4.43 (d, $^2J_{HH}$ = 6.0 Hz, $^1J_{SiH}$ = 188 Hz, 1 H, SiH), 3.64 (d, $^2J_{HH}$ = 7.8 Hz, 1 H, CNCMe$_2$CH_2O), 3.61 (d, $^2J_{HH}$ = 8.4 Hz, 1 H, CNCMe$_2$CH_2O), 3.58 (d, $^2J_{HH}$ = 8.4 Hz, 1 H, CNCMe$_2$CH_2O), 3.37 (d, $^2J_{HH}$ = 8.4 Hz, 1 H, CNCMe$_2$CH_2O), 2.01 (s, 3 H, *o*-C$_6$H$_2$$Me_3$), 1.99 (s, 3 H, *o*-C$_6H_2$$Me_3$), 1.89 (s, 3 H, *p*-C$_6H_2$$Me_3$), 1.16 (s, 3 H, CNC$Me_2CH_2$O *trans* to H), 1.15 (s, 3 H, CNCMe_2CH$_2$O *trans* to H), 1.08 (s, 3 H, CNCMe_2CH$_2$O *trans* to Si), 1.02 (s, 3 H, CNCMe_2CH$_2$O *trans* to Si), −13.22 (dd, $^1J_{RhH}$ = 21.3 Hz, $^3J_{HH}$ = 1.2 Hz, 1 H, RhH). ^{13}C{^{1}H} NMR (benzene-d_6, 150 MHz): δ 194.53 (d, $^1J_{RhC}$ = 51.0 Hz, 2C-N$_2$C$_3$H$_2$Mes), 186.4 (br, *C*NCMe$_2$CH$_2$O), 178.39 (d, $^1J_{RhC}$ = 40.5 Hz, CO), 144.1 (br, *ipso*-BC$_6$H$_5$), 139.10 (*ipso*-SiC$_6$H$_5$), 138.63 (*p*-C$_6$H$_2$Me$_3$), 137.25 (*ipso*-C$_6$H$_2$Me$_3$), 136.98 (*o*-BC$_6$H$_5$), 136.45 (*o*-SiC$_6$H$_5$), 135.86 (*o*-C$_6$H$_2$Me$_3$), 135.84 (*o*-C$_6$H$_2$Me$_3$), 129.69 (*m*-C$_6$H$_2$Me$_3$), 129.68 (*m*-C$_6$H$_2$Me$_3$), 127.87 (*m*-BC$_6$H$_5$), 127.81 (*p*-BC$_6$H$_5$), 127.41 (*p*-SiC$_6$H$_5$), 127.37 (*m*-SiC$_6$H$_5$), 124.93 (4,5C-N$_2$C$_3$H$_2$Mes), 121.86 (4,5C-N$_2$C$_3$H$_2$Mes), 80.81 (CNCMe$_2$CH$_2$O), 80.65 (CNCMe$_2$CH$_2$O), 69.11 (CNCMe$_2$CH$_2$O *trans* to Si), 67.04 (CNCMe$_2$CH$_2$O *trans* to H), 28.72 (CNCMe_2CH$_2$O *trans* to Si), 28.39 (CNCMe_2CH$_2$O *trans* to Si), 28.15 (CNCMe_2CH$_2$O *trans* to H), 27.33 (CNCMe_2CH$_2$O *trans* to H), 21.51 (*p*-C$_6$H$_2$$Me_3$), 19.78 (*o*-C$_6H_2$$Me_3$), 19.40 (*o*-C$_6H_2$$Me_3$). ^{11}B NMR (benzene-$d_6$, 192 MHz): δ −9.9. ^{15}N{^{1}H} NMR (benzene-d_6, 61 MHz): δ −161 (CNCMe$_2$CH$_2$O *trans* to Si), −172 (CNCMe$_2$CH$_2$O *trans* to H), −176 (N$_2$C$_3$H$_2$Mes), −187 (N$_2$C$_3$H$_2$Mes). ^{29}Si{^{1}H} NMR (benzene-d_6, 119 MHz): δ −21.37 (d, $^1J_{RhSi}$ = 30.2 Hz). IR (KBr, cm^{-1}): 2964 w, 2925 w, 2064 s (RhH), 2016 s (CO), 1998 s (SiH), 1593 m (CN), 1276 m, 967 m, 830 m. Anal. Calcd for $C_{35}H_{42}BN_4O_3RhSi$: C, 59.33; H, 5.98; N, 7.91. Found: C, 59.07; H, 5.64; N, 7.55. Mp: 124−127 °C.

{PhB(Ox^{Me2})$_2$Im^{Mes}}Ir(CO)CN^{t}Bu (15). {PhB(Ox^{Me2})$_2$Im^{Mes}}Ir(CO)$_2$ (7, 0.254 g, 0.354 mmol) and *tert*-butyl isocyanide (40.0 μL, 0.354 mmol) were allowed to react in benzene (10 mL). The transparent green-yellow reaction mixture was stirred at room temperature for 3 h. The solvent and volatiles were evaporated, and the resulting solid was triturated with pentane and dried *in vacuo* to afford the product as a greenish-yellow solid (0.246 g, 0.318 mmol, 89.8%). ^{1}H NMR (benzene-d_6, 600 MHz): δ 7.95 (d, $^3J_{HH}$ = 7.8 Hz, 2 H, *o*-C$_6$H$_5$), 7.67 (s, 1 H, N$_2$C$_3$H$_2$Mes), 7.44 (t, $^3J_{HH}$ = 7.2 Hz, 2 H, *m*-C$_6$H$_5$), 7.25 (t, $^3J_{HH}$ = 7.2 Hz, 1 H, *p*-C$_6$H$_5$), 6.76 (s, 2 H, *m*-C$_6$H$_2$Me$_3$), 6.32 (s, 1 H, N$_2$C$_3$H$_2$Mes), 3.68 (m, 4 H, CNCMe$_2$CH_2O), 2.20 (s, 6 H, *o*-C$_6$H$_2$$Me_3$), 2.11 (s, 3 H, *p*-C$_6H_2$$Me_3$), 1.32 (s, 6 H, CNC$Me_2CH_2$O), 1.27 (s, 6 H, CNC$Me_2CH_2$O), 0.73 (s, 9 H, CMe$_3$). ^{13}C{^{1}H} NMR (benzene-d_6, 150 MHz): δ 187 (br, *C*NCMe$_2$CH$_2$O), 177.53 (2C-N$_2$C$_3$H$_2$Mes), 176 (br, CO), 150 (br, *ipso*-C$_6$H$_5$), 138.49 (*p*-C$_6$H$_2$Me$_3$), 138.14 (*ipso*-C$_6$H$_2$Me$_3$), 136.84 (*o*-C$_6$H$_2$Me$_3$), 134.71 (*o*-C$_6$H$_5$), 129.64 (*m*-C$_6$H$_2$Me$_3$), 128.90 (*C*NCMe$_3$), 127.72 (*m*-C$_6$H$_5$), 126.38 (*p*-C$_6$H$_5$), 126.31 (4,5C-N$_2$C$_3$H$_2$Mes), 120.33 (4,5C-N$_2$C$_3$H$_2$Mes), 79.04 (CNCMe$_2$CH$_2$O), 68.89 (CNCMe$_2$CH$_2$O), 56.59 (CMe$_3$), 29.88 (CMe_3), 28.83 (CNCMe_2CH$_2$O), 28.68 (CNCMe_2CH$_2$O), 21.45 (*p*-C$_6$H$_2$$Me_3$), 19.30 (*o*-C$_6H_2$$Me_3$). ^{11}B NMR (benzene-$d_6$, 192 MHz): δ −8.5. ^{15}N{^{1}H} NMR (benzene-d_6, 61 MHz): δ −154 (CNCMe$_2$CH$_2$O), −176 (N$_2$C$_3$H$_2$Mes), −188 (N$_2$C$_3$H$_2$Mes), −196 (CNCMe$_3$). IR (KBr, cm^{-1}): 2959 w, 2920 w, 2852 w, 2144 m (CN), 1973 s (CO), 1616 w (CN), 1579 w (CN), 1461 w, 1185 w, 967 w, 731 w. Anal. Calcd for $C_{34}H_{43}BIrN_5O_3$: C, 52.84; H, 5.61; N, 9.06. Found: C, 53.27; H, 5.56; N, 9.35. Mp: 182−185 °C.

{PhB(Ox^{Me2})$_2$Im^{Mes}}Ir(CN^{t}Bu)$_2$ (16). *tert*-Butyl isocyanide (175.0 μL, 1.547 mmol) was added to a benzene solution (10 mL) of {PhB(Ox^{Me2})$_2$Im^{Mes}}Ir(η^4-C$_8$H$_{12}$) (**6**, 0.571 g, 0.742 mmol). The solution was stirred at room temperature for 3 h. Evaporation of the solvent and other volatile materials provided a solid that was triturated with pentane and immediately dried *in vacuo* to give the product as yellow solid (0.533 g, 0.644 mmol, 86.8%). ^{1}H NMR (benzene-d_6, 600 MHz): δ 8.00 (d, $^3J_{HH}$ = 6.8 Hz, 2 H, *o*-C$_6$H$_5$), 7.83 (s, 1 H, N$_2$C$_3$H$_2$Mes), 7.43 (t, $^3J_{HH}$ = 7.2 Hz, 2 H, *m*-C$_6$H$_5$), 7.25 (t, $^3J_{HH}$ = 7.2 Hz, 1 H, *p*-C$_6$H$_5$), 6.69 (s, 2 H, *m*-C$_6$H$_2$Me$_3$), 6.35 (s, 1 H, N$_2$C$_3$H$_2$Mes), 3.74 (m, 4 H, CNCMe$_2$CH_2O), 2.28 (s, 6 H, *o*-C$_6$H$_2$$Me_3$), 2.15 (s, 3 H, *p*-C$_6H_2$$Me_3$), 1.38 (s, 6 H, CNC$Me_2CH_2$O), 1.35 (s, 6 H, CNC$Me_2CH_2$O), 0.96 (br, 18 H, CMe$_3$). ^{13}C{^{1}H} NMR (benzene-d_6, 150 MHz): δ 185 (br, CNCMe$_2$CH$_2$O), 181.35 (2C-N$_2$C$_3$H$_2$Mes), 151 (br, *ipso*-C$_6$H$_5$), 139.15 (*o*-C$_6$H$_2$Me$_3$), 136.96 (*p*-C$_6$H$_2$Me$_3$), 136.41 (*ipso*-C$_6$H$_2$Me$_3$), 135.02 (*o*-C$_6$H$_5$), 129.46 (*m*-C$_6$H$_2$Me$_3$), 127.46 (*m*-C$_6$H$_5$), 125.92 (*p*-C$_6$H$_5$), 125.84 (4,5C-N$_2$C$_3$H$_2$Mes), 119.86 (4,5C-N$_2$C$_3$H$_2$Mes), 78.89 (CNCMe$_2$CH$_2$O), 68.95 (CNCMe$_2$CH$_2$O), 55 (br, CMe$_3$), 31 (br, CMe_3), 28.96 (CNCMe_2CH$_2$O), 28.85 (CNCMe_2CH$_2$O), 21.38 (*p*-C$_6$H$_2$$Me_3$), 20.38 (*o*-C$_6H_2$$Me_3$). ^{11}B NMR (benzene-$d_6$, 192 MHz): δ −8.7. ^{15}N{^{1}H} NMR (benzene-d_6, 61 MHz): δ −154 (CNCMe$_2$CH$_2$O), −176 (N$_2$C$_3$H$_2$Mes), −189 (N$_2$C$_3$H$_2$Mes), −231 (CNCMe$_3$). IR (KBr, cm^{-1}): 3137 w, 3044 w, 2979 s, 2962 s, 2926 m, 2865 m, 2124 s (CN), 2081 m, 2029 s (CN), 1653 w, 1616 m (CN), 1581 w (CN), 1559 w, 1492 m, 1458 m, 1401 m, 1365 m, 1338 m, 1324 m, 1284 m, 1230 s, 1211 s, 1185 m, 1162 m, 1130 m, 1000 m, 967 m, 851 w, 830 w, 729 m, 702 m. Anal. Calcd for $C_{38}H_{52}BIrN_6O_2$: C, 55.13; H, 6.33; N, 10.15. Found: C, 55.26; H, 6.61; N, 10.10. Mp: 174−177 °C.

{PhB(Ox^{Me2})$_2$Im^{Mes}}IrH(SiH$_2$Ph)CN^{t}Bu (17). Phenylsilane (32.0 μL, 0.259 mmol) was added to {PhB(Ox^{Me2})$_2$Im^{Mes}}Ir(CO)(CN^{t}Bu) (**15**, 0.200 g, 0.258 mmol) dissolved in benzene (10 mL). The resulting yellow transparent solution was heated at 60 °C for 4 h. The solvent and the volatiles were removed *in vacuo*, and the resulting solid was triturated with pentane and dried to give the product as yellow solid (0.205 g, 0.240 mmol, 93.0%). ^{1}H NMR (benzene-d_6, 600 MHz): δ 8.53 (d, $^3J_{HH}$ = 7.2 Hz, 2 H, *o*-BC$_6$H$_5$), 7.76 (d, $^3J_{HH}$ = 7.2 Hz, 2 H, *o*-SiC$_6$H$_5$), 7.58 (t, $^3J_{HH}$ = 7.2 Hz, 2 H, *m*-BC$_6$H$_5$), 7.42 (t, $^3J_{HH}$ = 7.8 Hz, 1 H, *p*-BC$_6$H$_5$), 7.19 (m, 3 H, *m*- and *p*-SiC$_6$H$_5$), 6.60 (d, $^3J_{HH}$ = 1.8 Hz, 1 H, N$_2$C$_3$H$_2$Mes), 6.50 (s, 1 H, *m*-C$_6$H$_2$Me$_3$), 6.47 (s, 1 H, *m*-C$_6$H$_2$Me$_3$), 6.00 (d, $^3J_{HH}$ = 1.8 Hz, 1 H, N$_2$C$_3$H$_2$Mes), 4.61 (d, $^2J_{HH}$ = 3.6 Hz, $^1J_{SiH}$ = 155 Hz, 1 H, SiH), 4.10 (d, $^2J_{HH}$ = 3.6 Hz, $^1J_{SiH}$ = 169 Hz, 1 H, SiH), 3.76 (d, $^2J_{HH}$ = 7.8 Hz, 1 H, CNCMe$_2$CH_2O), 3.68 (d, $^2J_{HH}$ = 3.6 Hz, 1 H, CNCMe$_2$CH_2O), 3.67 (d, $^2J_{HH}$ = 3.0 Hz, 1 H, CNCMe$_2$CH_2O), 3.47 (d, $^2J_{HH}$ = 7.8 Hz, 1 H, CNCMe$_2$CH_2O), 2.13 (s, 6 H, *o*-C$_6$H$_2$$Me_3$), 1.92 (s, 3 H, *p*-C$_6H_2$$Me_3$), 1.26 (s, 3 H, CNC$Me_2CH_2$O *trans* to H), 1.21 (s, 3 H, CNCMe_2CH$_2$O *trans* to H), 1.18 (s, 3 H, CNCMe_2CH$_2$O *trans* to Si), 1.13 (s, 3 H, CNCMe_2CH$_2$O *trans* to Si), 0.92 (s, 9 H, CMe$_3$), −18.76 (s, 1 H, IrH). ^{13}C{^{1}H} NMR (benzene-d_6, 150 MHz): δ 186.3 (br, *C*NCMe$_2$CH$_2$O), 185.1 (br, *C*NCMe$_2$CH$_2$O), 169.40 (2C-N$_2$C$_3$H$_2$Mes), 141.82 (*ipso*-C$_6$H$_2$Me$_3$), 138.03 (*p*-C$_6$H$_2$Me$_3$), 137.70 (*ipso*-SiC$_6$H$_5$), 137.08 (*o*-C$_6$H$_5$), 136.87 (*o*-C$_6$H$_5$), 136.13 (*o*-C$_6$H$_2$Me$_3$), 135.91 (*o*-C$_6$H$_2$Me$_3$), 129.49 (*m*-C$_6$H$_2$Me$_3$), 129.39 (*m*-C$_6$H$_2$Me$_3$), 127.79 (*m*-C$_6$H$_5$), 127.25 (*p*-C$_6$H$_5$), 126.70 (*m*- and *p*-C$_6$H$_5$), 124.28 (4,5C-N$_2$C$_3$H$_2$Mes), 121.32 (4,5C-N$_2$C$_3$H$_2$Mes), 80.51 (CNCMe$_2$CH$_2$O), 77.97 (CNCMe$_2$CH$_2$O), 70.97 (CNCMe$_2$CH$_2$O *trans* to H), 68.25 (CNCMe$_2$CH$_2$O *trans* to Si), 55.98 (*C*Me$_3$), 30.60 (CMe_3), 28.65 (CNCMe_2CH$_2$O), 28.27 (CNCMe_2CH$_2$O), 27.81 (CNCMe_2CH$_2$O), 27.35 (CNCMe_2CH$_2$O), 21.58 (*p*-C$_6$H$_2$$Me_3$), 19.94 (*o*-C$_6H_2$$Me_3$), 19.70 (*o*-C$_6H_2$$Me_3$). ^{11}B NMR (benzene-$d_6$, 192 MHz): δ −9.7. ^{15}N{^{1}H} NMR (benzene-d_6, 61 MHz): δ −176 (CNCMe$_2$CH$_2$O *trans* to Si), −189 (CNCMe$_2$CH$_2$O *trans* to H), −197 (CNCMe$_3$). ^{29}Si{^{1}H} NMR (benzene-d_6, 119 MHz): δ −56.14. IR (KBr, cm^{-1}): 3125 w, 3059 w, 3042 w, 2978 m,

dx.doi.org/10.1021/om500891h | *Organometallics* 2014, 33, 6840−6860

2963 m, 2925 m, 2879 m, 2139 s (IrH), 2094 m (CN), 2029 m (SiH), 2005 m (SiH), 1608 sh (CN), 1592 m (CN), 1489 m, 1472 w, 1368 w, 1336 w, 1279 w, 1202 m, 1185 m, 1160 m, 1134 m, 967 m, 835 m, 706 m. Anal. Calcd for $C_{39}H_{51}BIrN_5O_2Si$: C, 54.92; H, 6.03; N, 8.21. Found: C, 54.64; H, 6.56; N, 8.28. Mp: 266−269 °C.

■ ASSOCIATED CONTENT

Supporting Information

^1H and $^{13}C\{^1H\}$ NMR spectra of compounds **1**−**17**, rendered thermal ellipsoid illustrations of compounds **6** and **7**. Crystallographic information files (CIF) for compounds $PhB(Ox^{Me2})_2(Im^{tBu}H)LiCl(NCCD_3)$ (H[**1**]·LiCl·$NCCD_3$), K-[$PhB(Ox^{Me2})_2Im^{Mes}$] (K[**2**]), {$PhB(Ox^{Me2})_2Im^{tBu}$}Rh(η^4-C_8H_{12}) (**3**), {$PhB(Ox^{Me2})_2Im^{Mes}$}Rh(η^4-C_8H_{12}) (**4**), {PhB-$(Ox^{Me2})_2Im^{Mes}$}Rh(CO)$_2$ (**5**), {$PhB(Ox^{Me2})_2Im^{Mes}$}Ir(η^4-C_8H_{12}) (**6**), {$PhB(Ox^{Me2})_2Im^{Mes}$}Ir(CO)$_2$ (**7**), $To^MRh(\eta^4$-C_8H_{12}) (**8**), {κ^4-$PhB(Ox^{Me2})_2Im^{Mes\prime}CH_2$}Rh($\mu$-H)($\mu$-Cl)Rh-($\eta^2$-$C_8H_{14}$)$_2$ (**10**), {$PhB(Ox^{Me2})_2Im^{Mes}$}IrH(η^3-C_8H_{13}) (**11**), {κ^4-$PhB(Ox^{Me2})_2Im^{Mes\prime}CH_2$}RhH(CO) (**12**), {PhB-$(Ox^{Me2})_2Im^{Mes}$}IrH(Ph)CO (**13**), {$PhB(Ox^{Me2})_2Im^{Mes}$}RhH-($SiH_2Ph$)CO (**14**), {$PhB(Ox^{Me2})_2Im^{Mes}$}Ir(CO)$CN^tBu$ (**15**), and {$PhB(Ox^{Me2})_2Im^{Mes}$}IrH(SiH_2Ph)CN^tBu (**17**) are available free of charge via the Internet at http://pubs.acs.org.

■ AUTHOR INFORMATION

Corresponding Author

*E-mail: sadow@iastate.edu.

Present Address

‡Department of Chemistry, University of Chicago, 5735 S. Ellis Avenue, Chicago, Illinois 60637, United States.

Notes

The authors declare no competing financial interest.

■ ACKNOWLEDGMENTS

This research was supported by the U.S. Department of Energy, Office of Basic Energy Sciences, Division of Chemical Sciences, Geosciences, and Biosciences, through the Ames Laboratory (Contract No. DE-AC02-07CH11358).

■ REFERENCES

(1) (a) Bergman, R. G. *Science* **1984**, *223*, 902−908. (b) Labinger, J. A.; Bercaw, J. E. *Nature* **2002**, *417*, 507−514.

(2) Chaloner, P. A. *Homogeneous Hydrogenation*; Kluwer Academic Publishers: Dordrecht, 1993.

(3) Marciniec, B. *Hydrosilylation: A Comprehensive Review on Recent Advances*; Springer: Berlin, 2009.

(4) Leeuwen, P. W. N. M.; Claver, C. Rhodium Catalyzed Hydroformylation. In *Catalysis by Metal Complexes*; Springer: Dordrecht, 2002.

(5) (a) Bosnich, B. *Acc. Chem. Res.* **1998**, *31*, 667−674. (b) Leung, J. C.; Krische, M. J. *Chem. Sci.* **2012**, *3*, 2202−2209. (c) Roy, A. H.; Lenges, C. P.; Brookhart, M. *J. Am. Chem. Soc.* **2007**, *129*, 2082−2093.

(6) Doughty, D. H.; Pignolet, L. H. *J. Am. Chem. Soc.* **1978**, *100*, 7083−7085.

(7) Ho, H.-A.; Manna, K.; Sadow, A. D. *Angew. Chem., Int. Ed.* **2012**, *51*, 8607−8610.

(8) (a) Janowicz, A. H.; Bergman, R. G. *J. Am. Chem. Soc.* **1982**, *104*, 352−354. (b) Hoyano, J. K.; Graham, W. A. G. *J. Am. Chem. Soc.* **1982**, *104*, 3723−3725.

(9) Ho, H.-A.; Dunne, J. F.; Ellern, A.; Sadow, A. D. *Organometallics* **2010**, *29*, 4105−4114.

(10) Pawlikowski, A. V.; Gray, T. S.; Schoendorff, G.; Baird, B.; Ellern, A.; Windus, T. L.; Sadow, A. D. *Inorg. Chim. Acta* **2009**, *362*, 4517−4525.

(11) Purwoko, A. A.; Lees, A. J. *Inorg. Chem.* **1996**, *35*, 675−682.

(12) Duckett, S. B.; Haddleton, D. M.; Jackson, S. A.; Perutz, R. N.; Poliakoff, M.; Upmacis, R. K. *Organometallics* **1988**, *7*, 1526−1532.

(13) (a) Ghosh, C. K.; Hoyano, J. K.; Krentz, R.; Graham, W. A. G. *J. Am. Chem. Soc.* **1989**, *111*, 5480−5481. (b) Perez, P. J.; Poveda, M. L.; Carmona, E. *Angew. Chem., Int. Ed. Engl.* **1995**, *34*, 231−233.

(14) (a) Lian, T.; Bromberg, S. E.; Yang, H.; Proulx, G.; Bergman, R. G.; Harris, C. B. *J. Am. Chem. Soc.* **1996**, *118*, 3769−3770. (b) Bromberg, S. E.; Yang, H.; Asplund, M. C.; Lian, T.; McNamara, B. K.; Kotz, K. T.; Yeston, J. S.; Wilkens, M.; Frei, H.; Bergman, R. G.; Harris, C. B. *Science* **1997**, *278*, 260−263. (c) Yeston, J. S.; McNamara, B. K.; Bergman, R. G.; Moore, C. B. *Organometallics* **2000**, *19*, 3442−3446.

(15) Clot, E.; Eisenstein, O.; Jones, W. D. *Proc. Natl. Acad. Sci. U.S.A.* **2007**, *104*, 6939−6944.

(16) Blake, A. J.; George, M. W.; Hall, M. B.; McMaster, J.; Portius, P.; Sun, X. Z.; Towrie, M.; Webster, C. E.; Wilson, C.; Zarić, S. D. *Organometallics* **2007**, *27*, 189−201.

(17) Köcher, C.; Herrmann, W. A. *J. Organomet. Chem.* **1997**, *532*, 261−265.

(18) Xu, S.; Everett, W. C.; Ellern, A.; Windus, T. L.; Sadow, A. D. *Dalton Trans.* **2014**, *43*, 14368−14376.

(19) (a) Mazet, C.; Köhler, V.; Pfaltz, A. *Angew. Chem., Int. Ed.* **2005**, *44*, 4888−4891. (b) Köhler, V.; Mazet, C.; Toussaint, A.; Kulicke, K.; Häussinger, D.; Neuburger, M.; Schaffner, S.; Kaiser, S.; Pfaltz, A. *Chem.—Eur. J.* **2008**, *14*, 8530−8539.

(20) (a) Scepaniak, J. J.; Fulton, M. D.; Bontchev, R. P.; Duesler, E. N.; Kirk, M. L.; Smith, J. M. *J. Am. Chem. Soc.* **2008**, *130*, 10515−10517. (b) Scepaniak, J. J.; Young, J. A.; Bontchev, R. P.; Smith, J. M. *Angew. Chem., Int. Ed.* **2009**, *48*, 3158−3160.

(21) Scepaniak, J. J.; Vogel, C. S.; Khusniyarov, M. M.; Heinemann, F. W.; Meyer, K.; Smith, J. M. *Science* **2011**, *331*, 1049−1052.

(22) Gigler, P.; Bechlars, B.; Herrmann, W. A.; Kühn, F. E. *J. Am. Chem. Soc.* **2011**, *133*, 1589−1596.

(23) Schneider, N.; Finger, M.; Haferkemper, C.; Bellemin-Laponnaz, S.; Hofmann, P.; Gade, L. H. *Chem.—Eur. J.* **2009**, *15*, 11515−11529.

(24) Dunne, J. F.; Manna, K.; Wiench, J. W.; Ellern, A.; Pruski, M.; Sadow, A. D. *Dalton Trans.* **2010**, *39*, 641−653.

(25) Dunne, J. F.; Su, J.; Ellern, A.; Sadow, A. D. *Organometallics* **2008**, *27*, 2399−2401.

(26) Hernán-Gómez, A.; Herd, E.; Hevia, E.; Kennedy, A. R.; Knochel, P.; Koszinowski, K.; Manolikakes, S. M.; Mulvey, R. E.; Schnegelsberg, C. *Angew. Chem., Int. Ed.* **2014**, *53*, 2706−2710.

(27) Bucher, U. E.; Currao, A.; Nesper, R.; Rüegger, H.; Venanzi, L. M.; Younger, E. *Inorg. Chem.* **1995**, *34*, 66−74.

(28) Northcutt, T. O.; Lachicotte, R. J.; Jones, W. D. *Organometallics* **1998**, *17*, 5148−5152.

(29) Akita, M.; Ohta, K.; Takahashi, Y.; Hikichi, S.; Moro-oka, Y. *Organometallics* **1997**, *16*, 4121−4128.

(30) (a) Herrmann, W. A.; Goossen, L. J.; Spiegler, M. *Organometallics* **1998**, *17*, 2162−2168. (b) Ren, L.; Chen, A. C.; Decken, A.; Crudden, C. M. *Can. J. Chem.* **2004**, *82*, 1781−1787.

(31) Bonati, F.; Wilkinson, G. *J. Chem. Soc.* **1964**, 3156−3160.

(32) Bucher, U. E.; Fässler, T. F.; Hunziker, M.; Nesper, R.; Rüegger, H.; Venanzi, L. M. *Gazz. Chim. Ital.* **1995**, *125*, 181−188.

(33) Jeletic, M. S.; Jan, M. T.; Ghiviriga, I.; Abboud, K. A.; Veige, A. S. *Dalton Trans.* **2009**, 2764−2776.

(34) Bernskoetter, W. H.; Lobkovsky, E.; Chirik, P. J. *Organometallics* **2005**, *24*, 6250−6259.

(35) Batsanov, S. S. *Inorg. Mater.* **2001**, *37*, 871−885.

(36) Del Ministro, E.; Renn, O.; Rüegger, H.; Venanzi, L. M.; Burckhardt, U.; Gramlich, V. *Inorg. Chim. Acta* **1995**, *240*, 631−639.

(37) Albinati, A.; Bovens, M.; Rüegger, H.; Venanzi, L. M. *Inorg. Chem.* **1997**, *36*, 5991−5999.

(38) Netland, K. A.; Krivokapic, A.; Tilset, M. *J. Coord. Chem.* **2010**, *63*, 2909−2927.

(39) Cotton, F. A.; Wilkinson, G. *Advanced Inorganic Chemistry*, 4th ed.; Wiley: New York, 1980; p 947.

(40) Molinos, E.; Brayshaw, S. K.; Kociok-Köhn, G.; Weller, A. S. *Dalton Trans.* **2007**, 4829−4844.
(41) (a) Scott, N. M.; Dorta, R.; Stevens, E. D.; Correa, A.; Cavallo, L.; Nolan, S. P. *J. Am. Chem. Soc.* **2005**, *127*, 3516−3526. (b) Dorta, R.; Stevens, E. D.; Nolan, S. P. *J. Am. Chem. Soc.* **2004**, *126*, 5054−5055. (c) Huang, J.; Stevens, E. D.; Nolan, S. P. *Organometallics* **2000**, *19*, 1194−1197.
(42) Peters, J. C.; Feldman, J. D.; Tilley, T. D. *J. Am. Chem. Soc.* **1999**, *121*, 9871−9872.
(43) Turculet, L.; Feldman, J. D.; Tilley, T. D. *Organometallics* **2004**, *23*, 2488−2502.
(44) (a) Tanke, R. S.; Crabtree, R. H. *Inorg. Chem.* **1989**, *28*, 3444−3447. (b) Alvarado, Y.; Boutry, O.; Gutiérrez, E.; Monge, A.; Nicasio, M. C.; Poveda, M. L.; Pérez, P. J.; Ruíz, C.; Bianchini, C.; Carmona, E. *Chem.—Eur. J.* **1997**, *3*, 860−873.
(45) Ho, H.-A.; Gray, T. S.; Baird, B.; Ellern, A.; Sadow, A. D. *Dalton Trans.* **2011**, *40*, 6500−6514.
(46) Sexton, C. J.; Lopez-Serrano, J.; Lledos, A.; Duckett, S. B. *Chem. Commun.* **2008**, 4834−4836.
(47) McGhee, W. D.; Bergman, R. G. *J. Am. Chem. Soc.* **1988**, *110*, 4246−4262.
(48) (a) Scott, N. M.; Pons, V.; Stevens, E. D.; Heinekey, D. M.; Nolan, S. P. *Angew. Chem., Int. Ed.* **2005**, *44*, 2512−2515. (b) Corberán, R.; Sanaú, M.; Peris, E. *Organometallics* **2006**, *25*, 4002−4008. (c) Phillips, N.; Tang, C. Y.; Tirfoin, R.; Kelly, M. J.; Thompson, A. L.; Gutmann, M. J.; Aldridge, S. *Dalton Trans.* **2014**, *43*, 12288−12298.
(49) (a) Keyes, M. C.; Young, V. G., Jr.; Tolman, W. B. *Organometallics* **1996**, *15*, 4133−4140. (b) Slugovc, C.; Mereiter, K.; Trofimenko, S.; Carmona, E. *Chem. Commun.* **2000**, 121−122. (c) Conejero, S.; Esqueda, A. C.; Valpuesta, J. E. V.; Álvarez, E.; Maya, C.; Carmona, E. *Inorg. Chim. Acta* **2011**, *369*, 165−172.
(50) Cristóbal, C.; Hernández, Y. A.; López-Serrano, J.; Paneque, M.; Petronilho, A.; Poveda, M. L.; Salazar, V.; Vattier, F.; Álvarez, E.; Maya, C.; Carmona, E. *Chem.—Eur. J.* **2013**, *19*, 4003−4020.
(51) Belt, S. T.; Grevels, F. W.; Klotzbuecher, W. E.; McCamley, A.; Perutz, R. N. *J. Am. Chem. Soc.* **1989**, *111*, 8373−8382.
(52) Jones, W. D.; Hessell, E. T. *J. Am. Chem. Soc.* **1993**, *115*, 554−562.
(53) (a) Behrens, U.; Dahlenburg, L. *J. Organomet. Chem.* **1976**, *116*, 103−111. (b) Whited, M. T.; Zhu, Y.; Timpa, S. D.; Chen, C.-H.; Foxman, B. M.; Ozerov, O. V.; Grubbs, R. H. *Organometallics* **2009**, *28*, 4560−4570. (c) Salomon, M. A.; Braun, T.; Krossing, I. *Dalton Trans.* **2008**, 5197−5206. (d) Franken, A.; McGrath, T. D.; Stone, F. G. A. *J. Am. Chem. Soc.* **2006**, *128*, 16169−16177. (e) Franken, A.; McGrath, T. D.; Stone, F. G. A. *Organometallics* **2008**, *27*, 148−151. (f) Carr, M. J.; McGrath, T. D.; Stone, F. G. A. *Inorg. Chem.* **2008**, *47*, 713−722.
(54) Corey, J. Y. *Chem. Rev.* **2011**, *111*, 863−1071.
(55) Rosenberg, L.; Davis, C. W.; Yao, J. *J. Am. Chem. Soc.* **2001**, *123*, 5120−5121.
(56) (a) Drolet, D. P.; Lees, A. J. *J. Am. Chem. Soc.* **1992**, *114*, 4186−4194. (b) Lees, A. J.; Purwoko, A. A. *Coord. Chem. Rev.* **1994**, *132*, 155−160. (c) Ragaini, F.; Pizzotti, M.; Cenini, S.; Abbotto, A.; Pagani, G. A.; Demartin, F. *J. Organomet. Chem.* **1995**, *504*, 107−113. (d) Purwoko, A. A.; Lees, A. J. *Inorg. Chem.* **1995**, *34*, 424−425. (e) Purwoko, A. A.; Tibensky, S. D.; Lees, A. J. *Inorg. Chem.* **1996**, *35*, 7049−7055. (f) Lees, A. J. *J. Organomet. Chem.* **1998**, *554*, 1−11. (g) Dunwoody, N.; Lees, A. J. *Organometallics* **1997**, *16*, 5770−5778. (h) Panesar, R. S.; Dunwoody, N.; Lees, A. J. *Inorg. Chem.* **1998**, *37*, 1648−1650. (i) Dunwoody, N.; Sun, S.-S.; Lees, A. J. *Inorg. Chem.* **2000**, *39*, 4442−4451.
(57) Ghosh, C. K.; Rodgers, D. P. S.; Graham, W. A. G. *J. Chem. Soc., Chem. Commun.* **1988**, 1511−1512.
(58) Gridnev, A. A.; Mihaltseva, I. M. *Synth. Commun.* **1994**, *24*, 1547−1555.
(59) Occhipinti, G.; Jensen, V. R.; Törnroos, K. W.; Frøystein, N. Å.; Bjørsvik, H.-R. *Tetrahedron* **2009**, *65*, 7186−7194.
(60) Giordano, G.; Crabtree, R. H. *Inorg. Synth.* **1979**, *19*, 218−220.
(61) van der Ent, A.; Onderdelinden, A. L. *Inorg. Synth.* **1990**, *28*, 90−92.
(62) Powell, J.; Shaw, B. L. *J. Chem. Soc. A* **1968**, 211−212.
(63) Herde, J. L.; Lambert, J. C.; Senoff, C. V. *Inorg. Synth.* **1974**, *15*, 18−20.